12-2001

Automated Fault Detection in an Upflow Anaerobic Sludge Blanket Reactor: Comparisons of Biogas Production and Physicochemical Quantities

Alexandra Maria Almeida Carvalho Pinto
University of Tennessee - Knoxville

To the Graduate Council:

I am submitting herewith a dissertation written by Alexandra Maria Almeida Carvalho Pinto entitled "Automated Fault Detection in an Upflow Anaerobic Sludge Blanket Reactor: Comparisons of Biogas Production and Physicochemical Quantities." I have examined the final electronic copy of this dissertation for form and content and recommend that it be accepted in partial fulfillment of the requirements for the degree of Doctor of Philosophy, with a major in Biosystems Engineering.

D. Raj Raman, Major Professor

We have read this dissertation and recommend its acceptance:

Robert T. Burns, J. Wesley Hines, Lester O. Pordesimo, Luther R. Wilhelm

Accepted for the Council:
Carolyn R. Hodges

Vice Provost and Dean of the Graduate School

(Original signatures are on file with official student records.)

To the Graduate Council:

I am submitting herewith a dissertation written by Alexandra Maria Almeida Carvalho Pinto entitled “Automated Fault Detection in an Upflow Anaerobic Sludge Blanket Reactor: Comparisons of Biogas Production and Physicochemical Quantities.” I have examined the final electronic copy of this dissertation for form and content and recommend that it be accepted in partial fulfillment of the requirements for the degree of Doctor of Philosophy, with a major in Biosystems Engineering.

D. Raj Raman
Major Professor

We have read this dissertation
and recommend its acceptance:

Robert T. Burns

J. Wesley Hines

Lester O. Pordesimo

Luther R. Wilhelm

Accepted for the Council:

Dr. Anne Anne Mayhew
Vice Provost and
Dean of Graduate Studies

(Original signatures are on file in the Graduate Student Services Office.)

AUTOMATED FAULT DETECTION

IN AN UPFLOW ANAEROBIC SLUDGE BLANKET REACTOR:

COMPARISONS OF BIOGAS PRODUCTION AND

PHYSICOCHEMICAL QUANTITIES

A Dissertation

Presented for the

Doctor of Philosophy Degree

The University of Tennessee, Knoxville

Alexandra Maria Almeida Carvalho Pinto

December 2001

This dissertation is dedicated to:

my parents

José Leite and Ilca,

my husband

João Onofre,

and my son

João Vitor.

Esta tese é dedicada

aos meus pais

José Leite and Ilca,

ao meu esposo

João Onofre,

e ao meu filho

João Vitor.

ACKNOWLEDGEMENTS

It is very difficult for me to completely list from memory all the people who have been helpful during my journey throughout my Ph.D program to whom I am most grateful.

I would like to thank Dr. D. Raj Raman, my adviser, for his contributions and to the guidance on the research project.

In addition to Dr. Raman, I would like to thank the other members of my doctoral committee, Drs. Robert T. Burns, J. Wesley Hines, Lester O. Pordesimo, and Luther R. Wilhelm for their assistance and contributions to my research.

I also want to thank Dr. Ronald E. Yoder and my friend Dr. Renato Ribeiro for introducing me to the Biosystems Engineering graduate program at the University of Tennessee.

Special thanks go to Lara B. Moody, Gary L. Hawkins, and F. Henry Moody for contributions that were very relevant for my study. I also want to thank Catherine R. Mayhew, A. Renee Dyer, and Elizabeth L. Williams for the good time that I had with them.

I want to thank the staff at the department, especially Mr. Craig Wagoner for his help in the construction of the reactors; and Galina Melnichenko, Sarah Jenkins, Brenda Wallace, Frances Byrne, and Margaret Ann Taylor, for all their help and caring.

I want to thanks Anheuser-Busch Companies Inc. in Cartersville, GA for the donation of the biomass, and M&M Mars Inc. in Cleveland, TN for the confectionary wastewater used during my research.

There are some people that I met during my stay in the USA, whose friendship I will cherish forever. Among them are: Rozi and Demisio, Vanira and Túlio, Luciene and Ricardo, Burak and Alev, Ana and Renato, Luiz Eduardo and Zezé, Maria and Paulo, Márcia and Antonio, Carlos, Ibrahim, Maria, Leina and Rogério, Selma and Fábio, Iraci and Cyro, Ligia and Roberto, Claudia Werner, and Claudia and Samuel; and again, sorry if I left someone out.

Even physically separated from my family, I had their love and support to complete my education here. I also thank my sisters Andrea, Débora, and Lygia for their love and friendship. I also want to thank my other family: my mother-in-law “Dona Dazinha”, and my in-laws.

I also want to thank the family that came to be part of my life in Knoxville: Priscilla, Marinalva and Vinícius. They were very helpful and it was a joy to have their company. Finally, but not last, I would like to thank my husband João for all the support and love through my journey as a wife, mother, and graduate student. I also want to thank my son João Vitor for his love, kindness, and happiness. And for both of them, I am very sorry for the time that I was absent due to my studies.

And lastly, I would like to recognize the importance of CAPES (Coordenação de Aperfeiçoamento de Pessoal de Nível Superior) of Brazil and The Tennessee Agricultural Experiment Station via Regional Project S-1000 for financial support.

ACKNOWLEDGEMENTS CONT./AGRADECIMENTOS

Eu gostaria de dizer que é muito difícil para mim listar todas as pessoas para as quais eu gostaria de expressar minha gratitude durante minha jornada durante o programa de doutorado.

Eu gostaria de agradecer meu orientador Dr. D. Raj Raman pela suas contribuições e guia para o meu projeto de pesquisa.

Além de Dr. Raman, eu gostaria de agradecer aos outros membros do minha Banca Examinadora, Doutores Robert T. Burns, J. Wesley Hines, Lester O. Pordesimo, e Luther R. Wilhelm, pela assistência e contribuição prestadas à minha pesquisa.

Também gostaria de agradecer Dr. Ronald E. Yoder e meu amigo Dr. Renato Ribeiro por introduzir-me ao programa de pós-graduação da Universidade do Tennessee.

Agradecimentos especiais são dados à Lara e Henry Moody, e Gary L. Hawkins por contribuições que foram bastante relevantes para meu estudo. Também gostaria de agradecer Catherine R. Mayhew, Renee Dyer, and Elizabeth Williams pelas horas agradáveis que tivemos.

Gostaria de agradecer aos funcionários do departamento, especialmente o Sr. Craig Wagoner pelo seu auxílio and construção dos reatores; e Galina Melnichenko, Sarah Jenkins, Brenda Wallace, Frances Byrne, e Margaret Ann Taylor, por todo o auxílio e carinho.

Gostaria de agradecer Anheuser-Busch Companies Inc. de Cartersville, GA pela doação da biomassa, e também M&M Mars Inc. de Cleveland, TN pelo esgoto usados durante minha pesquisa.

Existem algumas pessoas que eu conheci durante minha estada nos E.U.A, e cuja amizade eu terei para sempre. Entre elas estão: Rozi e Demisio, Vanira e Túlio, Luciene e Ricardo, Burak e Alev, Ana e Renato, Luiz Eduardo e Zezé, Maria e Paulo, Márcia e Antonio, Carlos, Ibrahim, Leina e Rogério, Selma e Fábio, Iraci e Cyro, Ligia e Roberto, Claudia Werner, e Claudia and Samuel; de novo, me desculpem se eu me esqueci de alguém.

Mesmo estando fisicamente separada de minha família, eu tive o amor e o suporte deles para completar minha educação aqui. Eu também agradeço minhas irmãs Andrea, Débora e Lygia pelo amor e amizade. Também agradeço minha outra família: minha sogra Dona Dazinha e meus cunhados.

Também gostaria de agradecer uma parte da minha família que fez parte da minha vida em Knoxville, Priscilla, Marinalva e Vinícius, cuja presença foi muito agradável e de grande auxílio.

Finalmente, eu gostaria de agradecer meu esposo João por todo o encorajamento e amor por todos os caminhos de minha jornada como esposa, mãe, e estudante. Eu também agradeço meu filho João Vitor por seu amor, carinho, e alegria. E para ambos, que eu sinto muito pelo tempo que eu estive absente em razão do meu trabalho.

Terminando, gostaria de reconhecer a importância da CAPES (Coordenação de Aperfeiçoamento de Pessoal de Nível Superior) e ‘The Tennessee Agricultural Experiment Station’ através do projeto regional S-1000 pelo apoio financeiro.

ABSTRACT

A system capable of rapidly detecting toxic loads entering high-rate anaerobic reactors would greatly enhance their reliability, and could thereby increase their commercial acceptance. A high-rate anaerobic wastewater treatment process, called the failure-causing load detector (FCLD), consisting of a small (4-liter) upflow anaerobic sludge blanket (UASB) reactor having a short (10-min) hydraulic retention time (HRT), was used as a biosensor to rapidly detect potential problems with the influent wastewater. Sensors were used to monitor biogas production in the reactor, as well as pH, conductivity, and turbidity in the effluent from the reactor. The FCLD system was tested using the following failure-causing loads: organic overload, sodium toxic load (using NaCl), sodium hypochlorite (NaOCl, bleach), milk, sodium hydroxide (NaOH), and hydrochloric acid (HCl). Two different classifiers were implemented to identify the type of failure-causing load based upon the sensor outputs. Each classifier was tested using data collected during experiments with the FCLD system. The first classifier was a crisp classifier: it classified the failure-causing loads based on pH, conductivity, and turbidity, and was generated based on graph theory definitions. The second classifier was fuzzy logic based: it used a fuzzy inference system (FIS) to classify the failure-causing loads.

Biogas flow rate data under normal operating conditions was analyzed over ranges based on mean ± 1, ± 2, and ± 3 standard deviations, and was shown to be normally distributed. When using interval 2 (mean ± 2 sd), only 4 % of false positives (biogas alteration detection before addition of toxicant) were obtained, and it had 64 % of

false negatives (no alteration detection after addition of toxicant). However, 5 of the 9 failure-causing loads tests could still be detected using this interval. Due to variability in the biogas measurement and because classification could be performed using only pH, conductivity and turbidity as inputs, biogas was disregarded as an input for both classification processes. Even without biogas as an input for the classifiers, the FCLD reactor still was needed as part of the system because other monitored parameters (e.g. pH) in the effluent line are modified not only by changes in composition of the influent wastewater, but also from imbalances of by-products of the anaerobic digestion. The graph theory based classifier did not show false positives, and it reached 3.7 % correct classification 10 min after addition of the failure-causing load (test time), increasing to 48 % 15 min after test time, and reaching 100 % 20 min after test time. There were no false positives for FIS based classifier, and correct classification occurred with 7.4 % at 10 min after test time, 59 % 15 min after test time, increasing to 96 % 20 min after test time, and it reached 100 % correct classification 25 min after test time. Results from both classifiers showed that the FIS based classifier has more misclassifications (125 % more) than the graph theory based classifier. Response time was checked for biogas detection and for both classifiers. Biogas detection was 5 min faster than the classifiers for the loads that could be detected. One improvement for both classifiers would be the inclusion of biogas as an input, which would accelerate the detection of the failure-causing loads that cause significant change in biogas production.

TABLE OF CONTENTS

LIST OF TABLES

LIST OF FIGURES

LIST OF ABBREVIATIONS*

VFAs	volatile fatty acids
COD	chemical oxygen demand
UASB	upflow anaerobic sludge blanket
FCLD	Failure causing load detector
HRT	hydraulic retention time
NaCl	sodium chloride
NaOH	sodium hydroxide
HCl	hydrochloric acid
FIS	fuzzy inference system
AFO	animal feeding operation
MOS	Microorganisms
CO_2	carbon dioxide
O_2	free oxygen
H_2O	water
CH_4	methane
N	nitrogen
P	phophorus
VSS	volatile suspended solids
^oC	degrees Celsius
AF	anaerobic filter
AFBR	anaerobic fluidized bed reactor
ASBR	anaerobic sequential batch reactor
USEPA	US Environmental Protection Agency
AI	artificial inteligence
RHS	right hand side
DOF	degree of fulfillment
LHS	left hand side

* The abbreviations are listed in order of appearance

COA	center of area
COS	center of sums
MOM	mean of maxima
OUR	oxygen uptake rate
DO	dissolved oxygen
UAF	upflow anaerobic filter
F/M	food/microorganism ratio
PC	personal computer
PID	proportional-integral-derivative
Na^+	Sodium
NaOCl	sodium hypochlorite – common bleach
OO 50	organic overload at 50 g/L
20 Na	Na^+ at 20 g/L
blc 1% and bleach 1%	bleach at 1 %
blc 5% and bleach 5%	bleach at 5 %
10 Na	Na^+ at 10 g/L
OO 20	organic overload at 20 g/L
OO 40	organic overload at 40 g/L

CHAPTER 1

INTRODUCTION

High rate anaerobic treatment processes offer many advantages over aerobic processes: they require less energy to operate, they produce biogas that can be used as an energy source, they produce far less sludge as a byproduct when compared to aerobic treatment processes, and they do not require a large area to be implemented (Lettinga, 1995). However, high-rate anaerobic processes have a serious disadvantage: the possibility of reactor failure due to an organic overload or a toxic load, and the subsequent slow start-up typical of these systems.

When exposed to a toxic load, the composition of the liquid phase, as well as the biogas production and composition are expected to change. Some of the possible parameters that will vary in the liquid phase are alkalinity, volatile fatty acids (VFAs) concentration, chemical oxygen demand (COD) concentration, temperature, pH, dissolved hydrogen concentration (Moletta, 1994), and turbidity.

A system capable of detecting such toxic loads would greatly enhance the reliability of existing high-rate anaerobic reactors, and could thereby increase the commercial acceptance of high-rate anaerobic treatment systems. Several investigators have explored the possibility of monitoring anaerobic reactors to enhance system stability (Rozzi *et al*., 1997; Rozzi *et al*., 1999; Steyer *et al*., 1997a; Steyer *et al*., 1997b). Steyer *et al.* (1997a & 1997b) applied fuzzy logic to control influent flow rate, based on the output

gas flow rate in a high-rate anaerobic digester (120 L) (similar to a upflow anaerobic sludge blanket, or UASB), but did not use a surrogate short-retention time reactor in their work. Rozzi *et al*. (1997 & 1999) worked with a small (5 L) UASB-like reactor (called the Rantox), and demonstrated the ability to rapidly detect toxic loads. The Rantox was used to monitor the metabolism of acetoclastic methanogens in the presence of toxicants. Toxicity could be detected from the analysis of the Monod kinetic constants K_m (maximum substrate degradation) and K_S (half-saturation constant), under kinetically saturated conditions (high substrate conditions), which was achieved by the periodical addition of acetic acid to the reactor.

The need for a rapid toxicity detector motivated the development of a small-scale upflow anaerobic sludge blanket (UASB) reactor to be operated as a biosensor (Ervin *et al*., 1999). The device – called a failure-causing load detector (FCLD) – was designed to be placed alongside full-scale UASB reactors treating carbohydrate-rich wastewater. The FCLD has a hydraulic retention time (HRT) of 10 min, which is much shorter than the typical HRT of a full-scale UASB (ca. 2 – 8 h). Because of its short HRT, the FCLD responds more rapidly to a toxic event than does a full-scale reactor (Ervin *et al*., 1999).

The use of the FCLD together with sensors to monitor parameters in the effluent wastewater and gas phase originated what is called the FCLD system. Experiments with different failure modes were performed: organic overloads, and toxic loads with sodium chloride (NaCl), milk, household bleach, sodium hydroxide (NaOH) and hydrochloric acid (HCl) were performed. Biogas flow rate, pH, conductivity and turbidity were monitored continuously during experiments.

Because of the biological complexity inherent in the FCLD reactor, relationships among monitored parameters and toxicity are not expected to be exact; in other words, they involve some "fuzziness." By definition, fuzziness is the ambiguity that can be found in the definition of the meaning of a word (Terano, 1991). Fuzzy inference systems (FIS) are very useful in classification type problems, because FIS allows the making of input/output nonlinear mapping.

Therefore, the goal of this study was twofold:

(1) To run the FCLD system using both organic overloads and toxic loads to verify system performance and to generate sample data for the second goal.

(2) To develop and analyze expert system classification tools using FIS and graph theory for classifying the nature of the toxin entering the FCLD, based on easily measured macroscopic variables such as pH, biogas flow rate, conductivity and turbidity.

CHAPTER 2

LITERATURE REVIEW

2.1 – Wastewater treatment

Wastewater may be classified as municipal (domestic), industrial, and agricultural. Municipal waste consists of the wastewater that comes from residences, commercial buildings, schools and hospitals (Gray, 1989). Industrial wastewater comes from manufacturing plants, for instance, food processing plants, breweries, or paper mills (Gray, 1989). Agricultural wastewater is generated on animal feeding operations (AFO), such as livestock (beef and dairy cattle, swine) and poultry (broilers, layers, turkeys) operations.

Before wastewater is returned to surface waters or land, it must typically go through some method of treatment in order to avoid environmental degradation. Wastewater can be treated physically, chemically, and biologically (Metcalf and Eddy, 1991), or any combination of those methods. Physical treatment is achieved when physical forces are utilized; e.g., screening for the removal of solids, mixing to keep solids in suspension, flocculation to aggregate small particles into larger ones with the intention of sedimentation, and filtration to remove fine particles (Metcalf and Eddy, 1991). When a chemical reaction changes the composition of the wastewater it is known as chemical treatment. Some examples of chemical treatment are the precipitation for the removal of phosphorus, disinfection for the destruction of pathogenic organisms, and

dechlorination (Metcalf and Eddy, 1991). Biological treatment processes occur when living organisms, typically microbes, are used during the process. They can be used for the degradation of organic compounds, and the removal and/or sequestration of macronutrients such as nitrogen and phosphorus (Metcalf and Eddy, 1991). Biological treatment can be further subdivided into two major categories, aerobic and anaerobic processes.

2.1.1 – Aerobic wastewater treatment

Aerobic microorganisms require free oxygen to degrade the organics in the wastewater and to grow. Aerobic microorganisms (MOs) degrade organic contaminants in the wastewater when free oxygen is present, resulting in the growth of more microorganisms and the release of carbon dioxide (CO_2), water and energy (Gray, 1989), as equation 2.1 shows. Example aerobic wastewater treatment processes include activated sludge processes, aerated lagoons, trickling filters, rotating biological contactors and stabilization ponds (Metcalf and Eddy, 1991).

$$\text{Organics} + O_2 \xrightarrow{\text{Aerobic MOs}} \text{aerobic MOs} + CO_2 + H_2O + \text{energy} \qquad [2.1]$$

2.1.2 – Anaerobic wastewater treatment

Degradation of organics present in the wastewater by anaerobe microorganisms is called anaerobic digestion. This process takes place in the complete absence of free oxygen. Anaerobic degradation is a multistep process of different reactions that are

accomplished by a consortium of microorganisms (Pavlostathis and Giraldo-Gomez, 1991). It consists of three stages (Gray, 1989): hydrolysis, acid formation, and methane (CH_4) formation (methanogenic phase), as equation 2.2 shows.

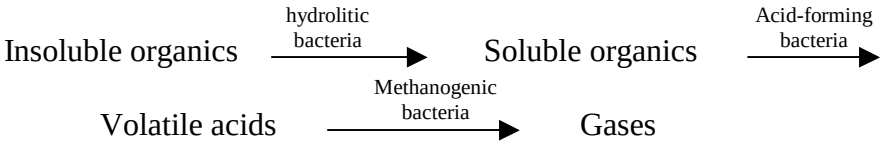

[2.2]

Even though described as a three-phase process, the reactions occur simultaneously; the microorganisms are therefore metabolically codependent on each other, as illustrated by figure 2.1. Anaerobic digestion starts as enzymes hydrolyze complex organic materials into smaller soluble products, amino acids, sugars, fatty acids and alcohol. Amino acids and sugars are products of the hydrolysis of proteins and carbohydrates, respectively. Amino acids and sugars are then fermented into intermediary products and acetate. Fatty acids and alcohol that are hydrolyzed from lipids are anaerobically oxidized into intermediary products, carbon dioxide and hydrogen. Acetate is produced from the homoacetogenesis of carbon dioxide and hydrogen. Finally, methanogenesis occurs via carbon dioxide reduction by hydrogen or from acetate. The anaerobic digestion produces biogas as an end product. Biogas is composed of methane (60-75%), carbon dioxide (25 – 30%) and trace amounts of nitrogen, hydrogen, and other gases (Gray, 1989). In order for the anaerobic digestion of complex organic materials to be efficient, several critical parameters must be in an

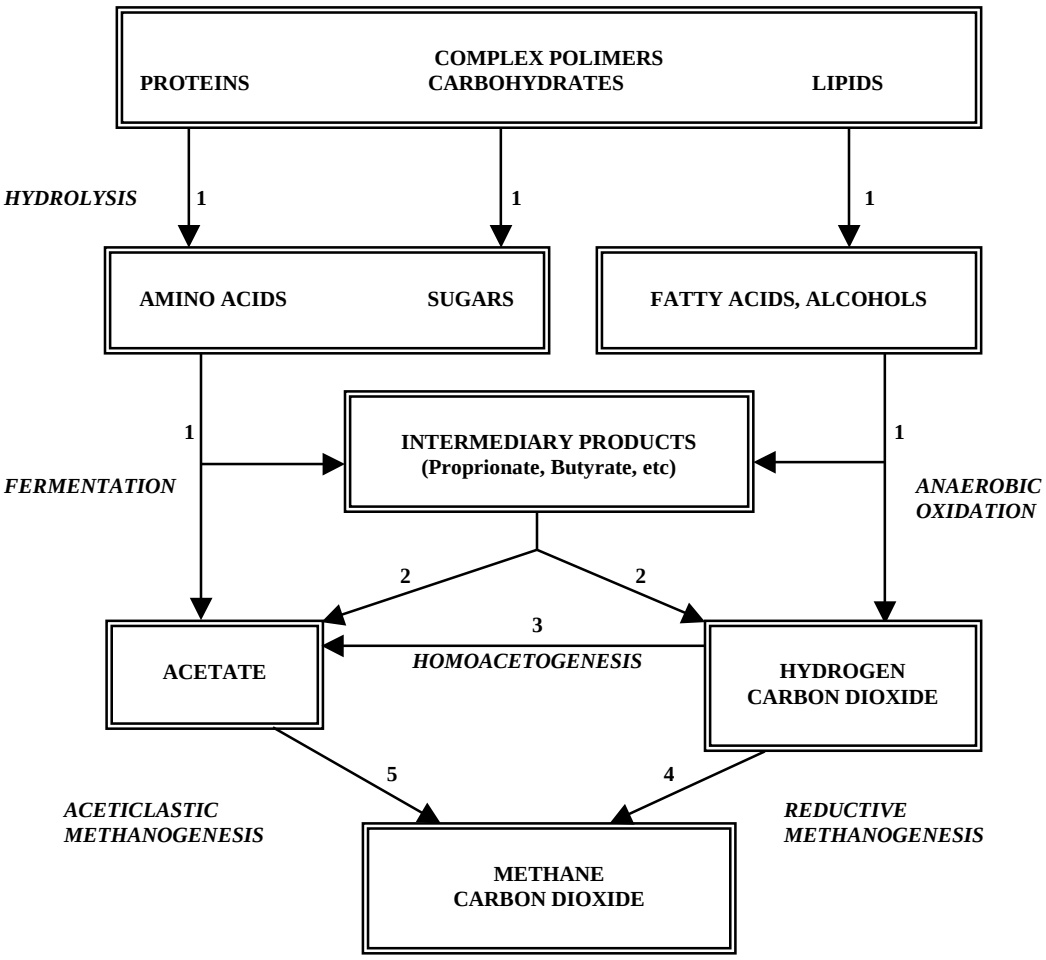

(1) fermentative bacteria,
(2) hydrogen-producing acetogenic bacteria,
(3) hydrogen-consuming acetogenic bacteria,
(4) carbon dioxide-reducing methanogens,
(5) aceticlastic methanogens

Figure 2.1 – Anaerobic digestion of complex organic material

optimal range, among them are pH, temperature, the concentration of macronutrients, carbon source, and electron donor.

The pH within an anaerobic reactor must be kept between 6.5 and 8.2 (Speece, 1996). If the methanogenic bacteria do not work properly, i.e., do not digest the intermediary products at a reasonable rate, these intermediary products will start to accumulate. The accumulation of these products, especially VFAs, will lower the pH inside the reactor. If the pH drops below 6.2, methane production will slow drastically and the process may fail (Winkler, 1981).

Nitrogen (N) and phosphorus (P) are essential nutrients for bacterial growth. Depending on the characteristics of the wastewater, these nutrients may have to be added to the influent. A COD:N ratio of 400:7 when having high loading rates (0.8 – 1.2 g COD/g VSS·d), and 1000:7 at low loading rates (< 0.5 g COD/g VSS·d) may be necessary as reviewed by Singh *et al.* (1998). The phosphorus requirement, described as P:N ratio, is 7:1 (Gray, 1989; Speece, 1996). The theoretical minimum COD:N:P ratio is thus 350:7:1 for high loading rates and 1000:7:1 for low loading rates, as reviewed by Speece, (1996). Other macronutrients and micronutrients that must be present in the wastewater are sulfide, iron, cobalt, nickel, and zinc (Speece, 1996).

The temperature range for anaerobic digestion is divided into three classes, psychrophilic, 5 – 25 degrees Celsius (^{o}C), mesophilic, 25 – 38^{o}C, and thermophilic, 50 – 70^{o}C (Gray, 1989). Usually, anaerobic reactors are operated under mesophilic conditions with an optimum temperature of 35^{o}C (Speece, 1996). Rates of substrate degradation and gas production are temperature dependent, with more gas production at high

temperatures. Gas production rate does not increase monotonically with temperature; it decreases above 55^{o}C (Gray, 1989).

Most of the microorganisms present in the anaerobic biomass are heterotrophic, which means that they need organic compounds that are present in the wastewater as source of carbon. In contrast, the methanogens that convert the H_2 to methane are autotrophic, their carbon source comes from the dissolved CO_2 within the reactor (Speece, 1996).

The electron donor comes from the biodegradable COD present in the wastewater. The electron donor provides energy for the metabolic activities of the biomass (Speece, 1996).

Anaerobic processes can be carried out in many ways, such as in anaerobic lagoons, digesters and filters. Some digesters and filters belong to a group that is called high rate digesters. These digesters can handle high organic loading rates such as 24 kg COD/m^3·d (Rajeshwari *et al.*, 1999). When using digesters or filters, anaerobic processes can be divided into two major categories: attached and suspended growth systems (Speece, 1996). In attached growth systems, microorganisms grow attached to some inert material such as plastic media, rocks, or sand. Anaerobic filters (AF) and fluidized bed reactors (AFBR) are examples of this category.

The anaerobic filter dissolved oxygen is an attached growth treatment process consisting of a reactor filled with solid media to which biomass grows and remains fixed. In most anaerobic filters, the wastewater enters from the bottom of the filter and flows

upward entering in contact with the biomass that is fixed to the media (Metcalf and Eddy, 1991); these filters are called upflow anaerobic filters.

In the AFBR, a film of biomass grows on a carrier medium that consists of very fine particles, such as sand, coal, porous glass beads, diatomaceous earth, and others (Speece, 1996). The particles must be small enough to be kept in suspension by the upward flow of wastewater to be treated (Winkler, 1981). Particles have very high surface area, resulting in a high density of biomass in contact with the wastewater (Winkler, 1981).

Suspended growth systems have the advantage that they do not need a packing media for biomass growth; microorganisms are suspended into the liquid (Metcalf and Eddy, 1991). Examples of suspended growth systems are the anaerobic sequential batch reactor (ASBR) and the UASB reactor.

The anaerobic treatment process using the ASBR involves the following steps: filling, reacting, settling and decanting (Speece, 1996). First, the reactor containing the biomass is filled with the wastewater to be treated. Next, the biomass and wastewater are mixed and the reaction takes place. Then, agitation ends and the biomass settles, leaving the clear and treated liquid on the top. Finally, the liquid on the top part is decanted.

Biomass inside UASB reactors is aggregated into small granules that have good settling properties when not exposed to rigorous mechanical agitation (Lettinga, 1995). Contact of granules to wastewater is obtained by the upward movement of biogas bubbles generated via anaerobic digestion and by the even distribution of influent wastewater in the bottom of the reactor (Lettinga, 1995). A very important part of the UASB reactor is

the gas solids separator (Lettinga, 1995). This device is located on the top of the reactor and separates the biogas from the biomass. The biogas exits the reactor from the top. Another device that can be used is a baffle in front of the effluent port to prevent the washout of granules.

Due to the difference in the sizes of the granules, sludge in the UASB is divided into three phases. The lower part of the biomass within the reactor is formed by larger granules, and is called the sludge bed. Just above this zone is the sludge blanket, formed by smaller grains and gas bubbles. The settling zone forms the upper part. Biomass attached to rising bubbles separate in the gas solids separator. Once separated, biomass settles in the settling zone, passes through the sludge blanket, and falls to the sludge bed. Figure 2.2 shows the schematic of a UASB reactor.

UASB technology is been used for treatment of different wastewaters, food processing units, breweries, tanneries, and municipal wastewater (Rajeshwari *et al.*, 1999). As reviewed by Speece (1996), some wastewaters, especially carbohydrates, have been treated by the UASB with great success. The fact that biomass in the UASB reactor does not need packing media to grow is one of the major advantages of this system (Speece, 1996). For these reasons, UASBs have fewer investments requirements compared to AFs and fluidized bed reactors (Rajeshwari *et al.*, 1999).

2.1.3 – Aerobic versus anaerobic process

Both aerobic and anaerobic processes have advantages and disadvantages. Some of the advantages of anaerobic systems over the aerobic systems are:

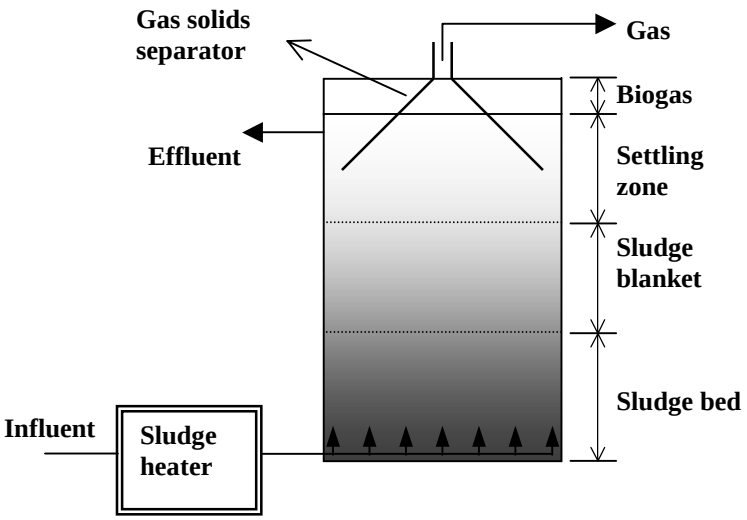

Figure 2.2 – Schematic of a UASB reactor showing the three phases

Low cost to implement – very simple reactors can be used. Also, treatment can occur with very little energy consumption (Lettinga *et al.*, 1980).

Less area required for implementation – anaerobic processes have higher loading rates (3.2 to 32 kg/m^3.d) compared to aerobic processes (0.5 to 3.2 kg/m^3.d) (Speece, 1996), so less area is required for the implementation of an anaerobic reactor.

Versatility of implementation – anaerobic processes can be applied at practically any place and at any scale (Lettinga *et al.*, 1980).

Reduction of biomass disposal cost – anaerobic processes produce much less excess sludge than aerobic processes. Disposal costs for anaerobic processes are approximately 10% of aerobic processes for the same effluent (Speece, 1996).

Conservation of energy –anaerobic processes can operate with very little energy consumption. Furthermore, the process generates useful energy in the form of methane (Speece, 1996; Lettinga *et al.*, 1980; Gray, 1989).

Long preservation of anaerobic microorganisms – the anaerobic microorganisms can be preserved unfed for more than one year without serious degradation of their activity (Lettinga *et al.*, 1980). This is a very important factor when the treatment is applied to seasonally produced wastewaters, like winery and sugar operations (Speece, 1996).

Off-gas air pollution eliminated – when using aerobic treatment some of the organic components are volatile and they can be air stripped before the biodegradation, which contributes to air pollution. However, this problem is completely eliminated when anaerobic processes are employed (Speece, 1996).

However, the anaerobic process has some significant drawbacks, such as:

Incomplete treatment – Lettinga *et al.* (1980) said that the anaerobic process is not a complete treatment; some mineralized components are left after the treatment. However, Moody and Raman, (2001), showed that when treating readily degradable food waste, a dual system consisting of a UASB followed by a DFAF could meet US Environmental Protection Agency (USEPA) effluent requirements.

Slow start up – the start up of a new reactor is very slow. However, if active biomass from another reactor is used to seed the new reactor this drawback can be overcome (Speece, 1996).

Vulnerability to toxins – the methanogens are very susceptible to toxins in certain wastewaters. However, methanogens can be acclimated to certain toxins when some precautions are taken, such as gradually increasing the toxicant concentration, and preventing the loss of biomass from the reactor until the biomass has acclimated (Speece, 1996).

In industrial settings, wastewater composition cannot always be predicted. For example, a sudden spill of some toxin into the wastewater can occur. Such events could adversely affect the anaerobic treatment process. The need to keep anaerobic treatment processes stable suggested the idea to create a biological sensor, the failure-causing load detector (FCLD) system to monitor high rate anaerobic processes. The FCLD system is described in detail in section 2.4.

2.2 - Artificial Intelligence

Human communication involves spoken and written language, and mathematics (Hopgood, 1993). Mathematics allows the exchange, storage and the expression of concepts that would be difficult to express with the spoken and written language (Hopgood, 1993).

The computer is one of the greatest achievements of technology. Initially, it was essentially one big calculator; with time it increased its storage capacity, its speed of processing, and many other functions. Computers are used everywhere and for a wide variety of tasks. One of the biggest questions facing computer science was how the computer could be used to think, in other words, to mimic human intelligence (Martin,

1988). This question created a new science called artificial intelligence (AI), which is the use of computational methods to create tools that simulate human intelligence, imagination, recognition, creativity and even emotions (Hopgood, 1993). AI covers many areas, such as engineering, medicine, linguistics, psychology, and computer science.

Recently, the term soft computing is being used as an alternative for artificial intelligence (Tsoukalas, 1997). Soft computing includes expert systems, neural networks, fuzzy logic, and genetic algorithms. All these technologies have a certain tolerance for the imprecision and ambiguity characteristic of human language.

2.3 - Fuzzy theory

Traditionally, science is viewed as certain, precise, specific, and uncertainty is not desired or allowed. However, many concepts in science and life itself are uncertain, imprecise, and vague. Fuzzy logic deals with concepts that can be classified as partial truth, i.e. imprecise concepts, which are values between completely true and completely false (FOLDOC, 1993). The following sections introduce fuzzy sets theory and other concepts used in fuzzy logic. For more details using fuzzy logic two books are recommended, *Fuzzy and Neural Approaches in Engineering* by Tsoukalas and Uhrig (1997), and *Fuzzy Sets and Fuzzy Logic Theory and Applications* by Klir and Yuan (1995).

2.3.1 -Fuzzy sets

The theory of fuzzy sets demonstrates that a set can have imprecise boundaries. The membership of an object to a fuzzy set is not a crisp value like yes or no, but a degree of pertinence to the set.

When dealing with classical (or crisp) set theory, an object *x* is a member of a set *A* that belongs to the universe of discourse *X*, which is the domain to which A belongs, namely the input space. This relationship is written as

$$x \in A \qquad [2.3]$$

or, if *x* does not belongs to the universe of discourse *X*,

$$x \notin A \qquad [2.4]$$

A set can be defined by a characteristic function that declares which elements of the universe of discourse *X* belong to the set *A*.

$$X_A(x) = \begin{cases} 1 & for \;\; x \in A \\ 0 & for \;\; x \notin A \end{cases} \qquad [2.5]$$

The characteristic function maps values of the universe of discourse *X* to the elements of the set {0,1}, and is expressed as

$$X_A : X \rightarrow \{0,1\} \qquad [2.6]$$

When using the theory of fuzzy sets, the function that denotes how an element *x* is a member of a fuzzy set is called membership function, and it is represented by

$$\mu_A : X \rightarrow [0,1] \qquad [2.7]$$

There are different ways to represent a membership function, such as triangular, trapezoidal, and Gaussian functions. Figure 2.3 represents a set of three triangular membership functions defined over a universe of discourse between 0 and 10. Figure 2.4 and 2.5 illustrate sets of three trapezoidal and three Gaussian membership functions over the same universe of discourse, respectively.

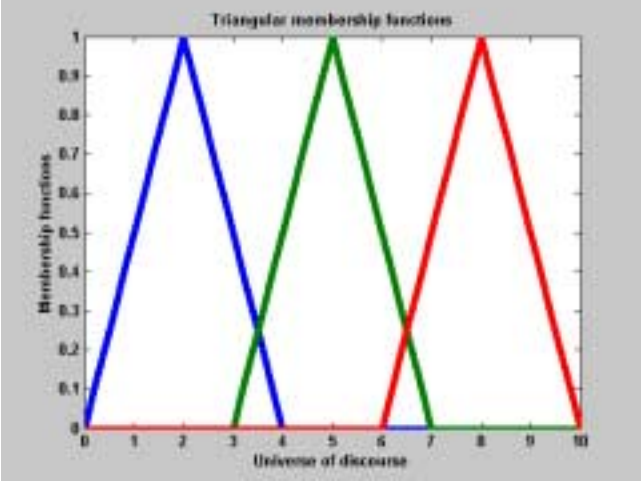

Figure 2.3 – Triangular membership functions

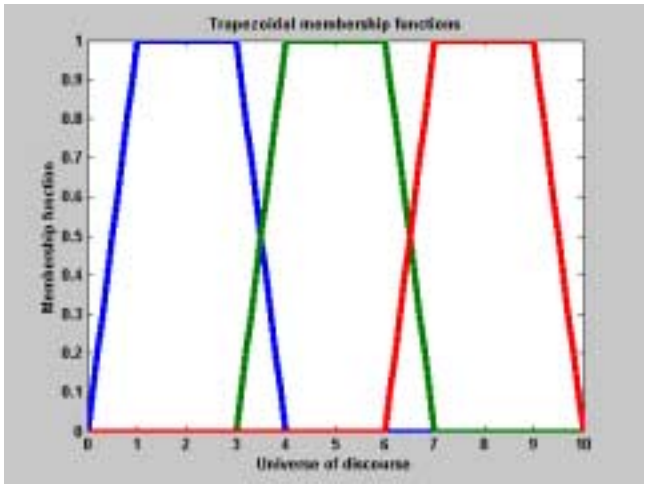

Figure 2.4 – Trapezoidal membership functions

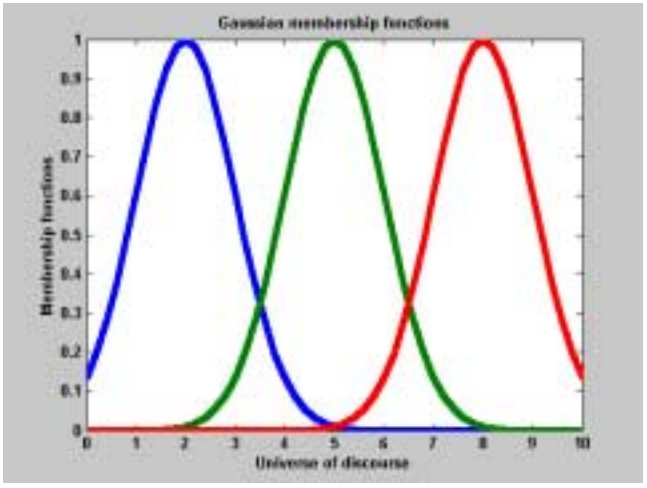

Figure 2.5 – Gaussian membership functions

Many variables can be represented by linguistic values that in traditional scientific terms are classified as uncertain, for example, high temperature, and low pH. Fuzzy set theory allows the representation of these linguistic values through membership functions. For instance, when dealing with high rate anaerobic digestion, pH can be classified as a fuzzy variable. Low pH can be represented by the trapezoidal membership function on the left side, while optimum pH can be represented by the triangular membership function, and high pH represented by a trapezoidal membership function on the right side of the figure. The universe of discourse for pH is between 4 and 11. Figure 2.6 represents a potential set of three triangular membership functions for pH values in an anaerobic reactor.

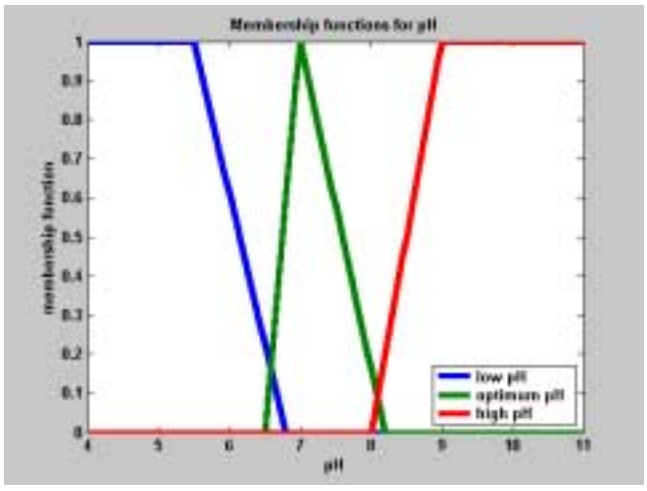

Figure 2.6 - Membership functions that represent a fuzzy set for pH

2.3.2-Basic concepts of fuzzy sets

Following are basic fuzzy operations applied to fuzzy sets *A* and *B*.

Empty fuzzy set (∅)

Any fuzzy set is classified as an empty fuzzy set if its membership function is zero for any value of its universe of discourse *X*.

$$A \equiv \varnothing \qquad if\ \mu_A(x) = 0, \forall\, x \in X \tag{2.8}$$

Normal fuzzy set

A fuzzy set is considered normal if there is at least one element x_0, on its universe of discourse, where its membership function equals one.

$$\mu_A(x_0) = 1 \tag{2.9}$$

Equality of fuzzy sets

Two fuzzy sets are equal if their membership functions are equal in the universe of discourse *X*.

$$A \equiv B \qquad if\ \mu_A(x) = \mu_B(x) \tag{2.10}$$

Complement of a fuzzy set

The complement of a fuzzy set is denoted by a new fuzzy set with membership function as followed.

$$\mu_{\bar{A}}(x) = 1 - \mu_A(x) \qquad [2.11]$$

Multiplication of a fuzzy set by a crisp number

A new fuzzy set is obtained when a crisp value multiplies a fuzzy set. This new fuzzy set has the following membership function.

$$\mu_{\alpha A}(x) \equiv \alpha \cdot \mu_A(x) \qquad [2.12]$$

Union ($\cup$) or max ($\vee$)

When this operation is applied to two fuzzy sets defined over the same universe of discourse *X*, a new fuzzy set is formed. The membership function for this new fuzzy set is formed by the maximum values of membership values for the two previous fuzzy sets. This property is illustrated in figure 2.7.

$$\mu_{A \cup B}(x) \equiv \mu_A(x) \vee \mu_B(x) \qquad [2.13]$$

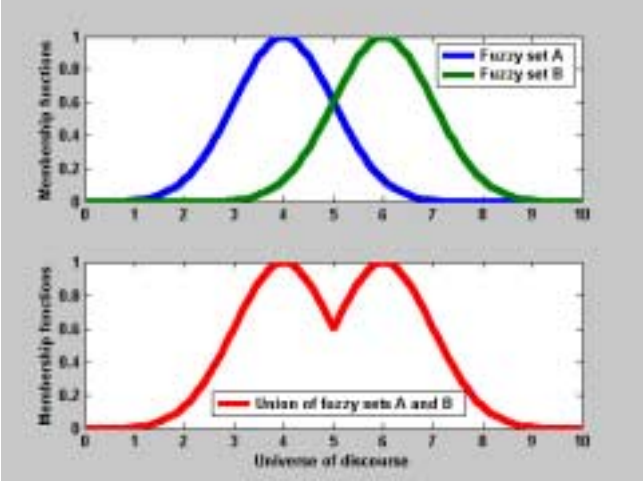

Figure 2.7 – Union of fuzzy sets *A* and *B*

Intersection (∩) or min (∧)

The intersection of two fuzzy sets is represented by a new fuzzy set with membership function that is derive from the minimum membership values of the original fuzzy sets. Figure 2.8 shows the intersection between two fuzzy sets, *A* and *B*.

$$\mu_{A\cap B}(x) \equiv \mu_A(x) \wedge \mu_B(x) \qquad [2.1]$$

Product (·)

The product of two fuzzy sets defined over the same universe of discourse *X* is a new fuzzy set. Membership function for the new fuzzy set is represented by the algebraic product of membership functions for the two fuzzy sets, i.e.,

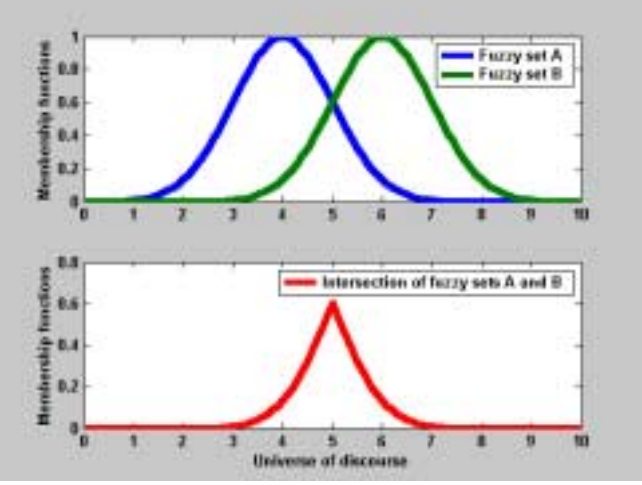

Figure 2.8 – Intersection of fuzzy sets *A* and *B*

$$\mu_{A\cdot B}(x) \equiv \mu_A(x) \cdot \mu_B(x) \qquad [2.15]$$

Power of a fuzzy set

When raising the membership function of a fuzzy set to a power α (positive real number), a new fuzzy set is formed, and it has the following membership function.

$$\mu_{A^\alpha}(x) \equiv [\mu_A(x)]^\alpha \qquad [2.16]$$

Concentration

When a variable linguistic is modified by the term VERY, like when saying ‘very low pH’, concentration is applied to the fuzzy set. Concentration of a fuzzy set, defined over the universe of discourse *X*, is defined as follows.

$$\mu_{CON(A)}(x) \equiv (\mu_A(x))^2 \qquad [2.17]$$

Dilation

If the term MORE OR LESS is applied to a linguistic variable, like 'more or less hot', dilation is applied to the fuzzy set. Dilation of a fuzzy set, over a universe of discourse *X*, is given by

$$\mu_{DIL(A)}(x) \equiv \sqrt{\mu_A(x)} \qquad [2.18]$$

Alpha-cut

Alpha-cut of a fuzzy set *A* is the crisp set A_α formed by all the elements of the universe of discourse whose memberships functions in the fuzzy set are greater than or equal to the value of α.

$$A_\alpha = \{x \in X / \mu_A(x) \geq \alpha\}, \quad where \quad \alpha \in [0,1] \qquad [2.19]$$

2.3.3 – Fuzzy propositions

A fuzzy proposition can be expressed as:

x is A [2.20]

Where, *x* is a variable that takes values from a universe of discourse. *A* is a fuzzy set on the universe of discourse that represents a predicate. *A* is called the *fuzzy variable*, or *linguistic variable*. Some examples of fuzzy prepositions are, 'pH is high', 'temperature is low', and 'x is a small number.' Fuzzy variables can be modified when a modifier is applied. Dilation (more or less), concentration (very) and negation (complement) are modifiers (Terano *et al*., 1991). Figure 2.9 represents membership functions for three fuzzy sets: *A*, '*Not A*, '*Very A*', and '*More or less A.*'

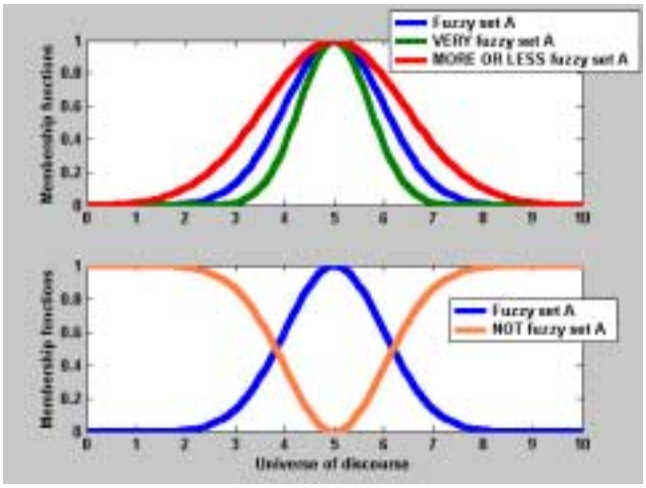

Figure 2.9 – Application VERY, MORE OR LESS, and NOT modifiers to a fuzzy set *A*

$$very\ A = A^2, \qquad \mu_{A^2}(x) = \left(\mu_A(x)\right)^2 \qquad [2.21]$$

$$more\ or\ less\ A = \sqrt{A}, \qquad \mu_{\sqrt{2}}(x) = \sqrt{\mu_A(x)} \qquad [2.22]$$

$$not\ A = 1 - A, \qquad \mu_{1-A} = 1 - \mu_A(x) \qquad [2.23]$$

2.3.4 - Fuzzy inference systems

Fuzzy logic is an AI technique that allows the making of input/output nonlinear mapping using the theory of fuzzy sets. This mapping is easily obtained from experimental data and from expert knowledge in the form of if/then rules, such as "*if x is A then y is B*", which are also called preposition rules, where the "if" part is the called antecedent and the "then" part is the consequent. The mapping from a given input into an output using fuzzy logic is called fuzzy inference. It can be applied in many fields, such as automatic control, data classification, decision analysis, and expert systems (Jang and Gulley, 1995). In order to better explain the FIS, some definitions have to be made. The design of an FIS is divided into five steps: fuzzification, fuzzy operation, implication relation, aggregation and defuzzification (Tsoukalas, 1996).

1 – **Fuzzification** is the first step in the inference system. A membership value between 0 and 1 is assigned for the input values (antecedents), which are the statements in the right hand side (RHS) of the if/then rule.

2- **Fuzzy operation.** When an element x_i belongs to a fuzzy set A on the antecedent of the rule, it means that the rule was fired. If more than one antecedent on the rule is fired, connectives are used to define the degree of fulfillment (DOF) for the rule, which is a single number between 0 and 1. The connective AND is modeled by the intersection (minimum) fuzzy set operation, while the OR is modeled by the union (maximum) fuzzy set operation, and NOT is the complement of a fuzzy set.

3 – **Implication relations** are obtained through fuzzy implication operators. The consequent that is the left hand side (LHS) of the if/then proposition is a fuzzy set and the implication method defines the shape of the consequent based on the DOF, which is the result from the last step. There are many implication operations (Tsoukalas, 1996). One of the most used is the Mamdani Min implication operator, it applies the min operation to define the shape of the consequent based on the DOF.

4 – **Aggregation** is used to unify the outputs of each rule. Fuzzy operators, such as maximum and sum, are used to aggregate the many outputs that were inferred in the last step, resulting in a unique fuzzy set output.

5 – **Defuzzification** is used to select the output crisp value that represents the output aggregate fuzzy set. There are many types of defuzzification methods, the most used are the centroid or center of area (COA), the center of sums (COS), and the mean of maxima (MOM).

The following example illustrates a FIS with two inputs, which are pH and biogas and one output, the operation mode. The FIS will map the inputs into one output that describe the type of operation mode based on if/then rules constructed based on knowledge of anaerobic wastewater treatment processes.

Suppose this inference system has three rules:

(1) If pH is acidic and biogas low then operation is overload

(2) If pH is basic and biogas is low than operation is toxic

(3) If pH is neutral and biogas is normal than operation is safe.

Implementation for this FIS follows the 5 steps, fuzzification of inputs, application of fuzzy operator, use of implication relations, aggregation of output, and output defuzzification. The basic structure for this problem is illustrated in figure 2.10, which is based on the example given by Jang and Gulley (2001). Information flows from two inputs to one output, and all rules are evaluated in parallel. Finally, results of the rules are combined and defuzzified. For this example, if the defuzzified output of the FIS is between 0 and 0.375 the operation mode is overload, if it is between 0.375 and 0.625 operation is normal, and more than 0.625 operation is toxic. Figure 2.11 represents the membership functions for the antecedents (pH (a) and biogas (b)) and consequent (operation mode) is illustrated in figure 2.12.

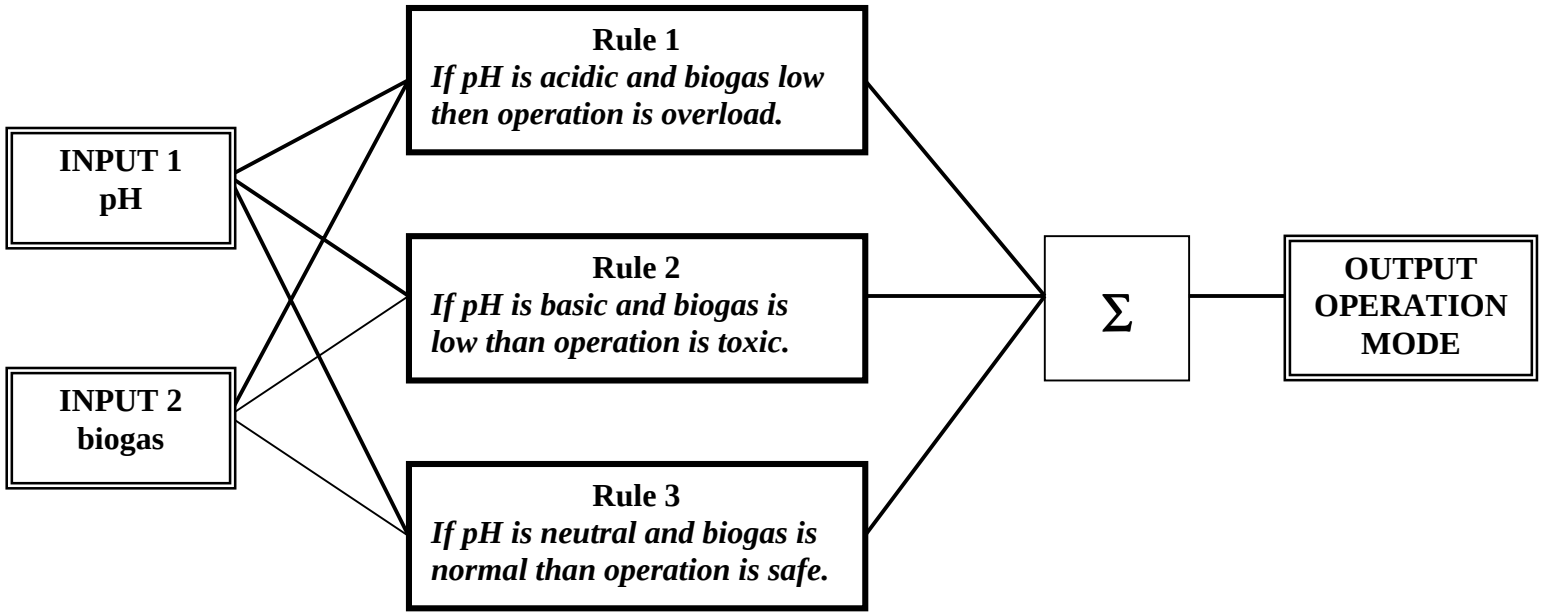

Figure 2.10 – FIS for classification of operation mode of an anaerobic treatment process based on pH and biogas production

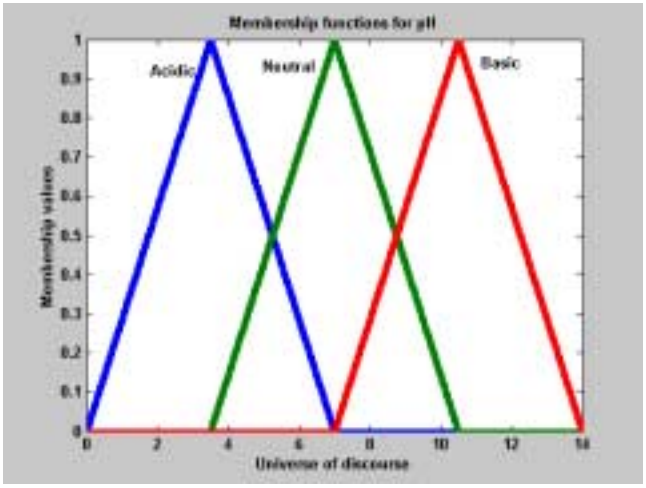

(a)

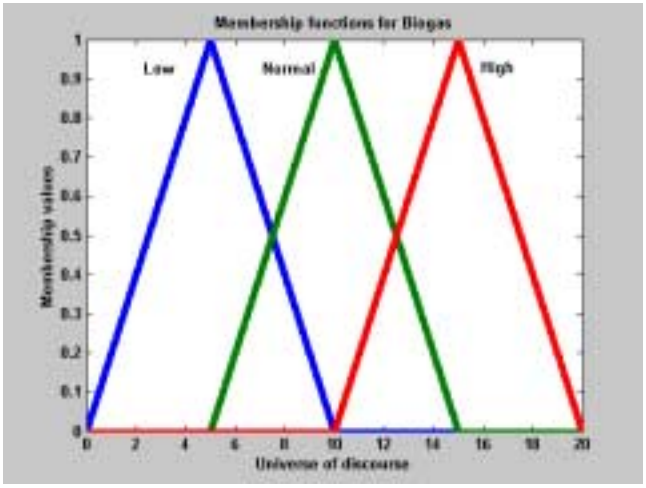

(b)

Figure 2.11 – Membership functions for the antecedents, pH (a) and biogas (b), of the fuzzy inference system

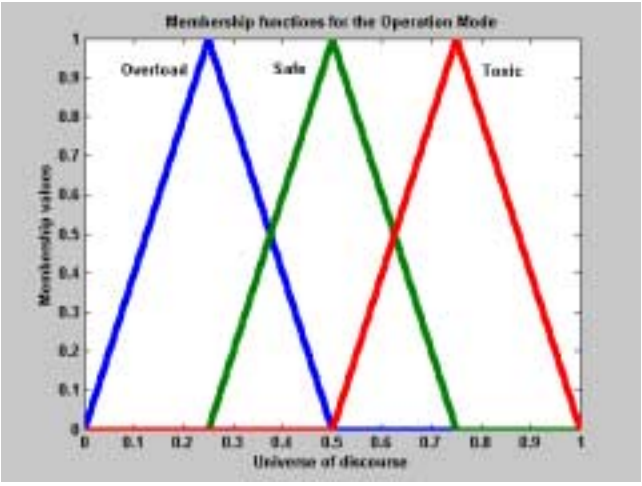

Figure 2.12 – Membership functions for the consequent, operation mode, of the fuzzy inference system

Fuzzification

Crisp inputs, which are measured values for the antecedents are:

pH = 4 and biogas = 3 mL/min.

Results for the fuzzification shows that a pH of 4 can be *acidic* with a membership value of 0.8, and *neutral* with a membership value of 0.2. The biogas flow rate of 3 mL/min is *low* with a membership value of 0.6. Figure 2.13 illustrates the fuzzified inputs, pH (a) and biogas (b).

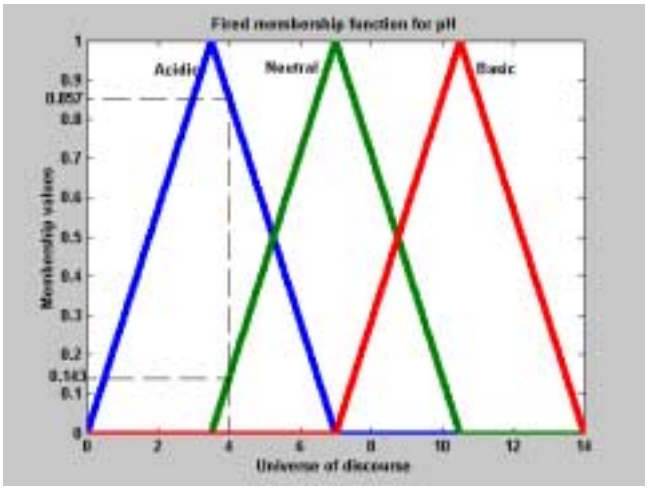

(a)

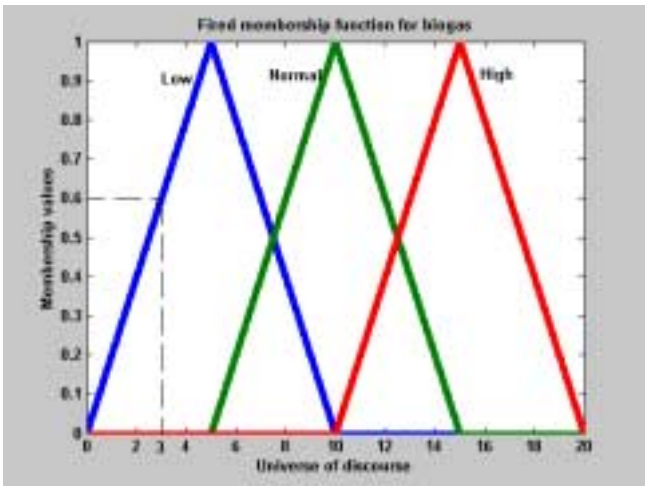

(b)

Figure 2.13 – Fuzzification of inputs pH (a) and biogas (b)

Fuzzy operation

More than one parameter is used in the RHS of the preposition (rule). Here, the connective AND (min) is used to select the DOF of each rule.

For rule 1, '*If pH is acidic and biogas low then operation is overload*', the two prepositions on the RHS were fired, with a membership value of 0.8 for pH (acidic) and 0.6 for biogas (low). Application of the AND operator results in the minimum between the membership values for acidic low, resulting a DOF of 0.6 for the rule. Figure 2.14 illustrates membership functions for the antecedents of rule 1, and membership values for each input.

Now, for rule 2 that is '*If pH is basic and biogas low then operation is toxic*', two prepositions on the RHS were fired: basic for pH, with zero membership value, and low biogas with membership value of 0.6. Applying the AND operator, zero is resulted as the DOF of the rule. Figure 2.15 illustrates membership functions for the antecedents of rule 2 with respective membership values for the inputs.

Finally, rule 3, '*If pH is neutral and biogas is normal then operation is safe*', is analyzed. Two prepositions on the RHS were fired: neutral for pH, with 0.143 for the membership value, and normal biogas with zero membership value. Applying the AND operator, the DOF for the rule is zero. Figure 2.16 illustrates membership functions for the antecedents of rule 3 with respective membership values for each input.

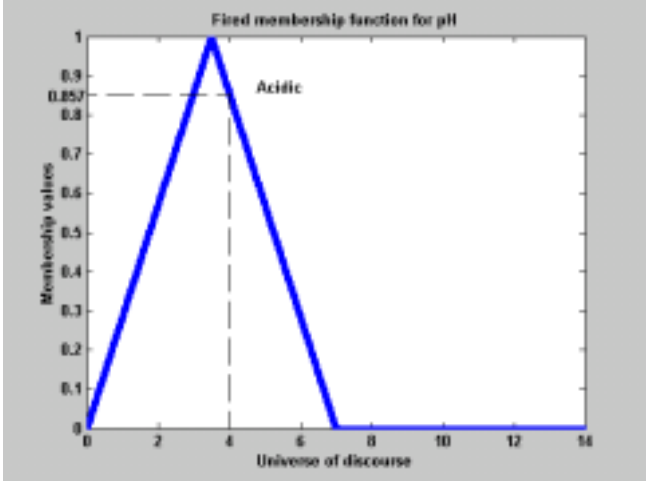

(a)

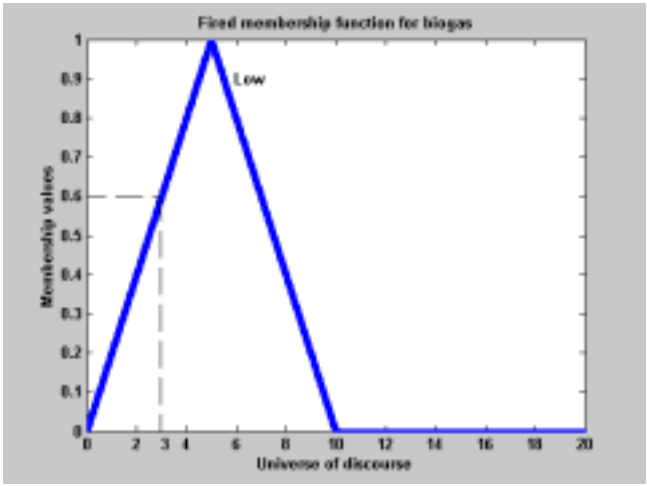

(b)

Figure 2.14 – Membership functions for acidic pH (a) and low biogas (b) for rule 1 and membership values for each input

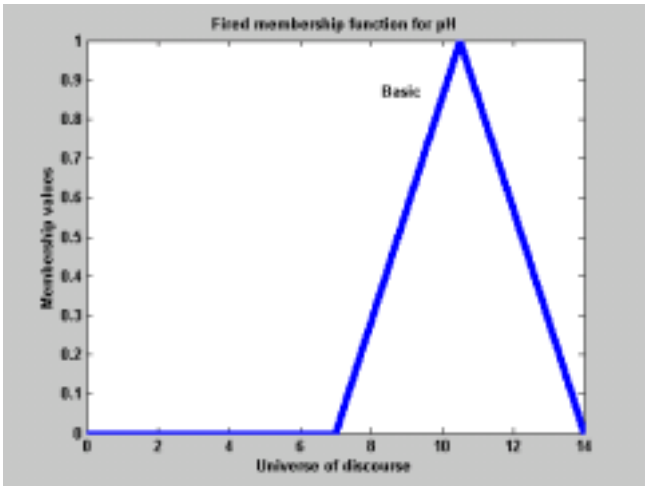

(a)

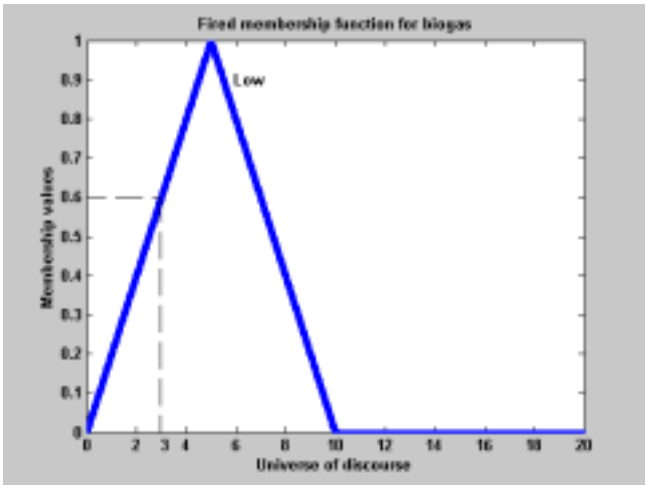

(b)

Figure 2.15 – Membership functions for basic pH (a) and low biogas (b) for rule 2 and membership values for each input

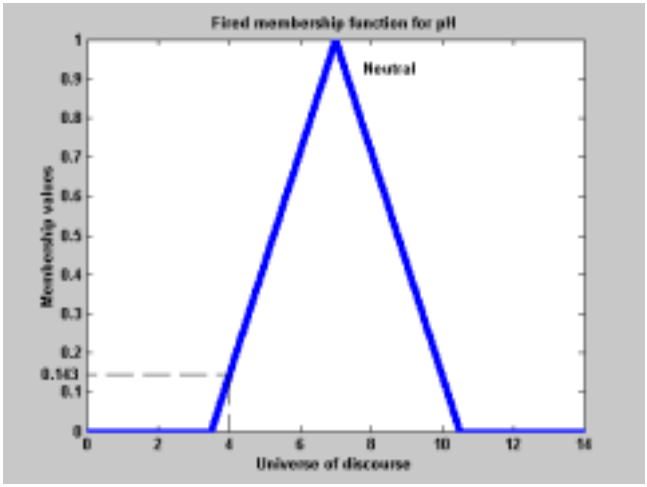

(a)

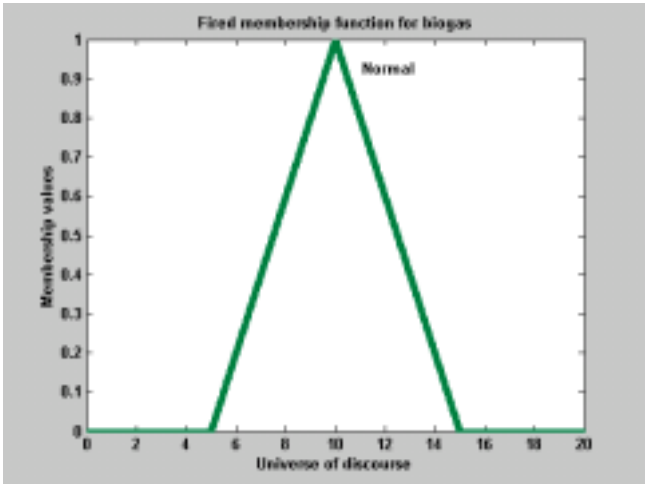

(b)

Figure 2.16 – Membership functions for neutral pH (a) and normal biogas (b) for rule 3 and membership values for inputs

Implication relation

Here, implication relation is obtained by the use of the Mamdani mim method. For each rule, the result will be the area of the consequent membership function under the DOF from last step.

For rule 1, '*If pH is acidic and biogas low then operation is overload*', the consequent states that operation is overload. Using the implication relation Mamdani mim and a DOF of 0.6, the result for this step is the area under 0.6 for the output membership function for overload, as illustrated in figure 2.17.

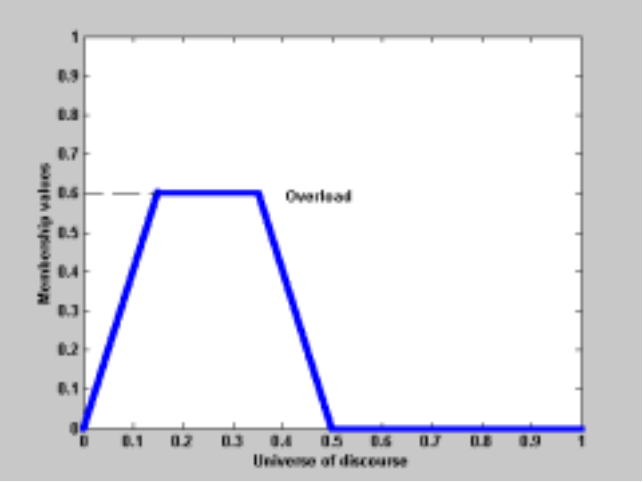

Figure 2.17 – Result of the implication relation Mamdani mim for rule 1

For rule 2, '*If pH is basic and biogas low then operation is toxic*', the consequent affirms that operation is toxic. However, fuzzy operation for rule 2 resulted in a DOF of zero. So, using Mamdani mim implication relation and zero for DOF, there is no fuzzy set to represent rule number 2.

The same occurs to rule 3, '*If pH is neutral and biogas is normal then operation is safe*', which does not have a fuzzy set to represent the output because the DOF for this rule is zero.

Aggregation

As said before, the aggregation is obtained by the application of the aggregation method to the results of the implication relation. The result is one fuzzy set that represents the output. Here, **max** is the method used to aggregate results of implication relation for rules 1, 2 and 3, which is represented in figure 2.18.

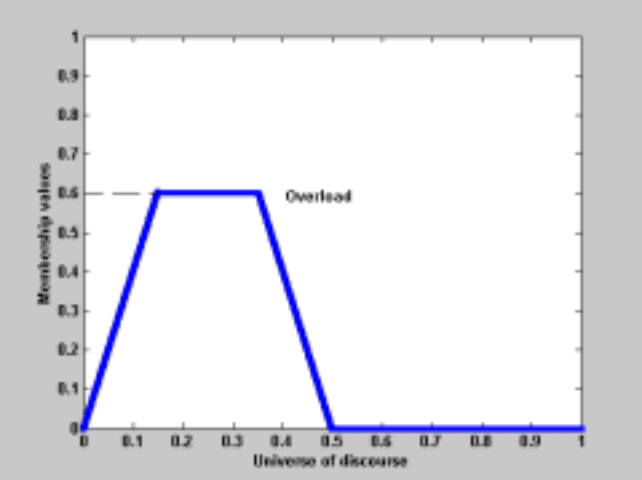

Figure 2.18 – Result of aggregation

Defuzzification

The defuzzification method used here is the centroid or center of area (COA), and is represented by the star in figure 2.19, which represents the results for this last step of the FIS for this problem. The defuzzified value is 0.25, which means that operation mode is organic overload, because it is between 0 and 0.375.

In this study, the FIS was implemented using FIS Editor from Fuzzy Logic Toolbox/MATLAB® (Jang and Gulley, 2001). The purpose was to use the parameters that were monitored during the tests with the FCLD system, biogas flow rate, pH, conductivity and turbidity, as the inputs of the FIS, and for the output of the FIS the state of operation of the anaerobic treatment, i.e.: safe operation, organic overload, or toxic loads with the classification of the toxicant. Base of rules and membership functions for the FIS were constructed using the data from experiments with the FCLD system.

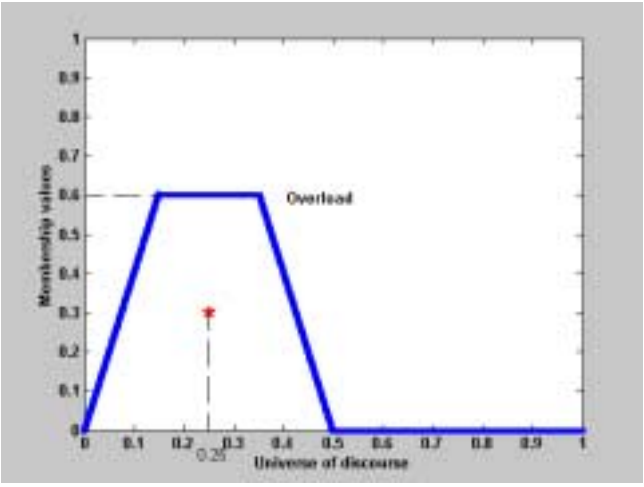

Figure 2.19 – Result from the defuzzification using centroid method

2.3.5 - Fuzzy logic applications

Fuzzy control is the most significant system based on fuzzy theory, and it is widely applied, especially in the field of engineering (Klir and Yuan, 1995). The following examples are representative of the applications for fuzzy logic:

- Fuzzy logic was used to select the best crane type to be used in a construction site (Hanna and Lotfallah, 1999).
- Ribeiro (1998) developed and implemented an irrigation control system that used climatic conditions and soil moisture as inputs for a fuzzy inference system, whose output was the operation of a solenoid valve.
- In medicine, fuzzy logic is used mainly for diagnosis of diseases (Klir and Yuan, 1995).
- Fuzzy logic is used in domestic appliances. A rice cooker uses fuzzy logic to control the cooking process; it is self-adjusting for rice and water conditions. Washing machines use fuzzy logic to select the water volume based on clothes volume, also if too much foam is detected an additional rinse cycle is used.

Fuzzy logic applications in the field of biological treatment processes will be described in section 2.5, along with other monitoring and control processes.

2.4 – Graph theory

Graph or network theory is very useful when constructing models for expert systems. Graphs are formed by nodes and links, which are represented by two sets, *X* and

L (Castillo *et al.*, 1997). In expert systems, the nodes represent prepositional variables and the links correspond to the relationship among the nodes (Castillo, 1997). Figure 2.20 illustrates one graph $G = (X, L)$ that is defined by the following sets *X* and *L*.

$$\begin{aligned} X &= \{A, B, C, D, E, F, G\} \\ L &= \{L_{AB}, L_{AC}, L_{BD}, L_{CE}, L_{DF}, L_{DG}\} \end{aligned} \qquad [2.24]$$

The next basic definitions describe concepts used in the graph theory. For more detailed information Castillo (1997) is suggested.

Directed graph: when all the links in the graph are directed links. When $L_{ij} \in L$ and $L_{ji} \notin L$, the link L_{ij} is a directed link. The order of the nodes defining a link is important here, and it is indicated by the arrow between the nodes. Figure 2.21 represents an directed graph, where

$$\begin{aligned} X &= \{A, B, C, D, E, F, G\} \\ L &= \{A \to B, B \to C, C \to E, E \to D, E \to G, D \to F, D \to G\} \end{aligned} \qquad [2.25]$$

When analyzing one link, for instance, $E \to D$, *E* is the **parent** node D, and *D* is the **children** of node *E*. The set that consists of a node and its parents is called the **family of a node**, for example, node *G* and its parents *D* and *E*.

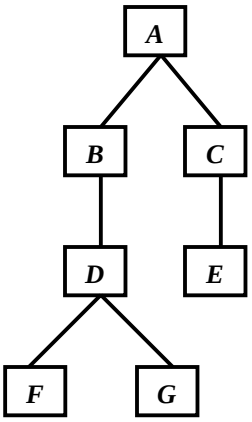

Figure 2.20 – Example of a graph

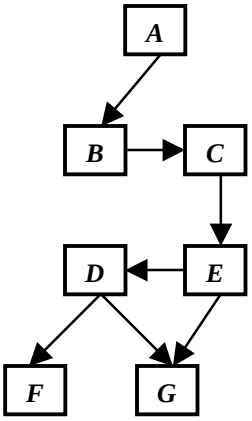

Figure 2.21 – Directed graph

Undirected graph: a graph that has only undirected links. When $L_{ij} \in L$ and $L_{ji} \in L$, the link between nodes X_i and X_j is and undirected link. The order of the nodes defining the link is not relevant in an undirected graph. Figure 2.22 represents an undirected graph, where

$$\begin{aligned} X &= \{A, B, C, D, E, F, G\} \\ L &= \{A-B, B-C, C-E, E-D, E-G, D-F, D-G\} \end{aligned} \qquad [2.26]$$

An undirected graph is a **complete graph** if all the nodes are linked to each other.

Neighbors are the nodes adjacent to a certain node; for instance, *C*, *D* and *G* are neighbors of node *E*.

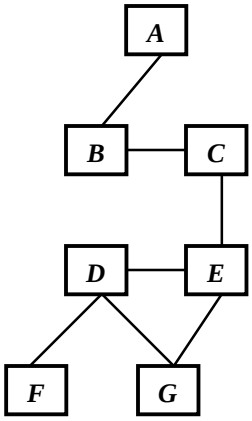

Figure 2.22 – Undirected graph

A **loop** is a closed path in an undirected graph.

An undirected graph is **connected** if there exist at least one link between every two nodes, otherwise it is **disconnected**.

A connected undirected graph is classified as a **tree** if for every pair of nodes there exist only one path. If this link is removed, there will be two disconnected trees.

A **multiply-connected graph** is an connected undirected graph that contains at least one pair of nodes that are connected by more than one link, which is the same of containing at least one loop.

Figure 2.23 shows an undirected disconnected graph (a), a tree graph (b) and a multiply-connected graph (c).

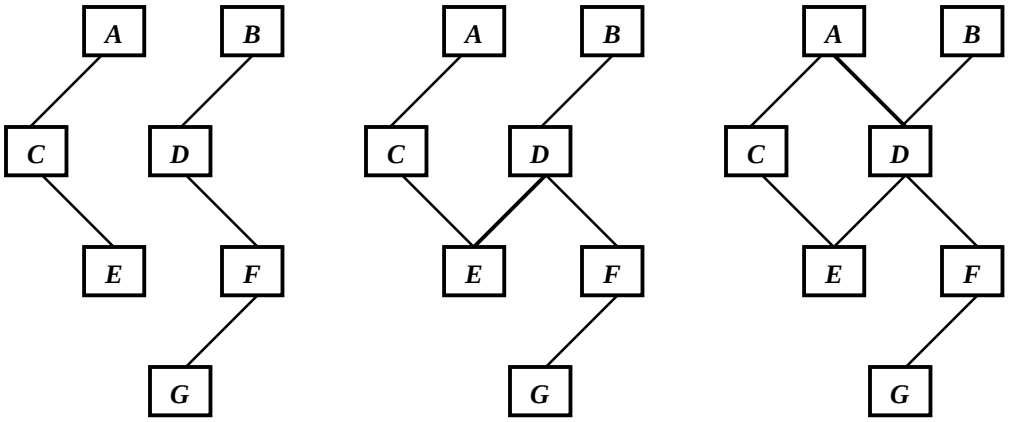

(a) (b) (c)

Figure 2.23 – undirected disconnected graph (a), tree graph (b), and multiply-connected graph (c)

When using graph theory to classify some data, the nodes represent questions and the links are the possible answers to the questions. Here, it will be used to classify the different failure modes within the FCLD system.

2.5 – Monitoring biological processes

The next sections describe how biological processes, aerobic and anaerobic, can be monitored to accomplish process stability.

2.5.1 – Respirometry

Aerobic microorganisms use oxygen as they consume the organics in the wastewater as equation 2.1 shows. Oxygen uptake rate (OUR) is the rate at which the microorganisms consume oxygen. OUR can be used to indicate biological activity: for instance, high OUR indicates high biological activity. The value of the OUR is measured using a sample of the mixed liquor, saturated with dissolved oxygen (DO). As time increases, the level of DO is measured; results are reported in terms of concentration of O_2 per volume per time (Metcalf and Eddy, 1991). The use of OUR to indicate biological activity can be called aerobic respirometry, and it is largely applied for the monitoring of activated sludge processes. Many systems, called respirometers, are available to measure OUR.

There are many examples of the use of respirometry, for instance:

- Ning *et al.* in 1999 used respirometry to identify and quantify nitrogen nutrient deficiency in activated sludge processes.

- Identification of activated sludge kinetics and wastewater characteristics using respirometric batch experiments (Brouwer *et al.*, 1998).
- Determination of the yield coefficient of aerobic activated sludge bacteria using a respirometric method (Strotmann *et al.*, 1999).

2.5.2 – Monitoring anaerobic wastewater treatment systems

With the advance of wastewater treatment technologies, the need for monitoring and controlling is a desired improvement. There are many examples of research that applied different techniques for the monitoring and even controlling to wastewater plants, anaerobic reactors, and other processes, the following examples illustrate some of the improvements that were made in the last decade:

- An automated control system was built to control a pilot scale fluidized bed reactor (2.8 m^3). Parameters monitored were gas production rate, hydrogen content in the gas phase, and pH in the liquid phase. Studies were made to avoid problems of recurrent organic overloads. Controlled variables were influent flow rate, and injections of HCl or NaOH (Moletta *et al.*, 1994).
- A biosensor called RANTOX, which is a small scale (5 L) anaerobic reactor, was used to detect organic overloads and/or toxic loads in the influent wastewater stream. Monitoring of the metabolism of the methanogenic microorganisms was indirectly made based on Monod kinetic parameters K_m (maximum substrate degradation rate) and K_s (half-saturation constant) under kinetically saturated conditions (high substrate conditions), which was

achieved by the periodical addition of acetic acid to the reactor. The biosensor was monitored by a computer that controlled the inputs (pumps and valves) and the outputs (pH and gas flow rate). Sodium acetate and acetic acid were used to induce the organic overloads, and sodium chloride and chloroform were used as toxins (Rozzi *et al.*, 1997, 1999; Pollice *et al.*, 2001).

- An anaerobic hybrid UASB- upflow anaerobic filter (UAF) bioreactor (1100-L) was monitored. Measurements were taken from the following devices to be analyzed on line, biogas flow meter, feed and recycling feed meters, thermometer, biogas analyzer, hydrogen analyzer and pH-meter. The behavior under steady state conditions and organic overload were studied (Puñal *et al.*, 1999).
- A sewage treatment plant localized in Morrinsville, New Zealand, received wastes mainly from a beef processing plant, a dairy factory, and municipal waste. During peak dairy production the admissible load increased considerably, the plant had to be upgraded and an ASBR was chosen. BOD, nitrification, and denitrification rates were estimated by a fuzzy system. In addition, ASBR control (normal operation, flow diversion, or reprocessing) was done by a fuzzy inference system. (Cohen *et al.*, 1997).
- A fuzzy control system for a pilot fluidized bed reactor system was developed by Estaben *et al.* (1997). Biogas flow rate and pH were used as input parameters, and the output parameter was influent flow rate. The control was based on a value of biogas production that ensured good COD reduction. If an

overload or other perturbation occurred, biogas production would change. Based on biogas change, the fuzzy control system would vary the feeding pump.

- Fuzzy logic was used to classify two types of problems in a fluidized bed reactor, change in influent concentration and/or feed rate, and foam inside the reactor (Steyer *et al.*, 1997 a).
- Fuzzy logic was used to control a fluidized bed reactor. Input variables were pH, temperature, and biogas flow rate. The output of control was influent flow rate. The objective was to avoid accumulation of VFA's within the reactor, keeping the process as stable as possible (Steyer *et al.*, 1997 b).
- A wastewater treatment consisting of anaerobic digestion, aerobic treatment, nitrification and denitrification, was controlled to detect dangerous loading situations. Fuzzy logic was used to classify input data (biogas flow rate and hydrogen in the off gas) into four classes: normal operation, toxic, overload or inhibition/underload (Marsili-Libelli and Muller, 1996; Muller *et al.*, 1997).
- An anaerobic/aerobic activated sludge system was controlled using fuzzy logic. The inputs were anaerobic food/microorganism (F/M) ratio and influent flow rate and the output was the recycle flow rate (Chang, *et. al*, 1996).

There are many other publications that show fuzzy logic related to anaerobic treatment processes, e.g., (Genovesi *et al.*, 1999; Tay and Zhang, 2000; Garcia *et al.*, 2000), however they will not be detailed here.

2.5.3 – First studies with the FCLD

The FCLD is a system that consists of a small-scale UASB reactor and some sensors to monitor the effluent wastewater. The FCLD was conceived by D. R. Raman and developed and tested by Ervin *et al* (1999) as a senior project at the Department of Biosystems Engineering and Environmental Science at The University of Tennessee. The FCLD is intended to work as a rapid toxicity detector, running in parallel with a full-scale UASB reactor. The short HRT (10 min) of the FCLD was intended to provide a rapid response to a toxic load in the waste stream. Since full-scale reactors typically operate at 2-8 h HRT's, a sub 1-h response time was expected to provide UASB operators with ample warning time to avoid failures in the main reactor.

The first prototype was built with PVC and plastic parts. The reactor volume was calculated based on expected biogas production, desired HRT, and maximum permissible up-flow velocity in the reactor to avoid biomass washout. Design calculations resulted in an actual volume of 6.5 L, with a working volume of 3.5 L. A PVC pipe 36 cm long with 15 cm nominal diameter was used as the reactor body. A 15 cm PVC cap was used for the bottom part of the reactor. To seal the reactor, a 15 cm flange was used at the top of the reactor. The reactor had one inlet port and three outlets ports. The inlet port was located in the bottom of the reactor. The effluent port was located in the middle side of the reactor, 17 cm above the bottom of the reactor. A port to accommodate the standpipe was located 9 cm below the effluent port. The biogas outlet port was 10 cm above the effluent port. Soft plastic tubes were used as influent, effluent wastewater and biogas lines. Figure 2.24 illustrates the UASB reactor used on the FCLD system.

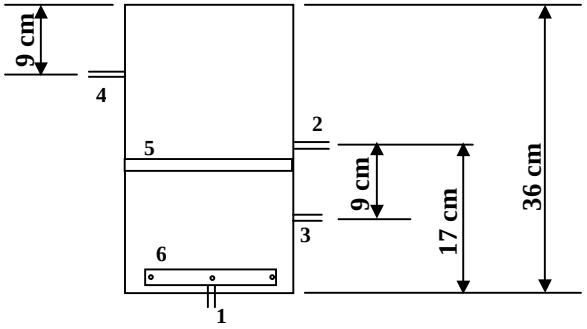

(a)

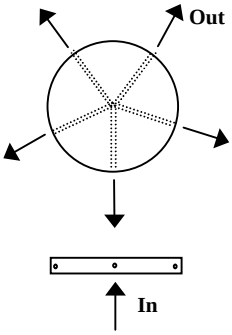

(b)

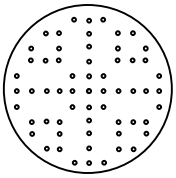

(c)

1 – influent port
2 – effluent port
3 – standpipe port
4 – biogas port
5 – influent manifold
6 – biomass biogas separator

Figure 2.24 – Diagram of the UASB reactor (a), with the influent manifold (b), and the biomass biogas separator (c)

A manifold was built to enhance the uniformity of wastewater distribution within the reactor. It consisted of a PVC disc with central inlet and 5 smaller radial outlets. As with all UASB reactors, a biogas-biomass separator was included, consisting of a disk (15 cm) with 61 holes (6 mm diameter each). It was positioned just below the effluent port. The objective of the separator was to reduce the effective cross-sectional area of the reactor, consequently increasing up-flow velocity, facilitating biogas separation from the biomass, and reducing biomass washout.

A 1 kW electrical heat exchanger was designed and built to heat influent wastewater. It consisted of a piece of copper tubing, wrapped with two 0.5 kW heating ropes. It was controlled by a microprocessor (PIC 16C57) in order to keep influent wastewater at a constant temperature.

A solenoid diaphragm-metering pump was selected (PULSAtron electronic metering pump, series E PLUS, PULSAFEEDER®, Punta Gorda, FL) for wastewater delivery to the FCLD. At each pulse, a constant wastewater volume was delivered to the reactor, thereby, maintaining a constant HRT. This pump had the ability to handle particulate-filled fluids, which was an important factor in the selection process because of the nature of the wastewater. The pulsed flow improved mixing within the reactor, and helped avoid clogging of the influent system.

Biogas flow rate was the variable used to monitor the failures of the FCLD system. A tipping bucket biogas flow meter (Beal, 1998) was used to monitor biogas flow rate. Its operation is similar to a tipping bucket rain gauge. It was made of clear acrylic, and consisted of a pivoting container divided into two equal size chambers with a port

that delivered biogas under the pivoting point. The tipping bucket was placed inside an acrylic box filled with water. When biogas released into one chamber reached 30 mL, the buoyancy of the gas would make the tipping bucket tip, thus releasing the biogas. The other side would then fill with biogas, and so on. Each tip was monitored with the use of a magnetic reed switch and by the microprocessor (PIC 16C57). Figure 2.25 shows the layout for the first prototype for the FCLD system.

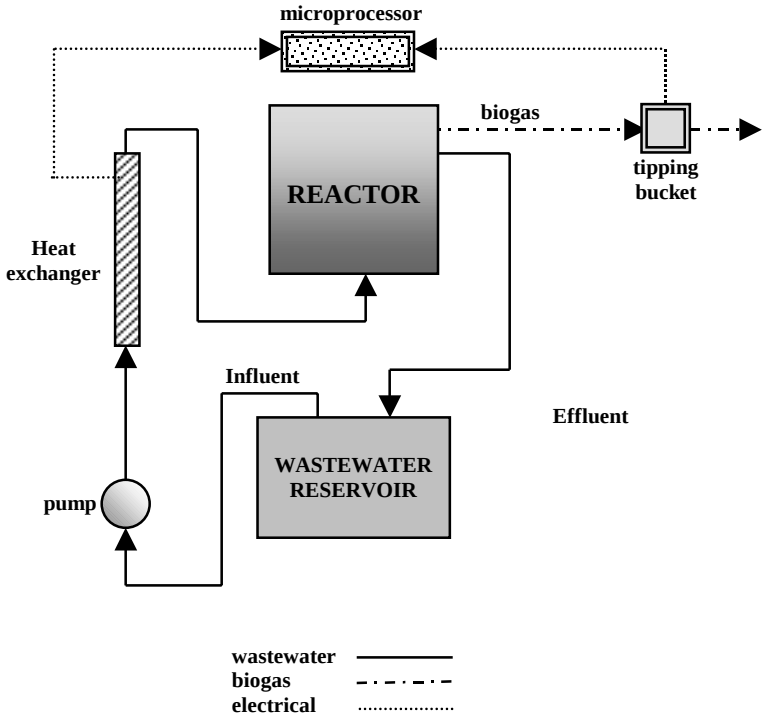

Figure 2.25 – Process flow diagram for the first prototype of the FCLD system

Ervin *et al.* (1999) used a standard testing protocol to do a series of laboratory tests. A 12-L carboy was used as wastewater reservoir. The wastewater used for the experiments was procured from a confectionary plant and the biomass from a brewery. Testing started by first acclimating the biomass to the confectionary wastewater that was diluted to approximately 10 g/L of COD. Sodium bicarbonate was added to the wastewater to achieve the desired alkalinity. The influent wastewater was pumped from the reservoir into the reactor. The effluent wastewater was then returned to the carboy; therefore the reactor was run undergoing recirculation.

Once the FCLD system was ready, with wastewater prepared and the reactor filled with fresh biomass, the process was initialized. When the system reached steady state, the failure-causing load was added to the influent wastewater. Ervin *et al.* (1999) used two types of failure mode separately to analyze the system: organic overload and sodium exposure with testing replicated three times. For the organic overload test COD concentration was increased from 10 g/L to 60 g/L. A high concentration of Na^+ is toxic to an unacclimated biomass (Speece, 1996). Significant cation toxicity is seen when Na^+ concentration exceeds 5 g/L (Speece, 1996). In the case of Na^+ load, a concentration of 20 g/L was tested. Results from the organic overload test showed that average biogas production approximately doubled in 25 min. Also, when Na^+ failure mode was performed, the average biogas production decreased by approximately 79% after approximately 34 min.

From their testing Ervin *et al* (1999) demonstrated that the FCLD system can easily and rapidly detect certain faults in the influent wastewater. Therefore, the FCLD

system was chosen to be used for another set of experiments with the addition of a pH sensor and further use of fuzzy logic for classification of failure modes within the anaerobic wastewater treatment process. The next chapter explains experiments and classification processes for the next phase of studies with the FCLD system.

CHAPTER 3

MATERIAL AND METHODS

3.1 – First stage of the FCLD project

Preliminary studies by Ervin *et al.* (1999) indicated that the FCLD system could be very useful in the monitoring of influent wastewater when using high rate anaerobic treatment. Therefore, improvements to the FCLD system were proposed, as explained in the following sections.

3.1.1 – System configuration

Initially, the FCLD was operated similar to Ervin *et al.* (1999). However, it was decided to monitor pH in the effluent line in addition to biogas. It is universally accepted that pH is a very powerful tool in the monitoring of anaerobic processes because of its relationship to the accumulation of volatile fatty acids in the reactor. To monitor pH, an electrode (ORION low maintenance triode model 9107, Boston, MA), and a meter (ORION model 290A, Boston, MA) were used. This meter has the ability to communicate with a personal computer via a RS232 port. A program written in Quick Basic was developed to monitor pH online every minute.

The tipping bucket used in the first study was improved to better measure the small flows of biogas produced by the reactor. A new, smaller, tipping bucket was fabricated of clear acrylic. The new tipping bucket was calibrated; each chamber could

hold 2.8 mL of biogas. The number of tips per minute was monitored using a micrologger (21X datalogger, Campbell Scientific-Inc, Logan, UT).

The recirculation mode was eliminated because in a real situation the wastewater will not be recycled. Recirculation was causing accumulation of byproducts of the degradation of the confectionary wastewater into the carboy, as well a decrease in COD concentration. Therefore, a larger, 100-L container for storage of influent wastewater was employed. Effluent wastewater was discharged to a drain.

Ervin *et al.* (1999) controlled temperature using a microprocessor (PIC 16C57). In this study temperature was initially controlled by the same micrologger that monitored the tipping bucket. However, temperature measured at the inlet port fluctuated excessively ($35 \pm 10^{o}C$) when using only the 21X to control the heat exchanger. The micrologger was therefore replaced by a proportional-integral-derivative (PID) controller (ETR-9090, OGDEN, Arlington Heights, IL), capable of much tighter control ($\pm 1^{o}C$ at steady state). Figure 3.1 shows a photo of the FCLD system used during this stage of the research, while figure 3.2 shows its material flow diagram.

3.1.2 – Failure tests

Concentrated sugary wastewater for the experiments was collected from the same regional confectionary plant. It was stored in 25-L containers and kept in a refrigerator at $4^{o}C$ to prevent natural degradation. The wastewater had a COD concentration of approximately 200 g/L. Biomass was procured from a regional brewery that uses a full-

Figure 3.1 – Photo of the FCLD system used during the first stage of the FCLD system project

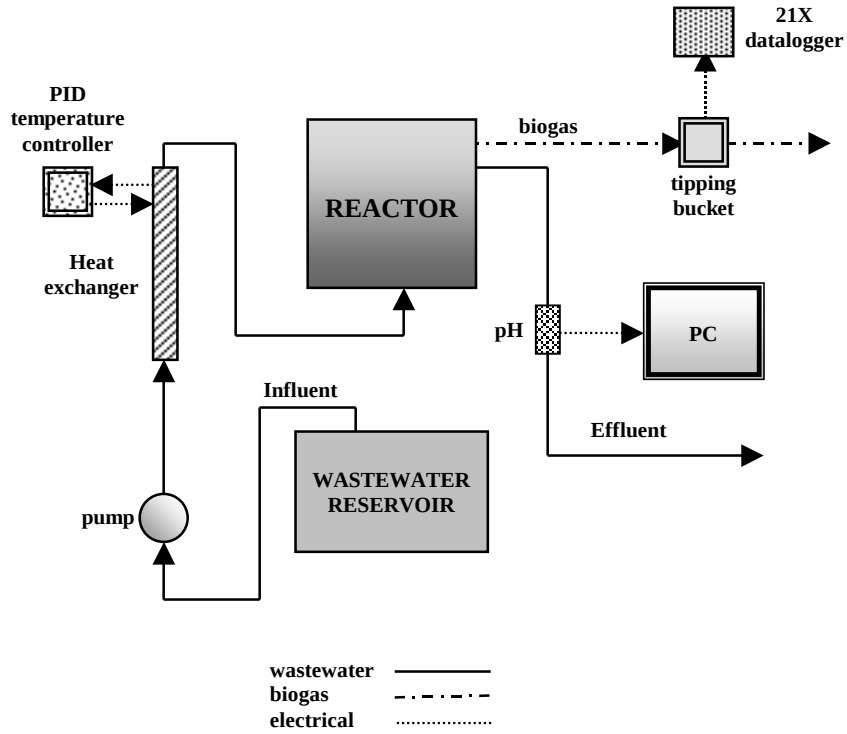

Figure 3.2 – Process flow diagram of the first stage of the FCLD system project

scale UASB reactor to treat its wastewater. Biomass consisted of black granules of approximately 1 mm in diameter. Biomass consisted of black granules of approximately 1 mm in diameter.

Tests runs of the FCLD were initialized in the same manner. First, confectionary wastewater was diluted to a COD concentration of approximately 10 g/L and enhanced with phosphorus (50 mg/L), nitrogen (200 mg/L) and sodium bicarbonate (1000 mg/L) in a 100-L container. For each test run, approximately 1.3 L of biomass was utilized. Once the reactor was loaded with fresh biomass, wastewater was mixed, and sensors were calibrated, the FCLD system could be initialized. Each test lasted approximately 4 h, the first 3 h was used to monitor the pH and biogas under steady state conditions. After 3 h, the failure-causing load was added to the wastewater container and the run finished 1 h later. There were two types of failure mode tests for this stage of the research, COD organic overload at 50 g/L and sodium toxic load at 20 g Na^+/L. After each test, data were processed using Microsoft® Excel. Biogas and pH data were averaged over 5 min intervals to reduce data fluctuation over time. Results from experiments are presented in chapter 4.

3.2 – Second stage of the FCLD project

The experience obtained during the first stage generated the desire to improve the FCLD system by testing more failure-causing modes and adding more sensors to monitor other physicochemical quantities. The next sections shows how these improvements were made and how experiments for this stage were performed.

3.2.1 – System configuration

Some of the failure modes used for the second stage testing could foam during experiments, resulting in the clogging of the biogas port that was very close to the wastewater level. Therefore, a taller version of the first reactor was constructed (54 cm vs. 36 cm). This modification allowed the gas output to be placed 6.5 cm higher than in the first reactor.

Studies from first stage of the FCLD project suggested that biogas and pH were effective monitoring parameters (Pinto *et al.,* 2000). However, a search for more parameters was made, and two more parameters were chosen: turbidity and conductivity.

When light passes through a liquid sample, it is scattered and absorbed by the particles present in the sample. Turbidity measures the relative amount of suspended particles in liquids, or how clear the sample is (OMEGA, 2001). When studying the influence of microbial activity under aerobic and anaerobic conditions to check the strength of activated sludge flocs, defloculation was noticed under anaerobic conditions and turbidity increased with the defloculation (Wilen, 2000). Increase in turbidity of reactor effluent can be due to loss of microorganisms, which decreases the efficiency of the treatment. Another motive to choose turbidity as a measurement parameter is the fact that some wastewaters, like the confectionary wastewater used for this research, have darker coloration when the COD concentration is higher. Finally, turbidity appears to be a good candidate for continuous, on-line monitoring, because of the simplicity of the turbidity sensors.

Conductivity is the ability of an aqueous solution to conduct an electric current. It depends on the concentration and type of ions in the solution. Habets and Knelissen (1998) measured conductivity along with other parameters to check the performance of an aerobic/anaerobic treatment system. Since some potential toxicants are ions, the use of a sensor to monitor conductivity appears to be very promising.

A search for a sensor to monitor turbidity located an online infrared sensor used in dishwashers and washing machines to monitor the performance of the rinsing cycle (APMS-10GRCF-KIT, Honeywell Inc, Freeport, IL). This sensor could also measure conductivity, so it was chosen to monitor turbidity and conductivity in the effluent wastewater. An RS232 port provided communication between sensor and PC. Consequently, the Quick Basic program that monitored the pH meter during first stage was enhanced by the addition of code to monitor the online infrared sensor.

The same biogas flow-meter was chosen to be used during this stage because of its good performance during the first stage of the FCLD system study. However, the 21X micrologger was replaced by a CR23X micrologger (Campbell Scientific Inc, Logan, UT) due to malfunctions with the older device. Figure 3.3 shows a photo of the new system, and figure 3.4 shows the process flow diagram for this setup.

3.2.2 – Failure tests

The first step on each experiment with the FCLD system was the preparation of the influent wastewater. Concentrated confectionary wastewater was diluted to a COD concentration of approximately 5 g/L. Also, it was enhanced with phosphorus (25 mg/L),

Figure 3.3 – Photo of the second stage of the FCLD system project

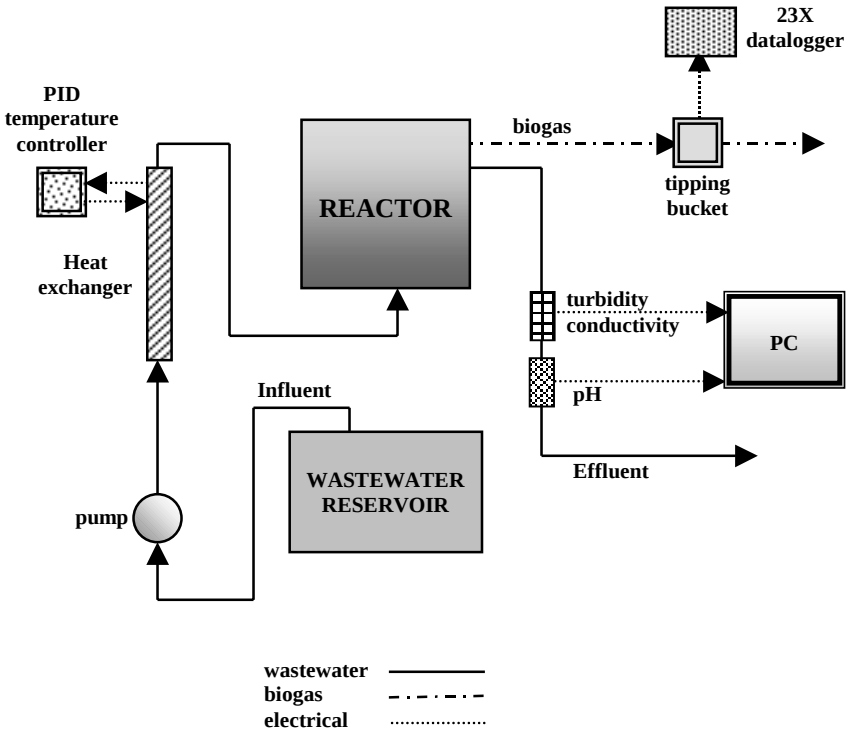

Figure 3.4– Process flow diagram of the second stage of the FCLD system project

nitrogen (100 mg/L) and sodium bicarbonate (1500 mg/L). Each failure test consumed 100 L of wastewater and lasted for approximately 4 h. Like in the first stage of the FCLD project, the first 3 h was used to monitor the parameters under steady state conditions. After these 3 h, approximately 30 L of wastewater remained in the container; at this time the failure-causing load was added to the wastewater container, and the experiment would finish 1 h later. Data processing was undertaken using Microsoft® Excel, and the monitored parameters were averaged into a 5 min interval to compromise between loss of temporal resolution and reduction in variability of signal.

Additional failure-causing modes were selected and added to the second stage of the FCLD project. These are listed as follows:

- **Organic overload at two COD concentrations, 20 and 40 g/L**. Increasing COD concentration from 5 g/L to 20 and 40 g/L would increase the influent COD concentration 400% and 800%, respectively. An organic overload may cause the pH to drop below 6.2 – 6.6 (Speece, 1996) and cause the failure of the process.
- **Na^+ at three different concentrations, 5, 10, and 20 g/L.** High Na^+ concentrations are toxic to the anaerobic biomass when they are not acclimated to it (Speece, 1996);
- **NaOH** to bring the pH from normal to a higher value. More than 8.2 can be harmful to the microorganisms (Speece, 1996). NaOH was added at 1 g/L to bring the pH to a much higher value (around 10);

- **HCl** to bring the pH from normal to a lower value. If pH goes below 6.5 (Speece, 1996), the microorganisms will be affected. So, 1.7 mL of HCl was added to 30 L of wastewater to lower the pH to a extreme value (around 5);
- **Milk fat** was simulated by adding 16 mL of heavy whipping cream per liter of wastewater. Milk fat can inhibit methanogenesis (Speece, 1996);
- **Sodium hypochlorite (NaOCl) that is the common household bleach** was used to simulate a chemical spill. Bleach concentrations used were 1% (10 mL/L) and 5% (5 mL/L) in volume.

Tests runs conducted for the second stage of the FCLD system project are summarized in table 3.1. Each type of test was replicated 3 times.

3.3 – Classification of failure modes

Data gathered during experiments with the FCLD system during first and second stages were used for classifying failure-causing modes. The following sections describe the fuzzy inference system (FIS) for first stage, biogas analysis for the second stage, and two classification methods, one using graph theory and other using an FIS, for the second stage.

Table 3.1 – Toxicants and concentrations used in the second stage of the FCLD system project

TOXICANT	*CONCENTRATION*
Organic overload (OO)	**20 g/l**
	40 g/l
Sodium (Na^+)	**5 g/l**
	10 g/l
	20 g/l
Sodium hydroxide (NaOH)	**1 g/l - to bring the pH to 10**
Hydrochloric acid (HCl)	**1.7 ml/l - to bring the pH to 5**
Heavy whipping cream - Milk	**16 ml/l**
Sodium hypochlorite (NaOCl)	**10 ml/1 - 1% in volume**
Bleach	**50 ml/l - 5% in volume**

3.3.1 – Fuzzy inference system (first stage)

After each experiment with the FCLD system was completed, data were processed using Microsoft® Excel. Biogas flow rate and pH data were averaged into a 5 min interval to reduce noise. These data sets were used to classify the type of failure mode (organic overload or sodium failure mode) into the FCLD system using an FIS using MATLAB®/Fuzzy Logic Toolbox/Simulink from MathWorks, Inc, Natick, MA.

Figure 3.5 illustrates the Simulink model that was used to run data from experiments with the FCLD system. The FIS block is a fuzzy logic controller block that is built in Simulink and implements an FIS. This block calls the FIS that was made using MATLAB®/Fuzzy Logic Toolbox using graphical user interface (GUI) tools, such as FIS Editor, Membership Functions Editor, and Rule Editor. This particular FIS has three inputs: biogas, pH, and change in pH. Each input has seven triangular membership functions: negative big (NB), negative medium (NM), negative small (NS), zero (ZE), positive small (PS), positive medium (PM), and positive big (PB). The universe of discourse for each input was scaled to be between -1 and 1. Figure 3.6 characterizes membership functions for inputs. Rules for the FIS were constructed using the Rule Editor. There are 3 inputs for the FIS, consequently a fuzzy operator is used to connect the inputs. Here, the fuzzy operator AND is used to connect the three inputs.

Mamdani min implication operator was used on the FIS. Aggregation was obtained using max operation. Finally, defuzzification was made using the centroid method. The output of the FIS was the classification of the failure mode. The output has three membership functions, sodium failure, normal operation, and organic overload. Figure 3.7 shows the output membership functions.

3.3.2 – Biogas analysis

Biogas production is a very important parameter when monitoring high rate anaerobic processes because of its intrinsic correlation to the performance of the

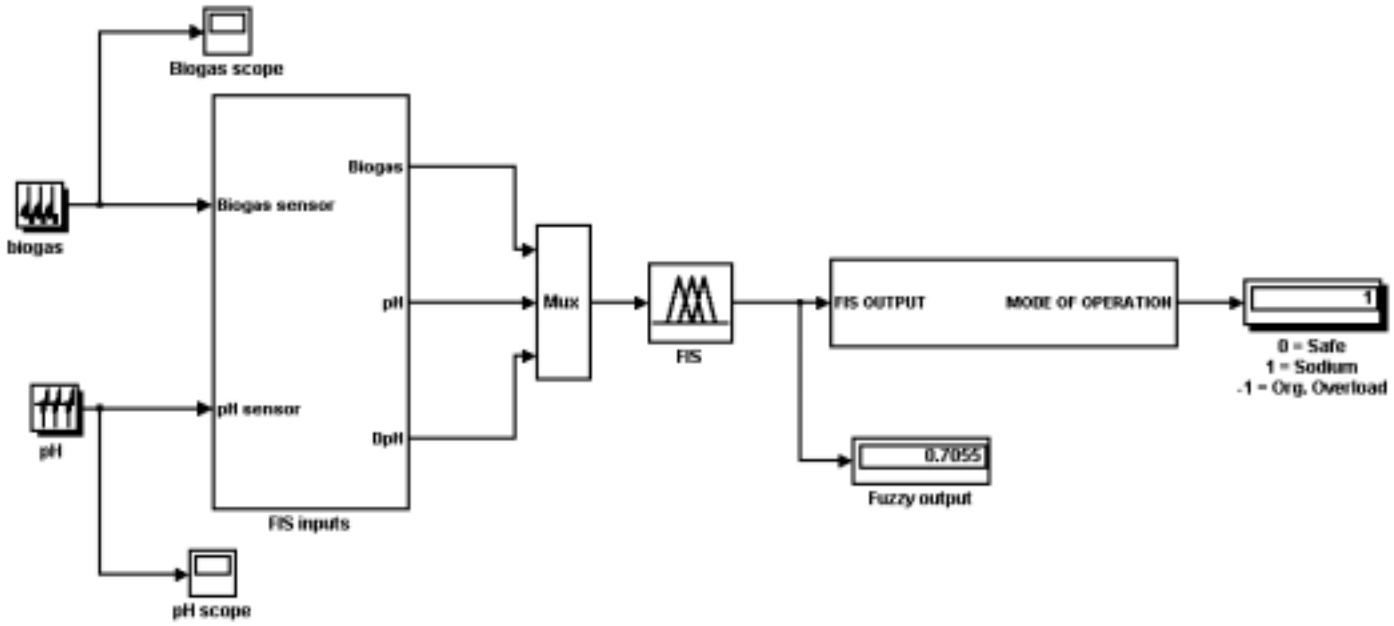

Figure 3.5 – Simulink model for fuzzy classification of failure mode for the first stage of the FCLD system

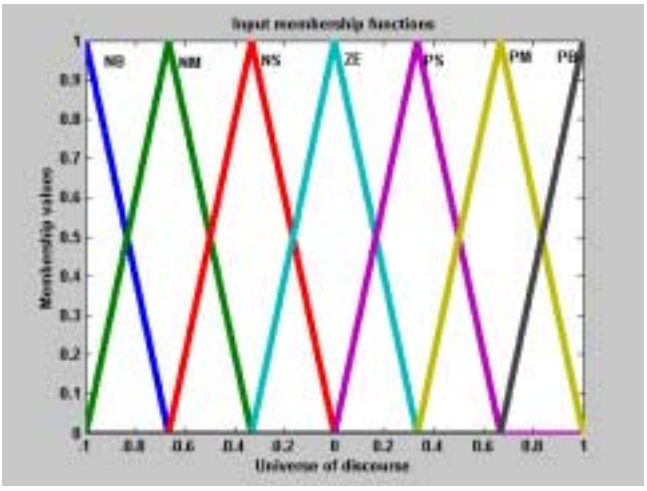

Figure 3.6 – Input membership functions for first stage of FCLD project

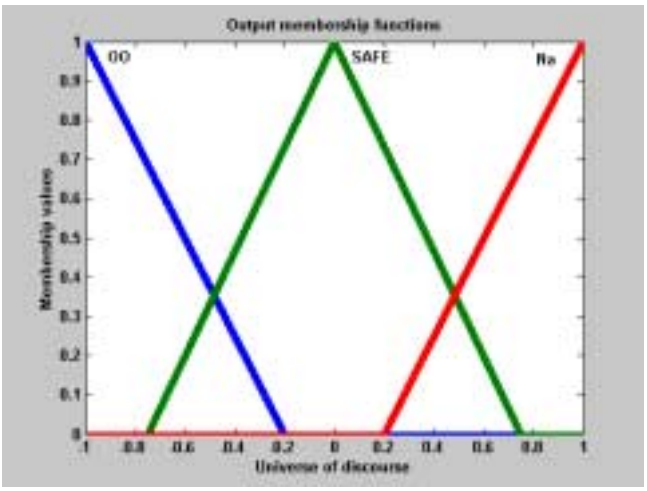

Figure 3.7 – Output membership functions for first stage of FCLD project.

anaerobic digester. If the metabolism of the methanogenic bacteria is affected somehow, they will not participate appropriately in the process of anaerobic digestion (Figure 2.1) thus biogas production can decrease. So, a separate analysis was used to understand how biogas flow rate changed during failure experiments for the second stage of the FCLD system. First, biogas flow rate data were processed using Microsoft® Excel. Data were averaged into a 5 min interval and plotted to visualize how each parameter responded for the different experiments that were performed with the FCLD system. The averaged data were analyzed using MATLAB® to check how biogas production behaved after addition of a failure mode (Table 3.1). This analysis was made comparing biogas production under faulty conditions to a range of values that defined the biogas under normal operation conditions. This interval was selected based on the mean value of biogas flow rate under normal operation for all the tests. Three biogas flow rate ranges were analyzed: mean ± 1 standard deviation, mean ± 2 standard deviations, and mean ± 3 standard deviations.

3.3.3 – Graph theory based classifier

Conductivity, turbidity, and pH data were first analyzed using Microsoft® Excel. Data were averaged into a 5 min interval to reduce variability and plotted to visualize how each parameter responded for the different experiments that were performed with the FCLD system.

A multiply-connected graph was built using pH, conductivity and turbidity data that were collected during failure mode experiments within the FCLD system. Based on

the multiply-connected graph, a MATLAB®/Simulink model was built, and a MATLAB® script was written to run this model. The script prompts the user for a filename, runs the Simulink model, and shows the result on the screen. These efforts are presented in the next chapter.

3.3.4 – Fuzzy inference system classifier

An FIS was implemented using MATLAB®/Fuzzy Logic Toolbox/Simulink from MathWorks, Inc. The three monitored parameters used as inputs for the FIS were, turbidity, pH and conductivity. The FIS was built to classify the 9 failure modes, and is shown in figure 3.8.

The FIS block calls the FIS that was generated using MATLAB®/Fuzzy Logic Toolbox using the graphical user interface (GUI) tools: FIS Editor, Membership Functions Editor, and Rule Editor. Membership functions for each input were selected based on the same intervals that were used for the classification using graph theory. Universe of discourse for inputs was scaled between 0 and 1. Figure 3.9 characterizes membership functions for turbidity, figure 3.10 illustrates membership functions for pH, while figure 3.11 shows membership functions for conductivity.

Rules for the FIS were constructed using the Rule Editor and they were based on the behavior of the monitoring parameters under each failure mode. Since there are 3 inputs for the FIS, a fuzzy operator was used to connect the inputs. Here, the fuzzy operator AND is used to connect the three inputs.

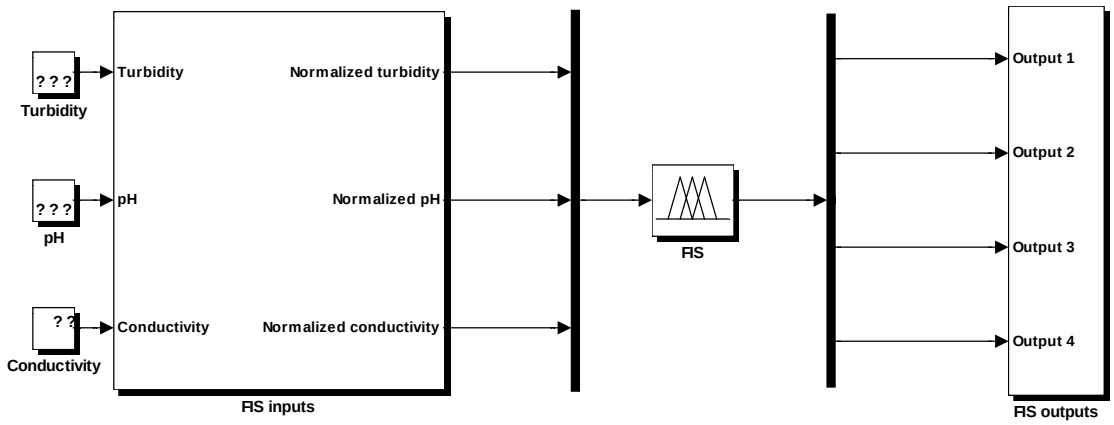

Figure 3.8 – Simulink model for fuzzy classification of failure mode for the second stage of the FCLD system.

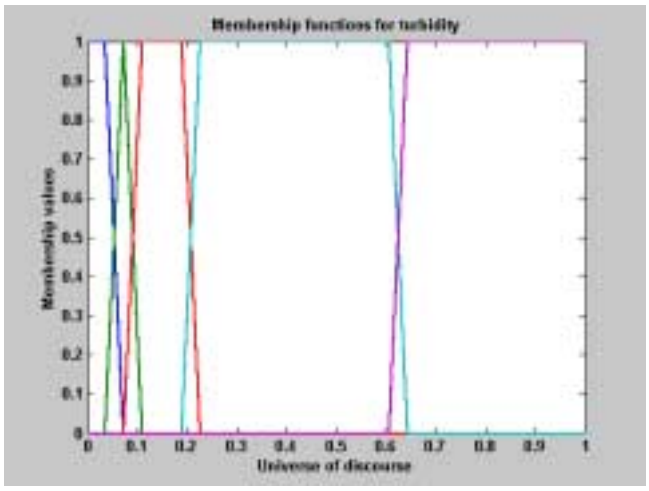

Figure 3.9 – Membership functions for turbidity

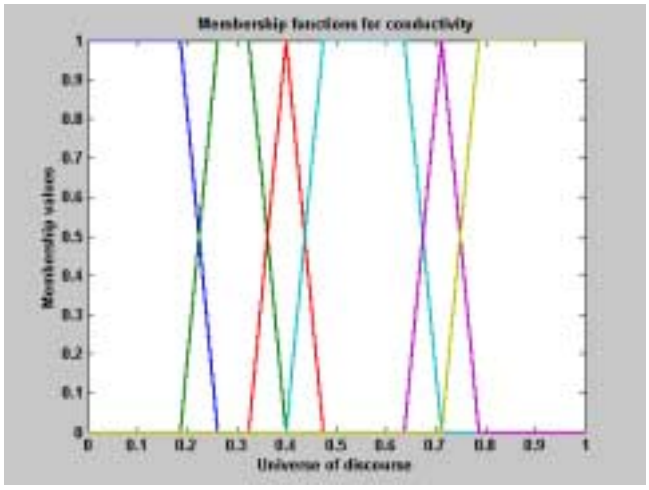

Figure 3.10 – Membership functions for conductivity

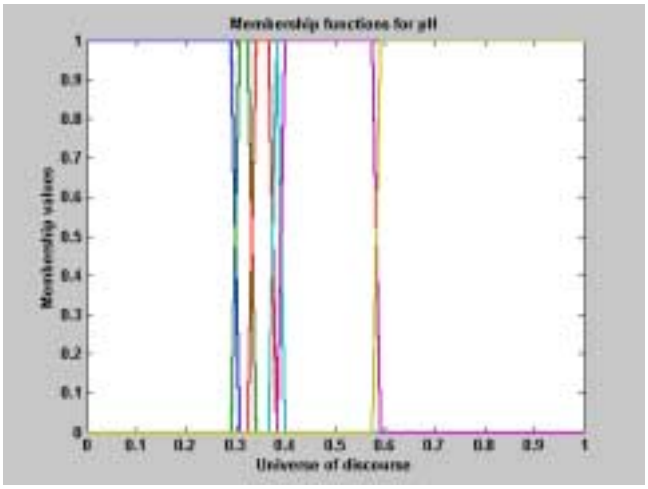

Figure 3.11 – Membership functions for pH

Mamdani min implication operator was used on the FIS. Aggregation was obtained using max operation. Finally, defuzzification was made using the centroid method.

The FIS has 4 outputs. Layout for the outputs was selected based on similarity among monitoring parameters for failure mode tests. Output 1 has membership functions for non-classification, organic overloads at 20 g/L and 40 g/L, and milk spill. Output 2 represents output membership functions for non-classification, HCl, and NaOH spills. Non-classification and Na^+ at 20 g/L are represented by output 3. Finally, output 4 represents membership functions for non-classification; bleach at 1 % and 5 %, and Na^+ at 10 g/L. Figures 3.12, 3.13, 3.14, and 3.15 illustrates outputs 1, 2, 3, and 4, respectively. Results for this FIS were obtained running the Simulink model for the second stage of the FCLD project.

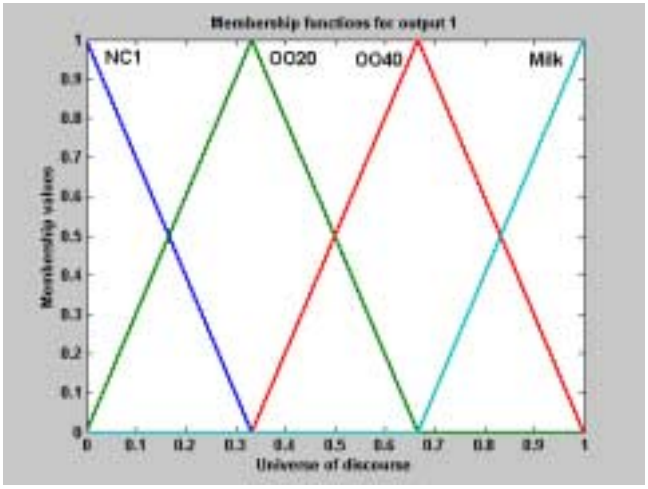

3.12 – Membership functions for output 1

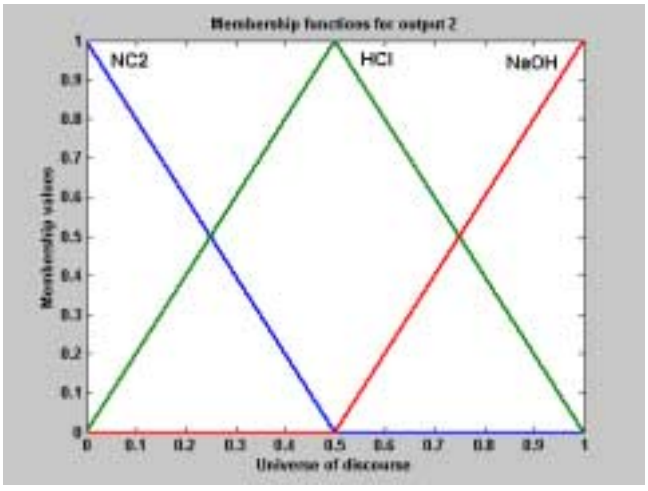

Figure 3.13 – Membership functions for output 2

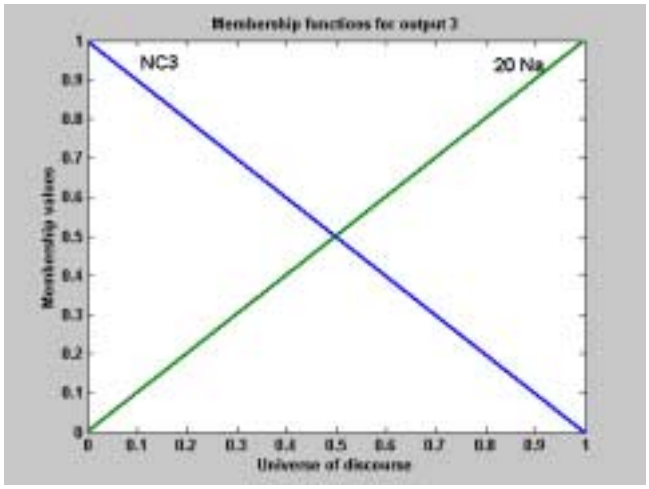

Figure 3.14 – Membership functions for output 3

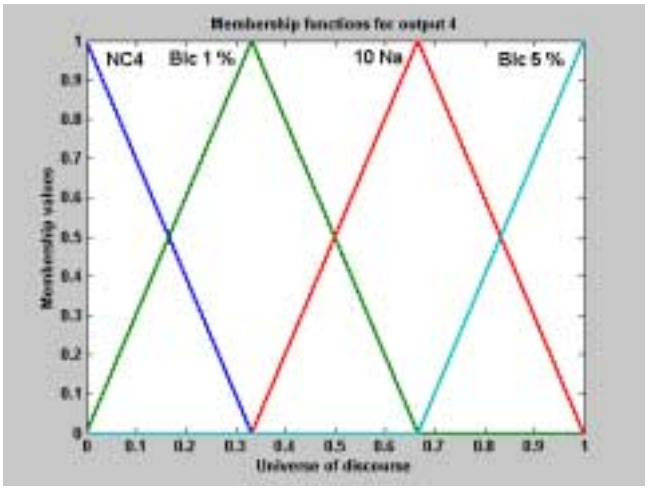

Figure 3.15 – Membership functions for output 4

CHAPTER 4

RESULTS AND DISCUSSIONS

4.1 – First stage

Results from experiments with the FCLD system during the first stage of the research are shown in the next section and they represent biogas flow rate and pH measurements for two types of failure modes: COD organic overload at 50 g/L and sodium toxicity using 20 g/L of Na^+. These results are also presented in Pinto *et al.* (2000).

4.1.1 – Toxic load experiments

As explained in section 3.1.2, each test lasted 4 h, however, for clarity, only the last two hours of data are shown on the following figures. Thus, the first 60 min on each graph represents steady state conditions from 2 h to 3 h for each variable. At t = 60 min, the failure-causing load was added. The response of each variable to the failure-causing load is shown from t = 60 to 120 min.

For the organic overload test, influent COD concentration was increased from 10 g/L to 50 g/L (OO 50). After 15 min, average biogas production increased by a factor 3×. Organic overload caused a noticeable pH drop after 10 min. For a 20 g/L Na^+ concentration (20 Na), biogas production ceased after 35 min, and pH had a mild

response (Pinto *et al.*, 2000). Figure 4.1 shows biogas flow rate for one OO 50 test and for one 20 Na test. Figure 4.2 shows pH response for the same tests.

4.1.2 – Fuzzy inference system responses

When simulating Na^+ failure mode tests, the FIS Simulink model detected the failure 20 min after the addition of NaCl to the influent wastewater stream, which is represented by the red vertical line in figure 4.3. In figure 4.3, zero values represent normal operation while 1 represents a failure mode due to Na^+ toxicity. When running data from organic overload tests, similar results were observed: failure mode was detected 15 min after the introduction of high COD solution. Figure 4.4 illustrates the FIS output that goes from normal operation (0) to a value of –1 (organic overload) at 75 min, 15 min after the application of the overload.

4.2 – Second stage

The next 2 sections show results from the experiments that were done with the FCLD system for the second stage, which used the failure modes summarized in table 3.1.

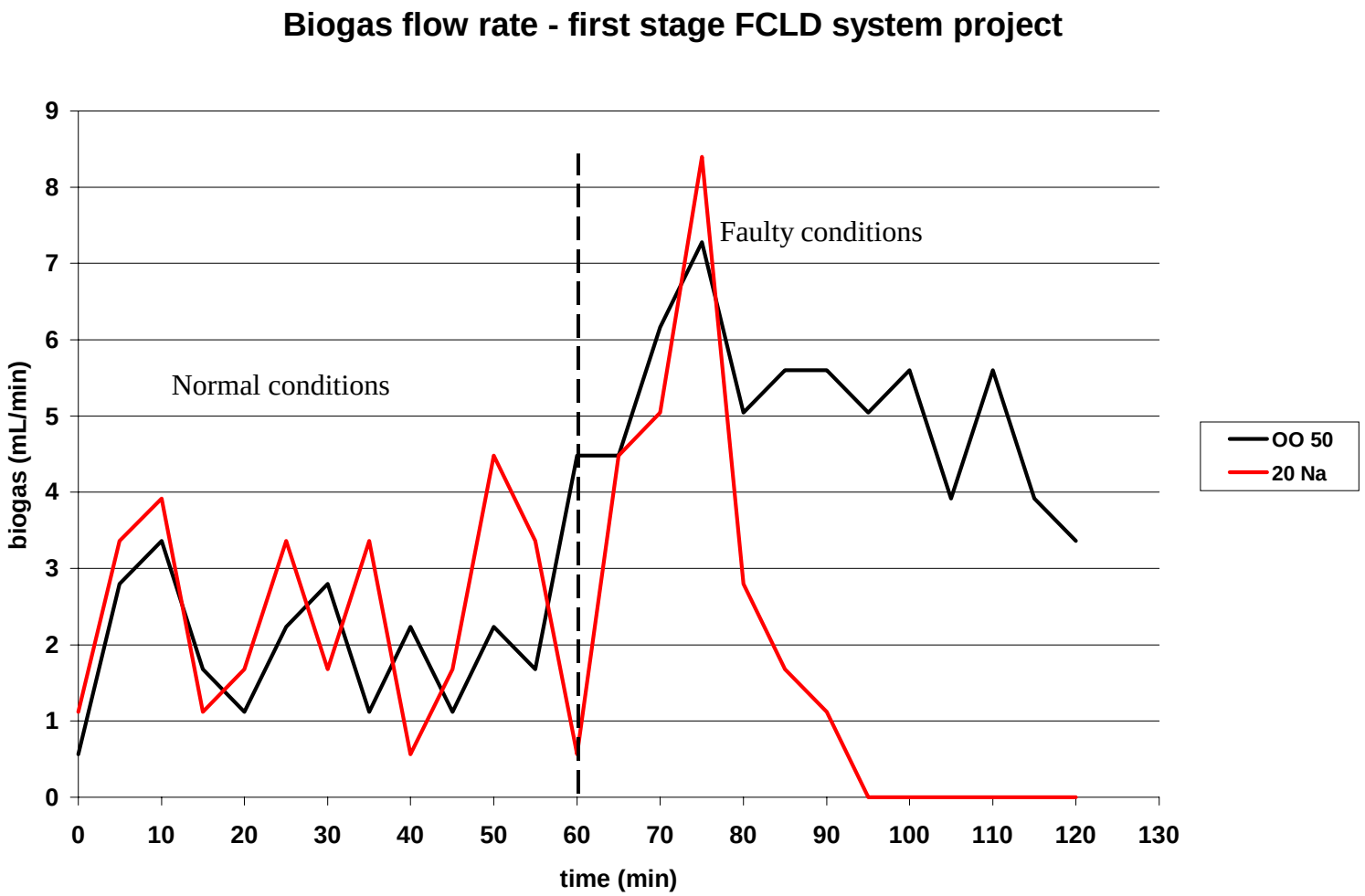

Figure 4.1 – Biogas response to organic overload in two separate experiments (vertical dashed line: test start time)

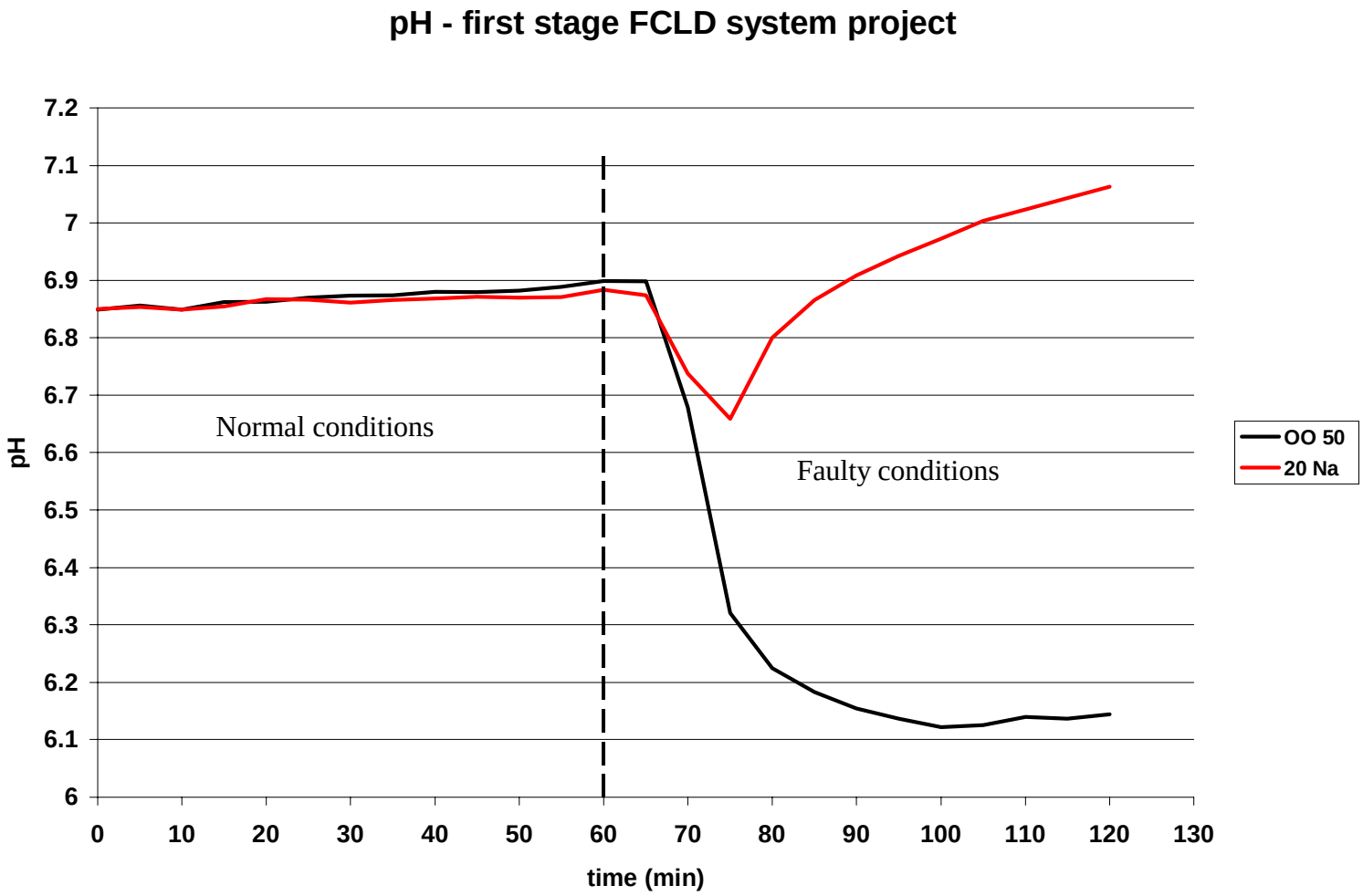

Figure 4.2 – pH response to organic overload in two separate experiments (vertical dashed line: test start time).

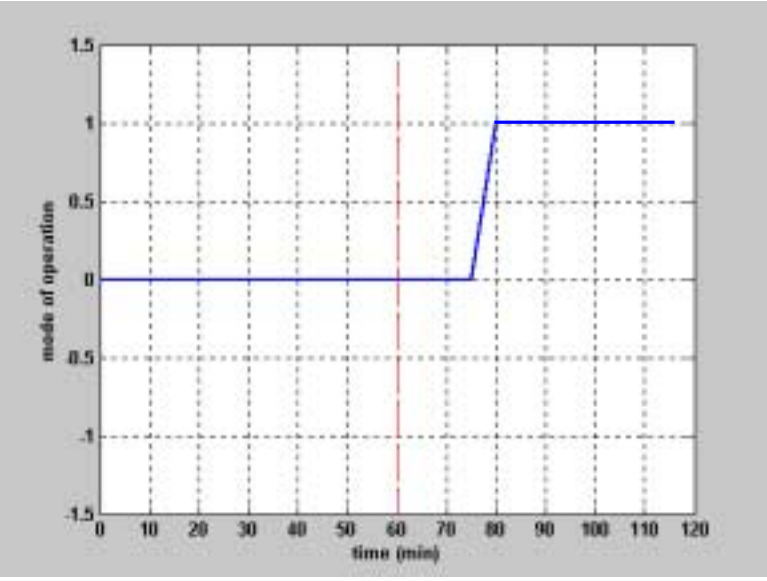

Figure 4.3 – Results from simulation of Na^+ toxic load (red doted line: test start time)

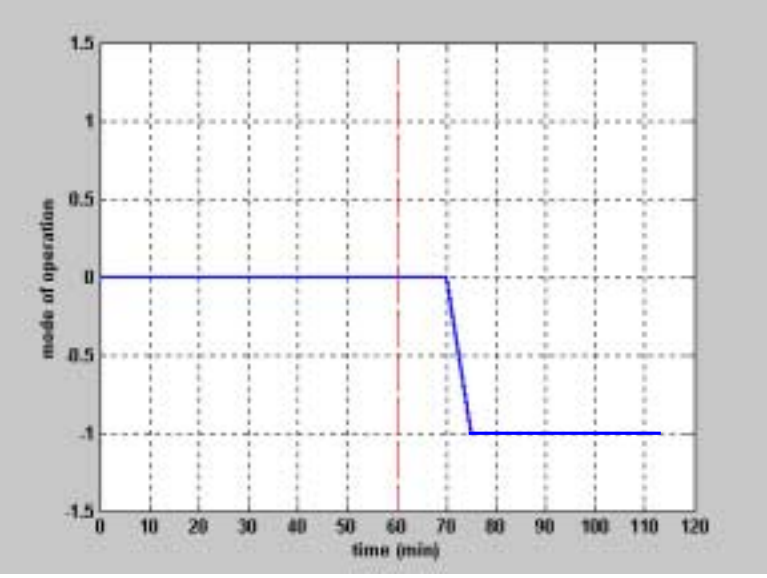

Figure 4.4 – Results from simulation of organic overload (red doted line: test start time)

4.2.1 – Toxic load experiments

Figure 4.5 represents example data (one of the three replicates) for biogas flow rate behavior for each type of failure-causing load tested. Figures 4.6, 4.7, and 4.8 illustrate similar example data (one of the replicates) for pH, conductivity, and turbidity responses, respectively.

From figures 4.5 to 4.8, it is clear that in certain tests, some monitored parameters respond very rapidly to the failure-causing load. Some responses can be seen as early as 5 min after the application of the load; others take much longer to respond. Based on this information, classification intervals were selected for pH, conductivity, and turbidity. The procedure for selection is explained in section 4.2.3.

4.2.2 – Biogas analysis

As can be seen by comparing figure 4.5 to figures 4.6-4.8, biogas flow rate measurements were not as stable as the other three variables. Furthermore, four of the toxicants did not cause clearly noticeable response in the biogas signal. For this reason, a separate analysis was done to classify faulty biogas flow rate from normal operation conditions. Normal biogas flow rate conditions were selected using mean (11.34 mL/min) and standard deviation (3.05 mL/min) values of steady-state biogas flow rate measurements for all 27 tests before the addition of the failure-causing load. Three intervals were analyzed: mean ± 1 standard deviation (8.29 - 14.39 mL/min), mean ± 2 standard deviations (5.24 - 17.44 mL/min), and mean ± 3 standard deviations (2.19 - 20.49 mL/min).

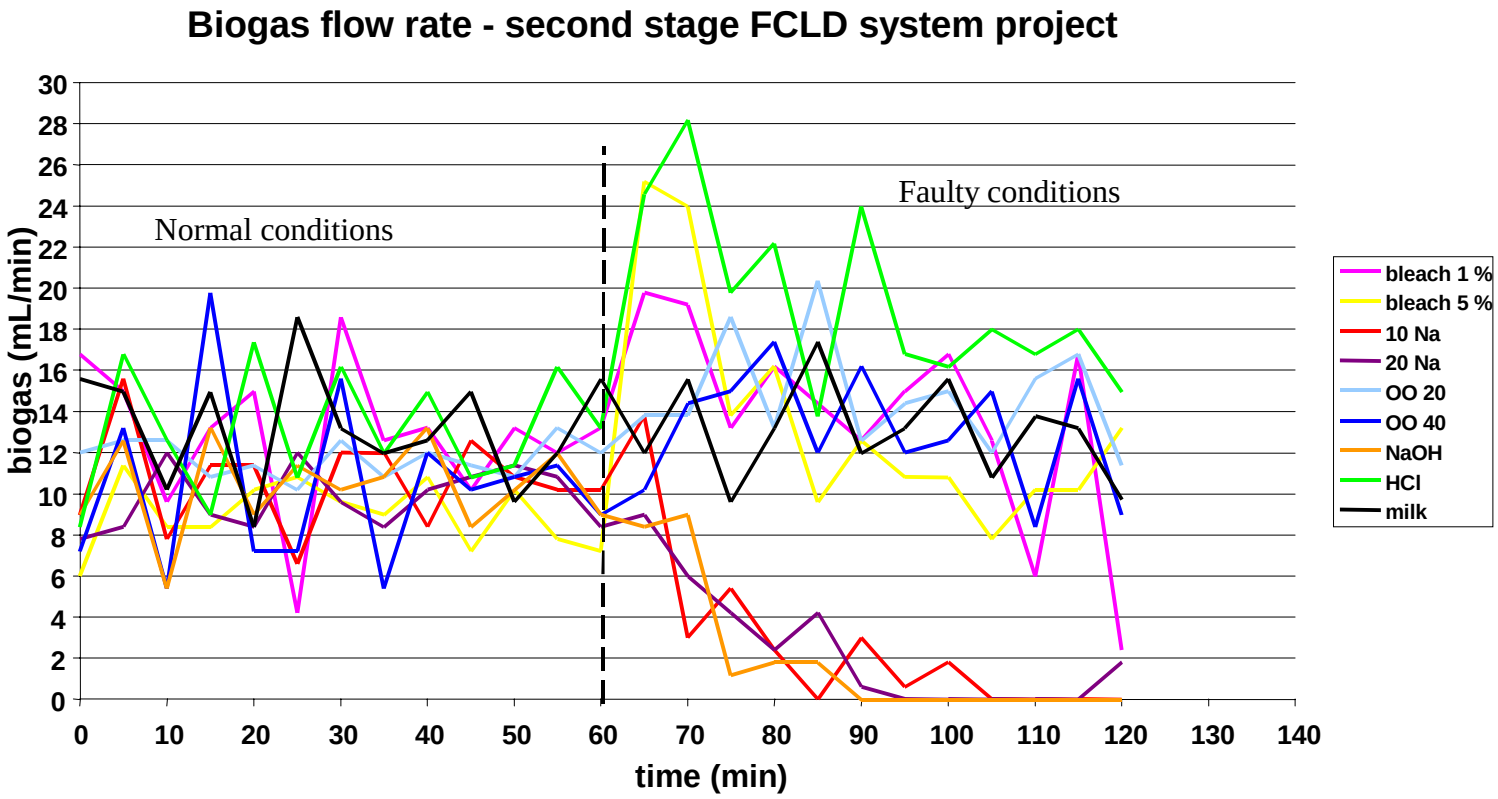

Figure 4.5 – Representative biogas response for failure tests with the FCLD system (vertical dashed line: test start time).

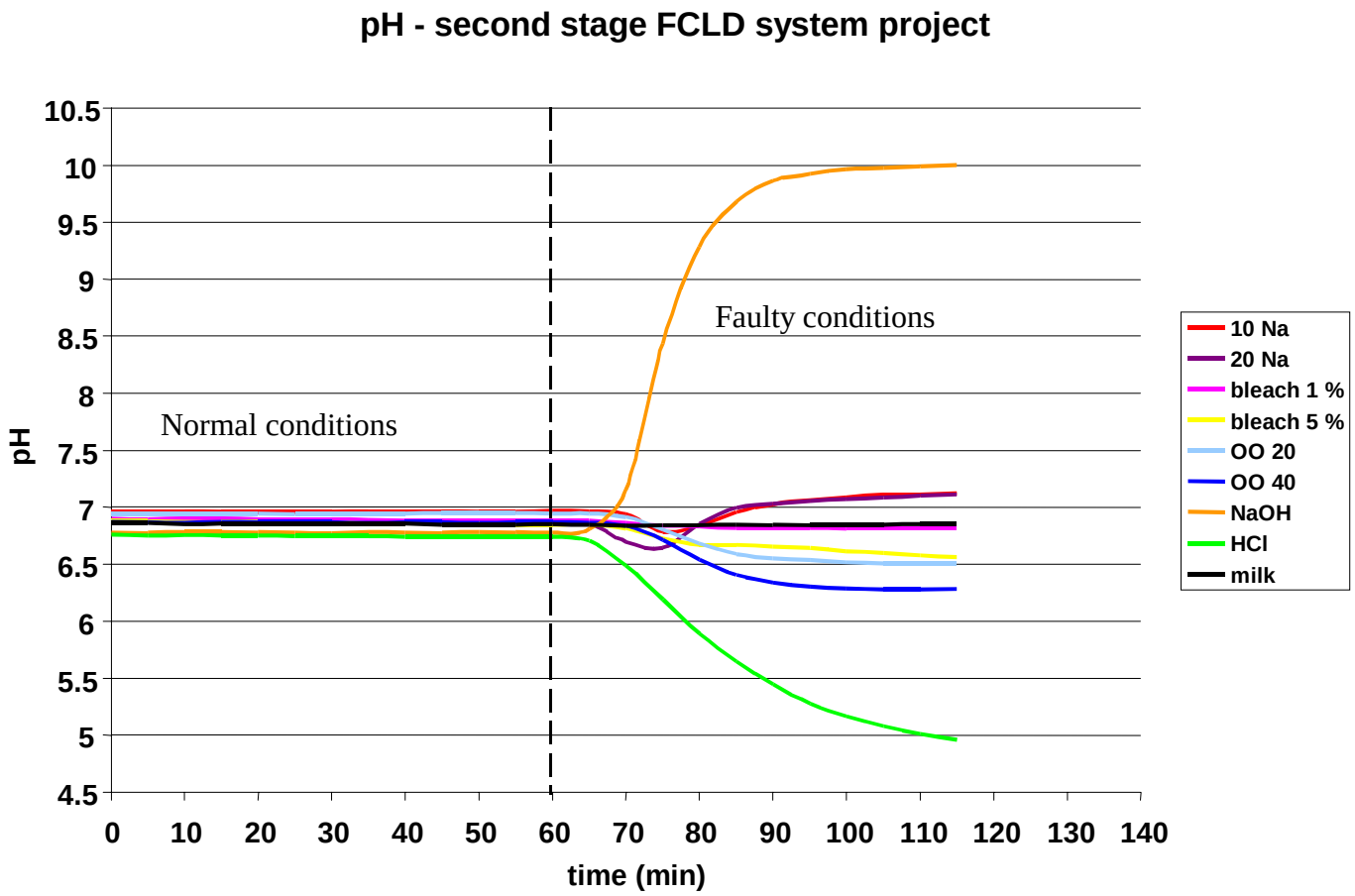

Figure 4.6 – Representative pH response for failure tests with the FCLD system (vertical dashed line: test start time).

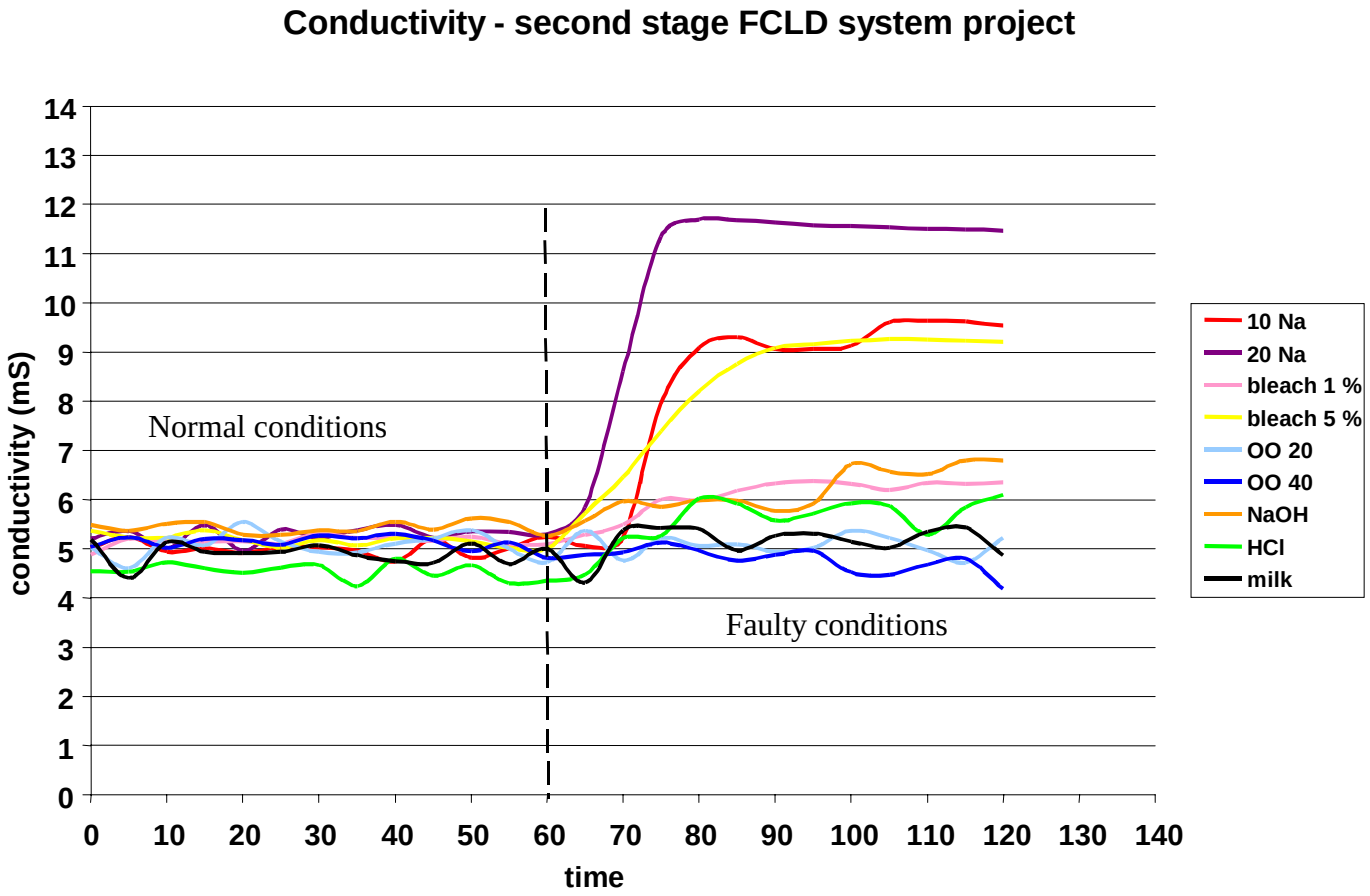

Figure 4.7 – Representative conductivity response for failure tests with the FCLD system (vertical dashed line: test start time).

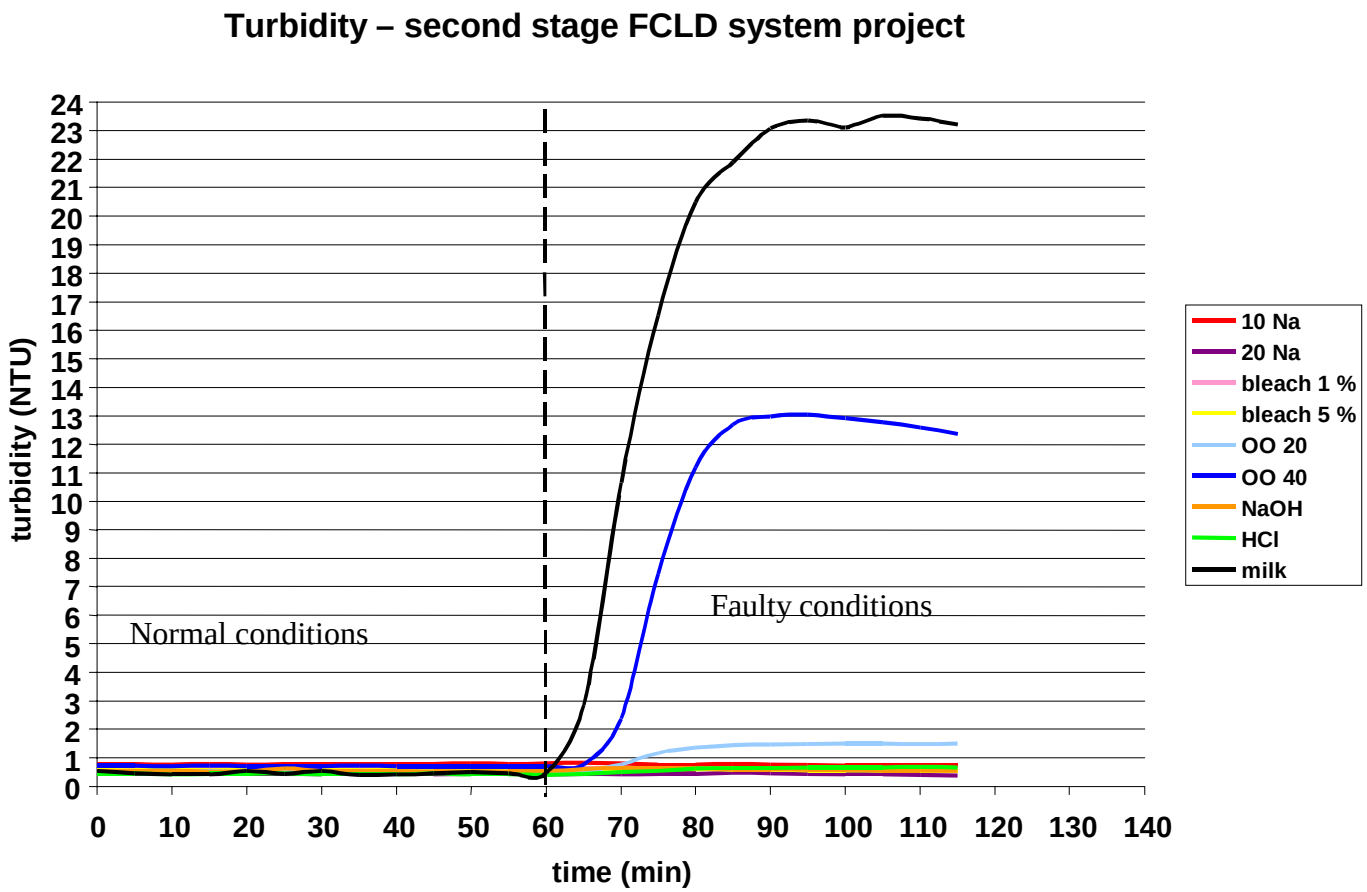

Figure 4.8 – Representative turbidity response for failure tests with the FCLD system (vertical dashed line: test start time).

Biogas flow rate data for all the 27 tests were evaluated in the three intervals, to determine when a fault-condition existed. Detailed results from the three analyses are provided in appendix A1 – Biogas analysis. Table 4.1 summarizes the results obtained from the analyses. False positives represent data points before test time (addition of toxicant) that are outside the comparison interval, and false negatives represent data points after test time that have values inside the comparison interval.

If biogas flow rate data under normal operation conditions is normally distributed, interval 1 must contain approximately 68 % of the measurements: results showed 68 %. Interval 2 must contain approximately 95 % of the measurements: results showed 96 %; interval 3 must contain approximately all the measurements, and it did. Interval 1 showed 32 % false positives, which is unacceptably high. Interval 2 showed only 4 % false positives, and had 64 % of false negatives (corresponding to a 36 % detection rate).

Table 4.1 – Results from biogas analysis for the second stage of the FCLD system project. Test time refers to time at which failure-causing load was introduced to the reactor.

		Interval 1 **mean ± 1 sd**	**Interval 2** **mean ± 2 sd**	**Interval 3** **mean ± 3 sd**
Before test time	**False positives**	32 %	4 %	0 %
After test time	**False negatives**	39 %	64 %	82 %

However, at mean ± 2 standard deviations interval, four of the nine failure-causing loads tests could still be detected within 5 to 15 min after addition of the loads. Interval 3 did not have false positives, however it had only 18 % detection; which is unacceptably low.

Even not using biogas as one input for the classifiers, the FCLD still need to be used as part of the system because other monitored parameters (e.g. pH) in the effluent line of the FCLD are modified not only by changes in composition of the influent wastewater, but also by imbalances of by-products (e.g. VFA's) of the anaerobic digestion process.

4.2.3 – Correlation of monitored parameters

Another step in the data analysis was to examine the correlation between monitored parameters. Correlations for pH-conductivity, pH-turbidity, pH-biogas, turbidity-conductivity, turbidity-biogas, and conductivity-biogas were calculated using post-failure causing load data. Complete results for this analysis are shown in appendix A2 – Correlation of monitored parameters. Table 4.2 represents the average values for the coefficient of determination (r^2) for each failure mode test that were used for both classifications.

Tests with Na^+ at 10 g/L and 20 g/L significantly decreased biogas, which was expected because of the toxicity of Na^+ at those concentrations; also, conductivity increased considerably due to the presence of more ions in solution. So, the observed high correlation between biogas and conductivity was unsurprising for Na^+ tests.

Table 4.2 – Results for the coefficient of determination (r^2) analysis. Yellow cells have $r^2 > 0.5$.

	pH-turb	pH-cond	pH-gas	turb-cond	turb-gas	cond-gas
Na10	0.5896	0.1271	0.1617	0.6021	0.4716	0.6993
Na20	0.2837	0.2190	0.4755	0.3326	0.3767	0.8379
blc1	0.3408	0.9072	0.1300	0.2644	0.0917	0.1201
Blc5	0.3861	0.8827	0.3776	0.1990	0.2182	0.2716
oo20	0.8771	0.3122	0.0672	0.2743	0.1227	0.0814
oo40	0.8662	0.5487	0.0129	0.3257	0.0629	0.0439
NaOH	0.0748	0.6949	0.7527	0.1717	0.0066	0.4630
HCl	0.7217	0.6230	0.2276	0.7790	0.1368	0.0814
Milk	0.3881	0.2128	0.0381	0.5247	0.0480	0.1352

Conductivity and pH were highly correlated for both bleach tests. When bleach (NaOCl) is added to water, it forms NaOH and hypochlorous acid (HOCl). The presence of NaOH (which dissociates into Na^+ and OH^-) probably increased the conductivity of the effluent, while HOCl decreased the pH, resulting in the observed high correlation between pH and conductivity for bleach experiments.

For both organic overload tests, pH and turbidity were highly correlated. One effect of an organic overload failure is the accumulation of volatile fatty acids (VFAs) in the reactor, due to the low activity of the methanogens (see figure 2.1); the accumulation

of VFAs drops the pH in the reactor. Turbidity increased because the confectionary wastewater used is darker (more particles) when the COD concentration is higher. This can explain the high correlation observed between pH and turbidity for both organic overloads.

Addition of NaOH to the wastewater raised pH significantly, slightly increased conductivity (due probably to the higher concentration of Na^+ and OH^-), and rapidly decreased biogas production. Therefore, high values for r^2 between pH-conductivity and pH-biogas were not surprising.

On the other hand, addition of HCl increased the concentration of H^+ and Cl^- and dropped the pH considerably. HCl slightly increased conductivity in the effluent, due presumably to the higher concentration of H^+ and Cl^- ions. Turbidity slightly increased, probably due to biomass lost after addition of the acid. These phenomena can explain the high correlation observed between pH-turbidity, pH-conductivity, and turbidity-conductivity.

Turbidity was the only parameter that was considerably affected by milk addition; all the other parameter showed insignificant changes.

4.2.4 – Implementing the graph theory based classifier

Each node of the classification using graph theory was defined based on values that could determine each failure mode. These values were selected based upon observation of the measured parameters at 20 min after addition of failure-causing load. Biogas was disregarded as an input because of the oscillation observed during the

monitoring, and because the classification of all failure mode tests could be performed using only pH, conductivity, and turbidity measurements.

As seen in figures 4.6, 4.7 and 4.8, some parameters have a very abrupt change after the addition of a failure mode. For instance, milk spill causes a rapid turbidity response, with values bigger than 15 Nephelometric Turbidity Units (NTU) 20 min after test time. Turbidity is also the relevant factor on the classification of organic overload at 40 g/L and 20 g/L. On the other hand, and unsurprisingly, pH is the parameter that was used as the main parameter on the classification of NaOH and HCl. For the classification of Na^+ at 20 g/L failure mode, conductivity was chosen because of its abrupt change from normal operation conditions. Na^+ at 10 g/L, bleach at 1 % and 5 % had slightly modifications from normal operation, needing closer observation from all the parameters. Table 4.3 shows pH, conductivity and turbidity intervals for the failure modes within the FCLD system. Based on these observations, a graph was made, and it is illustrated in figure 4.9.

4.2.5 – Performance of the graph theory based classifier

As explained in section 4.2.3, the failure modes can be classified using the limits shown in table 4.1, which are represented by the graph in figure 4.9. This graph was implemented using Simulink, and the block diagram for the classification using graph theory is illustrated in figure 4.10. The bigger block on the figure masks the graph used for the classification.

Table 4.3 – pH, conductivity and turbidity operational intervals 20 min after injection of failure mode into the influent wastewater of the FCLD system.

Parameter / Failure mode	pH	Conductivity (C) (mS)	Turbidity – T (NTU)
Milk			**T >= 15**
OO 40			**5 <= T < 15**
OO 20			**1.3 <= T <= 2.2**
Bleach 5%	**6.5 <= pH < 6.75**	**7.5 <= C < 9.4**	**T < 1.3**
NaOH	**6.5 <= pH < 6.75**		
Bleach 1%	**6.75 <= pH <= 6.85**	**5.8 <= C <= 6.9**	**T < 1.3**
10 Na	**6.75 <= pH < 8**	**7.5 <= C < 10**	**T < 1.3**
HCl	**pH <= 6.3**		**T < 1.3**
20 Na		**C >= 10**	

A MATLAB® program was used to run the Simulink model. Results are in matrix form: column 1 represents the time, and columns 2 to 10 represent the results for each type of failure mode. Number 1 in the matrix represents that the output for the failure mode is true, and 0 represent a false value. For example, when running the data set for test 15, fifteen min after the toxin was added (75 min) the failure mode organic overload at 20 g/L was detected (see the matrix immediately following figure 4.10).

All 27 tests were run, average results were calculated for the three replicates for each failure mode using another MATLAB® program. Average results for each one of the failure modes are shown in appendix A3 – Results for the classifiers.

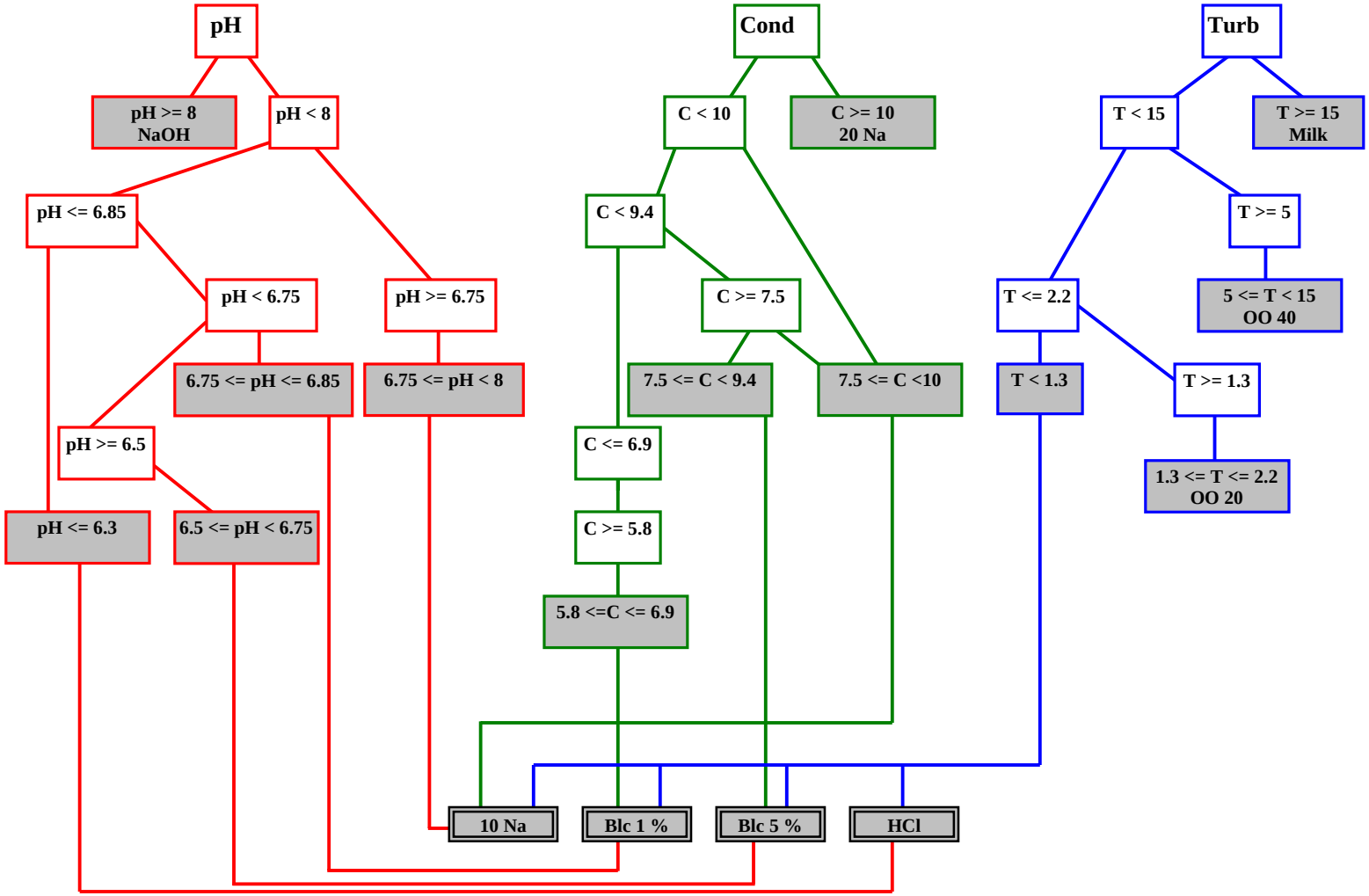

Figure 4.9 – Graph for the classification of failure modes

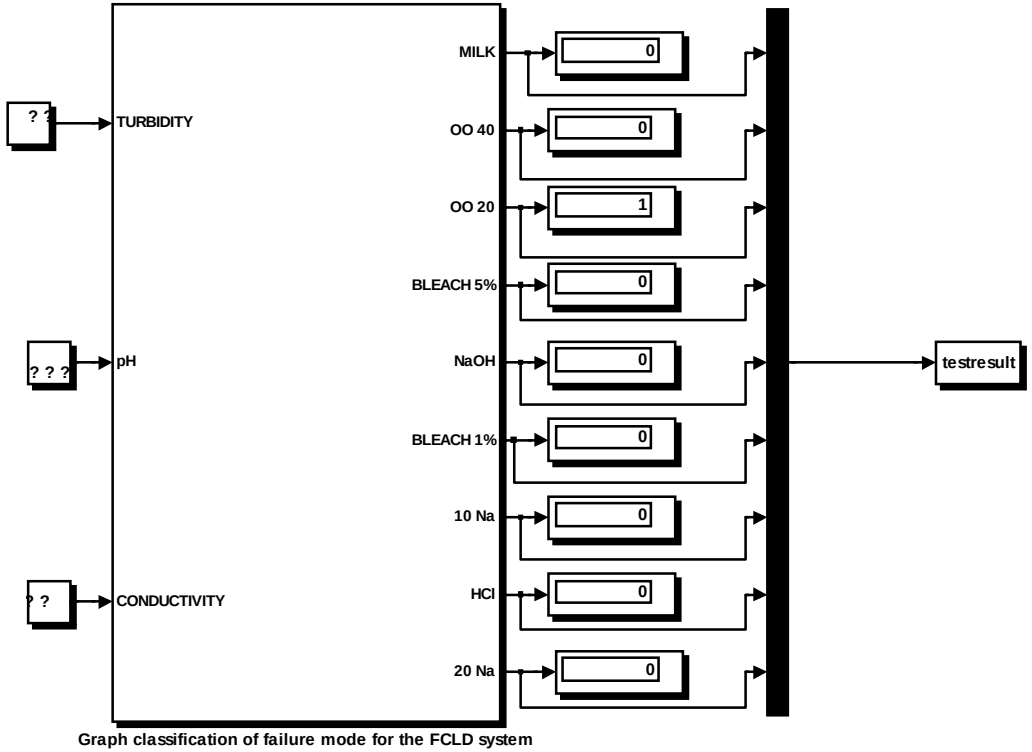

Figure 4.10 – Simulink model of graph theory based classifier

Classification of failure-causing loads using the graph theory based classifier did not show false positives. Furthermore, there were only 4 % misclassification, and they occurred in the transient period between the addition of the failure-causing load and the correct classification, which occurred 3.7 % of the time 10 min after addition of failure-causing load (time 70 min), increasing to 48 %, 15 min after test time (at 75 min), and 100 %, 20 min after test time (80 min).

```
What test do you want to run? (ex: test1, test2,...,test27): test15

**************************************************
The failure is due to organic overload at 20 g/L.
**************************************************
The results are:
```

time	milk	oo40	oo20	blc5	NaOH	blc1	Na10	HCl	Na20
0	0	0	0	0	0	0	0	0	0
5	0	0	0	0	0	0	0	0	0
10	0	0	0	0	0	0	0	0	0
15	0	0	0	0	0	0	0	0	0
20	0	0	0	0	0	0	0	0	0
25	0	0	0	0	0	0	0	0	0
30	0	0	0	0	0	0	0	0	0
35	0	0	0	0	0	0	0	0	0
40	0	0	0	0	0	0	0	0	0
45	0	0	0	0	0	0	0	0	0
50	0	0	0	0	0	0	0	0	0
55	0	0	0	0	0	0	0	0	0
60	0	0	0	0	0	0	0	0	0
65	0	0	0	0	0	0	0	0	0
70	0	0	0	0	0	0	0	0	0
75	0	0	1	0	0	0	0	0	0
80	0	0	1	0	0	0	0	0	0
85	0	0	1	0	0	0	0	0	0
90	0	0	1	0	0	0	0	0	0
95	0	0	1	0	0	0	0	0	0
100	0	0	1	0	0	0	0	0	0
105	0	0	1	0	0	0	0	0	0
110	0	0	1	0	0	0	0	0	0
115	0	0	1	0	0	0	0	0	0

4.2.6 – Performance of the fuzzy inference system classifier

This step, which is the use of an FIS to classify all the tests that were obtained during the second stage of the FCLD project, was made using MATLAB®/Fuzzy Logic Toolbox and the Simulink model illustrated in figure 4.10. To run the model, a script is run on the MATLAB® workspace. The program asks for the test that the user wants to classify, and then give the classification for that particular test. As explained in section 3.3.4, the FIS has 4 outputs and their membership functions can be seen in figures 3.12 to 3.14. The result from the simulation of the FIS model is shown in matrix form, where the column 1 represents the time interval for each test, 0 to 115 min, and columns 2 to 10 represent all the types of failure modes that were simulated using the FCLD system for the second stage of the research. The classification is shown as the possibility of the output been one of the failure modes. Here, the results are presented as the average for each type of failure-causing load.

The program runs the Simulink model using the data set for the selected test, and shows the classification results into the MATLAB® screen. The matrix in the next page shows the result for the average for sodium at 10 g/L. There were some misclassification during the transient period, but correct classification was reached 20 min after the toxin was added (at 80 min).

The average results for sodium at 10 g/L are:

time	oo20	oo40	Milk	HCl	NaOH	20Na	Blc1	10Na	Blc5
0	0	0	0	0	0	0	0	0	0
5	0	0	0	0	0	0	0	0	0
10	0	0	0	0	0	0	0	0	0
15	0	0	0	0	0	0	0	0	0
20	0	0	0	0	0	0	0	0	0
25	0	0	0	0	0	0	0	0	0
30	0	0	0	0	0	0	0	0	0
35	0	0	0	0	0	0	0	0	0
40	0	0	0	0	0	0	0	0	0
45	0	0	0	0	0	0	0	0	0
50	0	0	0	0	0	0	0	0	0
55	0	0	0	0	0	0	0	0	0
60	0	0	0	0	0	0	0	0	0
65	0	0	0	0	0	0	0	0	0
70	0	0	0	0	0	0	0	33	0
75	0	0	0	0	0	0	33	67	0
80	0	0	0	0	0	0	0	100	0
85	0	0	0	0	0	0	0	89	0
90	0	0	0	0	0	0	0	83	0
95	0	0	0	0	0	0	0	84	0
100	0	0	0	0	0	0	0	86	0
105	0	0	0	0	0	0	0	86	0
110	0	0	0	0	0	0	0	86	0
115	0	0	0	0	0	0	0	86	0

All 27 tests were run, and another matrix was built for each data set based on the results. If the possibility value of a test at a certain time was higher than 50, a value of 1 was assigned to that element, otherwise 0 was assigned. The objective of this new representation was to have results from the FIS in the same format as the results from the graph theory based classifier. For instance, the next matrix represents average values for sodium at 10 g/L. Test time was at 60 min, 10 min after test time one test was correctly classified as Na^+ at 10 g/L, 15 min after test time one test was classified as bleach at 1 %, and 2 were correctly. Finally, 20 min after test time all 3 tests were correctly classified. Also, there were no false positives when running the 3 data sets for Na^+ at 10 g/L.

The average for sodium at 10 g/L is:

time	milk	oo40	oo20	blc5	NaOH	blc1	Na10	HCl	Na20
0	0	0	0	0	0	0	0	0	0
5	0	0	0	0	0	0	0	0	0
10	0	0	0	0	0	0	0	0	0
15	0	0	0	0	0	0	0	0	0
20	0	0	0	0	0	0	0	0	0
25	0	0	0	0	0	0	0	0	0
30	0	0	0	0	0	0	0	0	0
35	0	0	0	0	0	0	0	0	0
40	0	0	0	0	0	0	0	0	0
45	0	0	0	0	0	0	0	0	0
50	0	0	0	0	0	0	0	0	0
55	0	0	0	0	0	0	0	0	0
60	0	0	0	0	0	0	0	0	0
65	0	0	0	0	0	0	0	0	0
70	0	0	0	0	0	0	33	0	0
75	0	0	0	0	0	33	67	0	0
80	0	0	0	0	0	0	100	0	0
85	0	0	0	0	0	0	100	0	0
90	0	0	0	0	0	0	100	0	0
95	0	0	0	0	0	0	100	0	0
100	0	0	0	0	0	0	100	0	0
105	0	0	0	0	0	0	100	0	0
110	0	0	0	0	0	0	100	0	0
115	0	0	0	0	0	0	100	0	0

Similar average results for all the failure-causing modes are shown in appendix A3 – Results for the classifiers together with average results from the graph theory based classifier.

Classification of failure-causing loads using the FIS classifier did not show false positives. This classifier showed 8 % misclassification during transient period. Correct classification occurred with 7.4 % 10 min after addition of failure-causing load (time 70 min), increasing to 59 % 15 min after test time (at 75 min), 96 % 20 min after test time, and reaching 100 % 25 min after test time (85 min).

4.2.7 – Response times

Figure 4.11 illustrates the response time for the detection of toxicants. Under normal operation conditions, biogas response (interval 1 – mean ± 1 sd) showed false positives, which was not observed when using the graph theory or the FIS based classifiers. However, it can be seen that biogas response is faster than the responses from the graph theory based and FIS classifiers. Biogas response does not reach 100 % classification because not all the failure-causing toxicants used to test the FCLD system generated substantial deviation from normal operation conditions.

Conductivity, turbidity, and pH were used as inputs for both classifiers; biogas was disregarded because of the high fluctuation found during monitoring. However, if biogas was used as an input for the classifiers, it could make the classification of the failure-causing modes that had significant change in biogas (NaOH, HCl, and Na^+ tests) approximately 10 min faster.

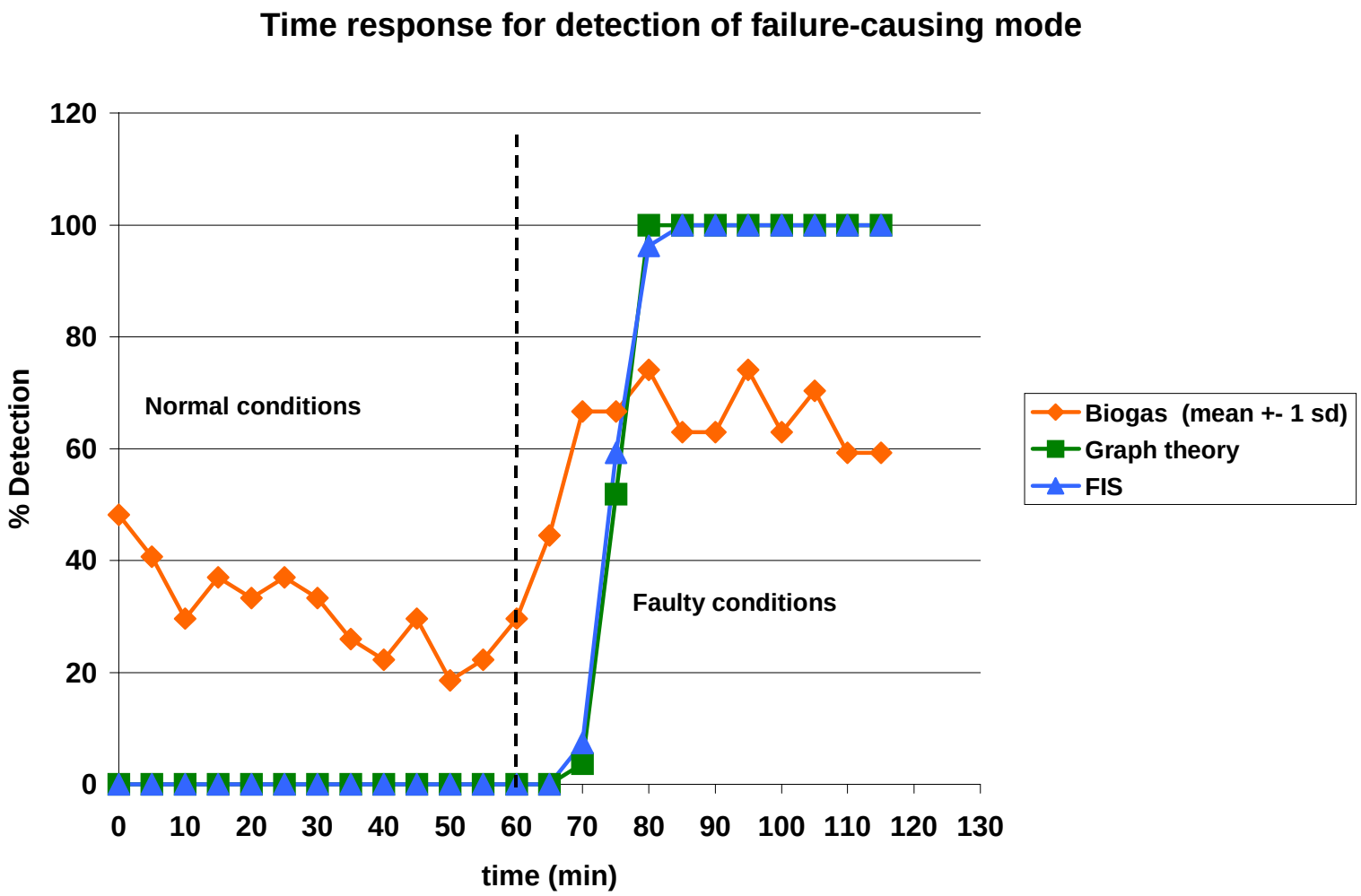

Figure 4.11 – Time response for detection of failure-causing modes using the FCLD system (vertical dashed line: test start time)

CHAPTER 5

SUMMARY AND CONCLUSIONS

5.1 – Conclusions

In this work a small UASB reactor (4-L volume; 10-min HRT) was used as a biosensor to detect failure-causing loads resulting from toxicants in the influent wastewater, in what is termed a failure-causing load detector (FCLD) system. Biogas flow rate, pH, conductivity, and turbidity were monitored during experiments with a variety of different types of failure-causing loads: organic overloads, sodium toxic loads, bleach, milk, HCl, and NaOH. Furthermore, data collected during these experiments were used as inputs for two classifiers capable of determining the different types of failure-causing loads entering the FCLD system. One classifier was developed using concepts of graph theory; the other used fuzzy inference system (FIS) techniques.

Biogas is the primary end product of anaerobic digestion (Figure 2.1), and it is mainly composed of CH_4 and CO_2. If the influent wastewater inhibits the metabolism of the methanogenic bacteria, biogas flow rate will decrease. Deviation from normal biogas production could be rapidly detected for some of the failure-causing loads. For the HCl tests, the change in biogas flow rate was detected within 5 min; for NaOH and sodium failure tests, detection was within 10 min. However, due to variability observed in biogas measurements and because classification could be performed using just pH, conductivity and turbidity as inputs, biogas was disregarded as an input for the classification of the failure-causing loads for the second stage of the FCLD.

The graph theory-based classifier is simpler than the FIS-based classifier. Also, it showed less misclassification than the FIS classifier: the FIS has 125 % more misclassification than the graph theory classifier. When comparing number of correct classifications in a specific time, both classifiers had similar performance: 10 min after test time, the FIS classifier correctly classified 2 of the 27 failure-causing loads and the graph theory based classified 1; 15 min after test time the FIS detected 16 tests correctly, and the graph theory based correctly classified 14; 20 min after test time, the graph theory based classifier correctly classified all the tests, and the FIS had correctly classified 26 tests; for the FIS based classifier, completely correct classification was reached at 25 min for all the tests.

For certain toxicants biogas measurement showed faster than the two physicochemical sensors based classifiers. The introduction of biogas as one input for both classifiers could speed the classification of the failure-causing loads that showed substantial biogas response.

5.2 – Recommendation for future work

This work proved that a small anaerobic digester (4-L) that has a short HRT (10 min) can detect faulty conditions in the influent wastewater within 5-20 min of any changes for the range of experiments that were performed. Also, when using expert system techniques such as graph theory and fuzzy logic, monitoring programs can be used to correctly classify the nature of the failure-causing load. However, there are some gaps to be filled in order to improve the overall understanding of this kind of system. The following suggestions can then be used as research topics in future works:

1. Integrate the biogas, pH, turbidity, and conductivity measurements to classify failure-causing loads to see if improvement in classification success rate and speed can be achieved.
2. Use historical toxicity information from a full-scale plant that uses a UASB, and test the FCLD system and the classifiers based on this information. Modify the classifiers if necessary.
3. Use other classification techniques together with the techniques used in this work, and compare the trade-offs of each one of them in order to rank them
4. Real time implementation of the two classifiers used in this work.

CHAPTER 5

SUMMARY AND CONCLUSIONS

5.1 – Conclusions

In this work a small UASB reactor (4-L volume; 10-min HRT) was used as a biosensor to detect failure-causing loads resulting from toxicants in the influent wastewater, in what is termed a failure-causing load detector (FCLD) system. Biogas flow rate, pH, conductivity, and turbidity were monitored during experiments with a variety of different types of failure-causing loads: organic overloads, sodium toxic loads, bleach, milk, HCl, and NaOH. Furthermore, data collected during these experiments were used as inputs for two classifiers capable of determining the different types of failure-causing loads entering the FCLD system. One classifier was developed using concepts of graph theory; the other used fuzzy inference system (FIS) techniques.

Biogas is the primary end product of anaerobic digestion (Figure 2.1), and it is mainly composed of CH_4 and CO_2. If the influent wastewater inhibits the metabolism of the methanogenic bacteria, biogas flow rate will decrease. Deviation from normal biogas production could be rapidly detected for some of the failure-causing loads. For the HCl tests, the change in biogas flow rate was detected within 5 min; for NaOH and sodium failure tests, detection was within 10 min. However, due to variability observed in biogas measurements and because classification could be performed using just pH, conductivity and turbidity as inputs, biogas was disregarded as an input for the classification of the failure-causing loads for the second stage of the FCLD.

The graph theory-based classifier is simpler than the FIS-based classifier. Also, it showed less misclassification than the FIS classifier: the FIS has 125 % more misclassification than the graph theory classifier. When comparing number of correct classifications in a specific time, both classifiers had similar performance: 10 min after test time, the FIS classifier correctly classified 2 of the 27 failure-causing loads and the graph theory based classified 1; 15 min after test time the FIS detected 16 tests correctly, and the graph theory based correctly classified 14; 20 min after test time, the graph theory based classifier correctly classified all the tests, and the FIS had correctly classified 26 tests; for the FIS based classifier, completely correct classification was reached at 25 min for all the tests.

For certain toxicants biogas measurement showed faster than the two physicochemical sensors based classifiers. The introduction of biogas as one input for both classifiers could speed the classification of the failure-causing loads that showed substantial biogas response.

5.2 – Recommendation for future work

This work proved that a small anaerobic digester (4-L) that has a short HRT (10 min) can detect faulty conditions in the influent wastewater within 5-20 min of any changes for the range of experiments that were performed. Also, when using expert system techniques such as graph theory and fuzzy logic, monitoring programs can be used to correctly classify the nature of the failure-causing load. However, there are some gaps to be filled in order to improve the overall understanding of this kind of system. The following suggestions can then be used as research topics in future works:

1. Integrate the biogas, pH, turbidity, and conductivity measurements to classify failure-causing loads to see if improvement in classification success rate and speed can be achieved.
2. Use historical toxicity information from a full-scale plant that uses a UASB, and test the FCLD system and the classifiers based on this information. Modify the classifiers if necessary.
3. Use other classification techniques together with the techniques used in this work, and compare the trade-offs of each one of them in order to rank them
4. Real time implementation of the two classifiers used in this work.

REFERENCES

REFERENCES

Beal, L. J. 1998. Laboratory scale testing of an anaerobic waste treatment system for a confectionery wastewater. Thesis, The University of Tennessee, Knoxville, Tennessee.

Brouwer, H., A. Klapwijk, and K. J. Keesman. 1998. Identification of activated sludge and wastewater characteristics using respirometric batch-experiments. *Water Research* 32(4):1240-1254.

Castillo, E., J. M. Gutiérrez, and A. S. Hadi. 1997. *Expert Systems and Probabilistic Network Models.* New York, NY: Springer-Verlag New York, Inc.

Chang, W. C., C. F. Ouyang, W. L. Chiang, and C. W. Hou. 1998. Sludge pre-recycle control of dynamic enhanced biological phosphorus removal system: an application of on-line fuzzy controller. *Water Research* 32(3):727-736.

Cohen, A., G. Janssen, S. D. Brewster, R. Seeley, A. A. Boogert, A. A. Graham, M. R. Mardani, N. Clarke, and N. K. Kasabov. 1997. Application of computational intelligence for on-line control of a sequencing batch reactor (SBR) at Morrinsville sewage treatment plant. *Water Science and Technology* 35(10):63-71.

Ervin, T., J. Hancock, and E. Wilkerson. 1999. An on-line sensor for predicting failure in high-rate anaerobic digesters. Unpublished final report for Biosystem Eng. 402 – Mentors: Raman, D. R. and Yoder, R. The University of Tennessee, Knoxville.

Estaben, M., M. Polit, and J. P. Steyer. 1997. Fuzzy control for an anaerobic digester. *Control Engineering Practice* 5(98):1303-1310.

Free On-Line Dictionary of Computing (FOLDOC). 1993. Definition for fuzzy logic (1995 Feb 21). Available from: URL: http://foldoc.doc.ic.ac.uk/foldoc/index.html

Garcia, F. J., V. Izquierdo, L. J. de Miguel, and J. R. Perán. 2000. Fault-diagnostic system using analytical fuzzy redundancy. *Engineering Application of Artificial Inteligence* 13:441-450.

Genovesi A., J. Harmand, and J-P. Steyer. 1999. A fuzzy logic based diagnosis system for the on-line supervision of an anaerobic digestor pilot-plant. *Biochemical Engineering Journal* 3:171-183.

Gray, N. F. 1989. *Biology of Wastewater Treatment*. New York, NY: Oxford University Press.

Habets, L. H. A., and H. J. Knelissen. 1997. In line biological water regeneration in a zero discharge recycle paper mill. *Water Science and Technology* 35(2-3):41-48

Hanna, A. S. and W. B. Lotfallah. 1999. A fuzzy logic approach to the selection of cranes. *Automation and Control* 8 (5):597- 608.

Hopgood, A. A. 1993. *Knowledge-Based Systems for Engineers and Scientists*. Boca Raton, FL: CRC Press, Inc.

Jang, J.-S. and N. Gulley. 2001. *Fuzzy Logic Toolbox for Use with MATLAB® User's Guide – Version 2*, Natick, MA: The Mathworks, Inc.

Klir, G. J. and B. Yuan. 1995. *Fuzzy Sets and Fuzzy Logic: Theory and Applications*. Upper Saddle River, NJ: Prentice Hall P T R.

Lettinga, G. 1995. Anaerobic digestion and wastewater treatment systems. *Antonie van Leeuwenhoek* 67:3-28.

Lettinga, G., A. F. M. van Velsen, S. W. Hobma, W. de Zeeuw, and A. Klapwijk. 1980. Use of upflow sludge blanket (USB) reactor concept for biological wastewater treatment, especially for anaerobic treatment. *Biotechnology and bioengineering* 22:699-734.

Masili-Libelli, S. and A. Muller. 1996. Adaptive fuzzy pattern recognition in the anaerobic digestion process. *Pattern Recognition Letters* 17:651-659.

Martin, J. and S. Oxman. 1988. *Building Expert Systems: A Tutorial, James Martin, Steven Oxman,* Englewood Cliffs, NJ: Prentice-Hall

Metcalf and Eddy, Inc., 1991. *Wastewater Engineering: Treatment, Disposal and Reuse. 3rd* Edition. New York, NY: McGraw-Hill, Inc.

Moletta, R., Y. Escoffier, F. Ehlinger, J. P. Coudert, and J. P. Leyris. 1994. On-line automatic control system for monitoring an anaerobic fluidized-bed reactor: response to organic overload. *Water Science and Technology* 30(12):11-20.

Moody, L. B. and D. R. Raman, 2001. A Dual-reactor anaerobic system for complete treatment of a food processing waste. *Journal of Agricultural Engineering Research* In press.

Muller, A., S. Marsili-Libelli, A. Aivasidis, T. Lloyd, S. Kroner, and C. Wandrey. 1997. Fuzzy control disturbances in a wastewater treatment process. *Water Research* 31(12):3157-3167.

Ning, Z., G. G. Patry, and H. Spanjers. 2000. Identification and quantification of nitrogen nutrient deficiency in the activated sludge process using respirometry. *Water Research* 34(13):3345-3354.

OMEGA Engineering. 2001. Turbidity measurement. Available from: URL: http://www.omega.com/techref/ph-6.html

Pavlostathis, S. G., and E. Giraldo-Gomez. 1991. Kinetics of anaerobic treatment: a critical review. *Critical Reviews in Environmental Control* 21(5,6): 411-490.

Pinto, A. M. A. C., D. R. Raman, and L. B. Moody. 2000. Using fuzzy logic to determine failure modes in a biological sensor for UASB reactors. Presented at July/12/2000 at the 2000 ASAE International Meeting – Milwaukee, WI. Paper No 006127.

Pollice, A., A. Rozzi, M. C. Tomei, A. D. Di Pinto, and G. Laera. 2001. Inhibiting effects of chloroform on anaerobic microbial consortia as monitored by the Rantox biosensor. *Water Research* 35(5):1179-1190.

Puñal, A., A. Lorenzo, E. Roca, C. Hernández, and J. M. Lema. 1999. Advanced monitoring of an anaerobic pilot plant treating high strength wastewaters. *Water Science and Technology* 40(8):237-244.

Rajeshwari, K. V., M. Balakrishna, A. Kansal, K. Lata, and V. V. N. Kishore. 1999. State-of-the-art of anaerobic digestion for industrial wastewater treatment. *Renewable and Sustainable Energy Reviews* 4:135-156.

Ribeiro, R. S. F. 1998. Fuzzy logic based automated irrigation control system optimized via neural networks. Dissertation. The University of Tennessee, Knoxville, Tennessee.

Rozzi, A., M. C. Tomei, A. C. Di Pinto, and N. Limoni. 1997. Monitoring toxicity in anaerobic digesters by the RANTOX biosensor: theoretical background. *Biotechnology and Bioengineering* 55(1):33-40.

Rozzi, A., M. C. Tomei, A. C. Di Pinto, and N. Limoni. 1999. Monitoring toxicity in anaerobic digesters by utilizing the RANTOX biosensor: calibration tests. *Bioresource Technology* 68:155-163.

Singh, R. P., S. Kumar, and C. S. P. Ojha. 1998. Nutrient requirement for UASB process: a review. *Biochemical Engineering Journal* 3:35-54.

Speece, R. E. 1996. *Anaerobic Biotechnology for Industrial Wastewaters*. Nashville, TN: Archae Press.

Steyer, J-P., D. Rolland, J-C Bouvier, and R. Moletta. 1997. Hybrid fuzzy neural network for diagnosis – Application to the anaerobic treatment of wine distillery wastewater in a fluidized bed reactor. *Water Science Technology* 36(6-7): 209-217.

Steyer, J-P., Estaben M. and M. Polit. 1997. Fuzzy control of an anaerobic digestion process for the treatment of an industrial wastewater. *Proceedings of the 6th IEEE International Conference on Fuzzy Systems* 3:1245-1249.

Strotmann, U. J., A. Geldern, A. Kuhn, C. Gendig, and S. Klein. 1999. Evaluation of a respirometric test method to determine the heterotrophic yield coefficient of activated sludge bacteria. *Chemosphere* 38(15):3555-3570.

Tay, J-H. and X. Zhang. 2000. A fast predicting neural fuzzy model for high-rate anaerobic wastewater treatment systems. *Water Research* 34(11):2849-2860.

Terano, T., K. Asai, and M. Sugeno. 1991. *Fuzzy Systems Theory and its Applications.* San Diego, CA: Academic Press, Inc.

Tsoukalas, L. H. and R. E. Uhrig. 1997. *Fuzzy and Neural Approaches in Engineering.* New York, NY: John Wiley & Sons, Inc.

Wilen, B-M, J. L. Nielsen, K. Keiding, and P. H. Nielsen. 2000. Influence of microbial activity on the stability of activated sludge flocs. *Colloides and Surfaces B: Biointerfaces*. 18(2):145-156.

Winkler, M. A. 1981. *Biological Treatment of Wastewater*. West Sussex, England: Ellis Horwood Ltd.

APPENDICES

A1 – Biogas analysis

The next three pages show the results obtained for the biogas anlysis. Normal biogas flow rate conditions were selected using mean (11.34 mL/min) and standard deviation (3.05 mL/min) values at steady-state operation before the addition of the failure-causing load (test time). Three intervals were analyzed: mean ± 1 standard deviation (8.29 - 14.39 mL/min), mean ± 2 standard deviations (5.24 – 17.44 mL/min), and mean ± 3 standard deviations (2.19 – 20.49 mL/min)

For instance, when observing results for the interval composed by mean biogas flow rate ± 1 standard deviation, and looking at the column that represents Na^+ at 10 g/L (Na10), it can be seen that at times 0, 5, 10, and 35 min, 1 out of 3 tests had biogas flow rate outside the interval, at 25 min 2 tests for Na10 shown biogas flow rate outside normal operation conditions, and times 15, 20, 30, and 40 to 60 had all the 3 tests with biogas flow rate within the normal operation interval. Time 60 min represents the time when the failure modes were added to the influent wastewater. At time 65 min for Na10 there is one observation of biogas flow rate outside the limits for normal conditions, and from 70 to 115 min all three replicates were detected as being outside the normal operation range. Similar observation can be done for all the other tests, and for the other 2 intervals that defined normal operation conditions.

```
==========================================================================
Analysis using normal biogas production as the interval between mean +-
1 standard deviation.
==========================================================================
Biogas production interval: 8.29 <= BIOGAS <= 14.39 (mL/min)
Biogas detection = (1)
No biogas detection = (0)
  time    milk  oo40  oo20  blc5  NaOH  blc1  Na10  HCl   Na20
     0     1     3     0     1     2     2     1     2     2
     5     2     1     0     1     1     2     1     2     1
    10     0     3     0     1     1     1     1     1     0
    15     3     3     1     1     0     0     0     2     0
    20     0     1     0     2     2     2     0     1     1
    25     2     2     0     0     1     0     2     1     2
    30     0     2     1     2     0     1     0     3     0
    35     1     1     0     0     0     1     1     2     1
    40     1     0     0     1     2     0     0     2     0
    45     1     0     1     2     1     1     0     2     0
    50     1     1     1     0     0     0     0     1     1
    55     0     0     1     3     0     0     0     2     0
    60     1     0     0     2     1     1     0     2     1
    65     1     0     1     3     0     3     1     3     0
    70     2     1     0     3     2     1     3     3     3
    75     2     2     2     0     3     0     3     3     3
    80     0     2     2     2     2     3     3     3     3
    85     2     1     2     0     3     2     3     1     3
    90     0     3     1     0     3     1     3     3     3
    95     1     0     3     2     3     2     3     3     3
   100     2     1     1     1     3     1     3     2     3
   105     1     2     2     3     3     0     3     2     3
   110     0     1     1     1     3     2     3     2     3
   115     0     2     2     0     3     1     3     2     3

**************************************************************************
Before test time there were, in percentage:
False positive biogas production before test time is 31.79 percent.
No biogas detection before test time is 68.21 percent.
And after test time the results are:
Biogas detection after test time is 61.111 percent.
No biogas detection after test time is 38.889 percent.
**************************************************************************
```

```
==========================================================================
Analysis using normal biogas production as the interval between mean +-
2 standard deviation.
==========================================================================
Biogas production interval: 5.24 <= BIOGAS <= 17.44 (mL/min)
Biogas detection = (1)
No biogas detection = (0)
  time    milk  oo40  oo20  blc5  NaOH  blc1  Na10  HCl   Na20
     0     0     0     0     0     0     1     0     1     0
     5     0     0     0     0     0     0     0     0     0
    10     0     0     0     0     0     1     0     1     0
    15     0     1     0     0     0     0     0     0     0
    20     0     0     0     1     0     0     0     0     0
    25     2     0     0     0     0     0     0     0     0
    30     0     0     0     1     0     1     0     0     0
    35     0     0     0     0     0     0     0     0     0
    40     0     0     0     1     0     0     0     0     0
    45     0     0     1     0     0     0     0     0     0
    50     0     0     0     0     0     0     0     0     0
    55     0     0     0     0     0     0     0     0     0
    60     0     0     0     1     0     0     0     0     0
    65     0     0     0     2     0     2     0     3     0
    70     1     0     0     3     2     1     3     3     0
    75     0     0     1     0     2     0     0     3     1
    80     0     1     1     0     2     0     3     2     3
    85     0     0     1     0     3     0     3     1     3
    90     0     0     0     0     3     0     3     1     3
    95     0     0     0     1     3     0     3     1     3
   100     0     0     0     1     3     0     3     1     3
   105     0     1     0     0     3     0     3     2     3
   110     0     0     0     1     3     0     3     1     3
   115     0     0     0     0     3     0     3     2     3

**************************************************************************
Before test time there were, in percentage:
False positive biogas production before test time is 3.7037 percent.
No biogas detection before test time is 96.296 percent.
And after test time the results are:
Biogas detection after test time is 36.111 pecent.
No biogas detection after test time is 63.889 percent.
**************************************************************************
```

```
==========================================================================
Analysis using normal biogas production as the interval between mean +-
3 standard deviation.
==========================================================================
Biogas production interval: 2.19 <= BIOGAS <= 20.49 (mL/min)
Biogas detection = (1)
No biogas detection = (0)
  time    milk  oo40  oo20  blc5  NaOH  blc1  Na10  HCl   Na20
     0      0     0     0     0     0     0     0     0      0
     5      0     0     0     0     0     0     0     0      0
    10      0     0     0     0     0     0     0     0      0
    15      0     0     0     0     0     0     0     0      0
    20      0     0     0     0     0     0     0     0      0
    25      0     0     0     0     0     0     0     0      0
    30      0     0     0     0     0     0     0     0      0
    35      0     0     0     0     0     0     0     0      0
    40      0     0     0     0     0     0     0     0      0
    45      0     0     0     0     0     0     0     0      0
    50      0     0     0     0     0     0     0     0      0
    55      0     0     0     0     0     0     0     0      0
    60      0     0     0     0     0     0     0     0      0
    65      0     0     0     0     0     0     0     0      0
    70      0     0     0     0     0     0     1     0      0
    75      0     0     0     0     2     0     0     0      0
    80      0     0     0     0     1     0     1     0      0
    85      0     0     0     0     3     0     2     0      2
    90      0     0     0     0     3     0     2     0      2
    95      0     0     0     0     3     0     3     0      3
   100      0     0     0     0     3     0     2     0      3
   105      0     0     0     0     3     0     2     0      2
   110      0     0     0     0     3     0     2     0      2
   115      0     0     0     0     3     0     2     0      3

**************************************************************************
Before test time there were, in percentage:
False positive biogas production before test time is 0 percent.
No biogas detection before test time is 100 percent.
And after test time the results are:
Biogas detection after test time is 17.901 percent.
No biogas detection after test time is 82.099 percent.
```

A2 – Correlation of monitored parameters

The next two matrices show the results from the correlation analysis among the monitored parameters biogas, pH, conductivity, and turbidity.

Next matrix represents correlation coefficients for the following:

test	ph-turb	ph-cond	ph-gas	turb-cond	turb-gas	cond-gas
Na10	0.6352	0.3960	0.4037	0.8899	0.7771	0.8338
Na10	0.7881	0.2735	0.3478	0.7006	0.5111	0.8155
Na10	0.8627	0.3870	0.4487	0.7237	0.7413	0.8590
Na20	0.3331	0.4394	0.7102	0.0078	0.3062	0.8799
Na20	0.1206	0.4687	0.6765	0.5577	0.4767	0.9442
Na20	0.8518	0.4942	0.6814	0.8288	0.8995	0.9208
Blc1	0.2745	0.9820	0.4179	0.2516	0.0149	0.4090
Blc1	0.9082	0.9418	0.3334	0.7910	0.3439	0.3888
Blc1	0.3494	0.9328	0.3229	0.3230	0.3955	0.2049
Blc5	0.4700	0.9657	0.5929	0.3561	0.3496	0.4931
Blc5	0.5091	0.9345	0.7759	0.3456	0.4823	0.6854
Blc5	0.8236	0.9178	0.4233	0.5922	0.5475	0.3191
oo20	0.9653	0.0934	0.1862	0.1177	0.2887	0.1441
oo20	0.9350	0.9416	0.1382	0.8993	0.2656	0.2863
oo20	0.9085	0.2030	0.3845	0.0168	0.4630	0.3763
oo40	0.9595	0.5304	0.1906	0.3650	0.3429	0.2269
oo40	0.8686	0.8966	0.0386	0.6313	0.2534	0.2806
oo40	0.9610	0.7489	0.0314	0.6672	0.0828	0.0378
NaOH	0.1554	0.7223	0.9622	0.1880	0.0684	0.6642
NaOH	0.3322	0.8522	0.7577	0.4683	0.0057	0.7153
NaOH	0.3000	0.9147	0.8707	0.5103	0.1231	0.6606
HCl	0.9601	0.7651	0.7401	0.8809	0.6228	0.4747
HCl	0.8655	0.7686	0.1232	0.8080	0.1026	0.0833
HCl	0.7029	0.8324	0.3465	0.9529	0.1095	0.1095
Milk	0.3851	0.1056	0.1823	0.4681	0.0802	0.0479
Milk	0.5359	0.4481	0.0530	0.8315	0.2725	0.5901
Milk	0.8537	0.6532	0.2795	0.8147	0.2516	0.2345

Next matrix represents r^2 for the following:

test	ph-turb	ph-cond	ph-gas	turb-cond	turb-gas	cond-gas
Na10	0.4035	0.1568	0.1630	0.7920	0.6039	0.6952
Na10	0.6210	0.0748	0.1210	0.4908	0.2612	0.6650
Na10	0.7442	0.1498	0.2013	0.5237	0.5496	0.7379
Na20	0.1110	0.1931	0.5044	0.0001	0.0938	0.7743
Na20	0.0145	0.2197	0.4576	0.3110	0.2273	0.8914
Na20	0.7256	0.2442	0.4644	0.6869	0.8091	0.8479
Blc1	0.0754	0.9644	0.1746	0.0633	0.0002	0.1673
Blc1	0.8249	0.8871	0.1112	0.6257	0.1183	0.1512
Blc1	0.1221	0.8700	0.1042	0.1043	0.1564	0.0420
Blc5	0.2209	0.9326	0.3516	0.1268	0.1222	0.2432
Blc5	0.2591	0.8734	0.6020	0.1194	0.2326	0.4698
Blc5	0.6783	0.8423	0.1791	0.3507	0.2997	0.1018
oo20	0.9317	0.0087	0.0347	0.0139	0.0834	0.0208
oo20	0.8742	0.8867	0.0191	0.8087	0.0705	0.0820
oo20	0.8253	0.0412	0.1478	0.0003	0.2143	0.1416
oo40	0.9205	0.2814	0.0363	0.1332	0.1176	0.0515
oo40	0.7545	0.8040	0.0015	0.3986	0.0642	0.0787
oo40	0.9236	0.5608	0.0010	0.4452	0.0069	0.0014
NaOH	0.0241	0.5217	0.9257	0.0353	0.0047	0.4411
NaOH	0.1103	0.7263	0.5741	0.2193	0.0000	0.5117
NaOH	0.0900	0.8368	0.7582	0.2604	0.0152	0.4363
HCl	0.9218	0.5854	0.5477	0.7760	0.3879	0.2254
HCl	0.7492	0.5907	0.0152	0.6529	0.0105	0.0069
HCl	0.4941	0.6929	0.1201	0.9081	0.0120	0.0120
Milk	0.1483	0.0111	0.0332	0.2191	0.0064	0.0023
Milk	0.2872	0.2008	0.0028	0.6913	0.0742	0.3483
Milk	0.7288	0.4266	0.0781	0.6637	0.0633	0.0550

A3 – Results for the classifiers

Average results for the graph theory and FIS classifiers using the 27 data sets are showed in the following pages. The results on the top are from the graph theory based classifier and the results on the bottom are from the FIS classifier. Values in each of the columns (2-10) are percentage of detections.

Graph theory classifier:

The average for sodium at 10 g/L is:

time	milk	oo40	oo20	blc5	NaOH	blc1	Na10	HCl	Na20
0	0	0	0	0	0	0	0	0	0
5	0	0	0	0	0	0	0	0	0
10	0	0	0	0	0	0	0	0	0
15	0	0	0	0	0	0	0	0	0
20	0	0	0	0	0	0	0	0	0
25	0	0	0	0	0	0	0	0	0
30	0	0	0	0	0	0	0	0	0
35	0	0	0	0	0	0	0	0	0
40	0	0	0	0	0	0	0	0	0
45	0	0	0	0	0	0	0	0	0
50	0	0	0	0	0	0	0	0	0
55	0	0	0	0	0	0	0	0	0
60	0	0	0	0	0	0	0	0	0
65	0	0	0	0	0	0	0	0	0
70	0	0	0	0	0	0	33	0	0
75	0	0	0	0	0	0	67	0	0
80	0	0	0	0	0	0	100	0	0
85	0	0	0	0	0	0	100	0	0
90	0	0	0	0	0	0	100	0	0
95	0	0	0	0	0	0	100	0	0
100	0	0	0	0	0	0	100	0	0
105	0	0	0	0	0	0	100	0	0
110	0	0	0	0	0	0	100	0	0
115	0	0	0	0	0	0	100	0	0

FIS classifier:

The average for sodium at 10 g/L is:

time	milk	oo40	oo20	blc5	NaOH	blc1	Na10	HCl	Na20
0	0	0	0	0	0	0	0	0	0
5	0	0	0	0	0	0	0	0	0
10	0	0	0	0	0	0	0	0	0
15	0	0	0	0	0	0	0	0	0
20	0	0	0	0	0	0	0	0	0
25	0	0	0	0	0	0	0	0	0
30	0	0	0	0	0	0	0	0	0
35	0	0	0	0	0	0	0	0	0
40	0	0	0	0	0	0	0	0	0
45	0	0	0	0	0	0	0	0	0
50	0	0	0	0	0	0	0	0	0
55	0	0	0	0	0	0	0	0	0
60	0	0	0	0	0	0	0	0	0
65	0	0	0	0	0	0	0	0	0
70	0	0	0	0	0	0	33	0	0
75	0	0	0	0	0	33	67	0	0
80	0	0	0	0	0	0	100	0	0
85	0	0	0	0	0	0	100	0	0
90	0	0	0	0	0	0	100	0	0
95	0	0	0	0	0	0	100	0	0
100	0	0	0	0	0	0	100	0	0
105	0	0	0	0	0	0	100	0	0
110	0	0	0	0	0	0	100	0	0
115	0	0	0	0	0	0	100	0	0

Graph theory classifier:

The average for sodium at 20 g/L is:

time	milk	oo40	oo20	blc5	NaOH	blc1	Na10	HCl	Na20
0	0	0	0	0	0	0	0	0	0
5	0	0	0	0	0	0	0	0	0
10	0	0	0	0	0	0	0	0	0
15	0	0	0	0	0	0	0	0	0
20	0	0	0	0	0	0	0	0	0
25	0	0	0	0	0	0	0	0	0
30	0	0	0	0	0	0	0	0	0
35	0	0	0	0	0	0	0	0	0
40	0	0	0	0	0	0	0	0	0
45	0	0	0	0	0	0	0	0	0
50	0	0	0	0	0	0	0	0	0
55	0	0	0	0	0	0	0	0	0
60	0	0	0	0	0	0	0	0	0
65	0	0	0	0	0	0	0	0	0
70	0	0	0	67	0	0	0	0	0
75	0	0	0	0	0	0	0	0	100
80	0	0	0	0	0	0	0	0	100
85	0	0	0	0	0	0	0	0	100
90	0	0	0	0	0	0	0	0	100
95	0	0	0	0	0	0	0	0	100
100	0	0	0	0	0	0	0	0	100
105	0	0	0	0	0	0	0	0	100
110	0	0	0	0	0	0	0	0	100
115	0	0	0	0	0	0	0	0	100

FIS classifier:

The average for sodium at 20 g/L is:

time	milk	oo40	oo20	blc5	NaOH	blc1	Na10	HCl	Na20
0	0	0	0	0	0	0	0	0	0
5	0	0	0	0	0	0	0	0	0
10	0	0	0	0	0	0	0	0	0
15	0	0	0	0	0	0	0	0	0
20	0	0	0	0	0	0	0	0	0
25	0	0	0	0	0	0	0	0	0
30	0	0	0	0	0	0	0	0	0
35	0	0	0	0	0	0	0	0	0
40	0	0	0	0	0	0	0	0	0
45	0	0	0	0	0	0	0	0	0
50	0	0	0	0	0	0	0	0	0
55	0	0	0	0	0	0	0	0	0
60	0	0	0	0	0	33	0	0	0
65	0	0	0	0	0	67	0	0	0
70	0	0	0	0	0	0	100	0	0
75	0	0	0	0	0	0	0	0	100
80	0	0	0	0	0	0	0	0	100
85	0	0	0	0	0	0	0	0	100
90	0	0	0	0	0	0	0	0	100
95	0	0	0	0	0	0	0	0	100
100	0	0	0	0	0	0	0	0	100
105	0	0	0	0	0	0	0	0	100
110	0	0	0	0	0	0	0	0	100
115	0	0	0	0	0	0	0	0	100

Graph theory classifier:

The average for bleach at 1 percent is:

time	milk	oo40	oo20	blc5	NaOH	blc1	Na10	HCl	Na20
0	0	0	0	0	0	0	0	0	0
5	0	0	0	0	0	0	0	0	0
10	0	0	0	0	0	0	0	0	0
15	0	0	0	0	0	0	0	0	0
20	0	0	0	0	0	0	0	0	0
25	0	0	0	0	0	0	0	0	0
30	0	0	0	0	0	0	0	0	0
35	0	0	0	0	0	0	0	0	0
40	0	0	0	0	0	0	0	0	0
45	0	0	0	0	0	0	0	0	0
50	0	0	0	0	0	0	0	0	0
55	0	0	0	0	0	0	0	0	0
60	0	0	0	0	0	0	0	0	0
65	0	0	0	0	0	0	0	0	0
70	0	0	0	0	0	0	0	0	0
75	0	0	0	0	0	67	0	0	0
80	0	0	0	0	0	100	0	0	0
85	0	0	0	0	0	100	0	0	0
90	0	0	0	0	0	100	0	0	0
95	0	0	0	0	0	100	0	0	0
100	0	0	0	0	0	100	0	0	0
105	0	0	0	0	0	100	0	0	0
110	0	0	0	0	0	100	0	0	0
115	0	0	0	0	0	100	0	0	0

FIS classifier:

The average for bleach at 1 % is:

time	milk	oo40	oo20	blc5	NaOH	blc1	Na10	HCl	Na20
0	0	0	0	0	0	0	0	0	0
5	0	0	0	0	0	0	0	0	0
10	0	0	0	0	0	0	0	0	0
15	0	0	0	0	0	0	0	0	0
20	0	0	0	0	0	0	0	0	0
25	0	0	0	0	0	0	0	0	0
30	0	0	0	0	0	0	0	0	0
35	0	0	0	0	0	0	0	0	0
40	0	0	0	0	0	0	0	0	0
45	0	0	0	0	0	0	0	0	0
50	0	0	0	0	0	0	0	0	0
55	0	0	0	0	0	0	0	0	0
60	0	0	0	0	0	0	0	0	0
65	0	0	0	0	0	0	0	0	0
70	0	0	0	0	0	0	0	0	0
75	0	0	0	0	0	67	0	0	0
80	0	0	0	0	0	100	0	0	0
85	0	0	0	0	0	100	0	0	0
90	0	0	0	0	0	100	0	0	0
95	0	0	0	0	0	100	0	0	0
100	0	0	0	0	0	100	0	0	0
105	0	0	0	0	0	100	0	0	0
110	0	0	0	0	0	100	0	0	0
115	0	0	0	0	0	100	0	0	0

Graph theory classifier:

The average for bleach at 5 percent is:

time	milk	oo40	oo20	blc5	NaOH	blc1	Na10	HCl	Na20
0	0	0	0	0	0	0	0	0	0
5	0	0	0	0	0	0	0	0	0
10	0	0	0	0	0	0	0	0	0
15	0	0	0	0	0	0	0	0	0
20	0	0	0	0	0	0	0	0	0
25	0	0	0	0	0	0	0	0	0
30	0	0	0	0	0	0	0	0	0
35	0	0	0	0	0	0	0	0	0
40	0	0	0	0	0	0	0	0	0
45	0	0	0	0	0	0	0	0	0
50	0	0	0	0	0	0	0	0	0
55	0	0	0	0	0	0	0	0	0
60	0	0	0	0	0	0	0	0	0
65	0	0	0	0	0	0	0	0	0
70	0	0	0	0	0	100	0	0	0
75	0	0	0	0	0	0	33	0	0
80	0	0	0	100	0	0	0	0	0
85	0	0	0	100	0	0	0	0	0
90	0	0	0	100	0	0	0	0	0
95	0	0	0	100	0	0	0	0	0
100	0	0	0	100	0	0	0	0	0
105	0	0	0	100	0	0	0	0	0
110	0	0	0	100	0	0	0	0	0
115	0	0	0	100	0	0	0	0	0

FIS classifier:

The average for bleach at 5 % is:

time	milk	oo40	oo20	blc5	NaOH	blc1	Na10	HCl	Na20
0	0	0	0	0	0	0	0	0	0
5	0	0	0	0	0	0	0	0	0
10	0	0	0	0	0	0	0	0	0
15	0	0	0	0	0	0	0	0	0
20	0	0	0	0	0	0	0	0	0
25	0	0	0	0	0	0	0	0	0
30	0	0	0	0	0	0	0	0	0
35	0	0	0	0	0	0	0	0	0
40	0	0	0	0	0	0	0	0	0
45	0	0	0	0	0	0	0	0	0
50	0	0	0	0	0	0	0	0	0
55	0	0	0	0	0	0	0	0	0
60	0	0	0	0	0	0	0	0	0
65	0	0	0	0	0	67	0	0	0
70	0	0	0	0	0	100	0	0	0
75	0	0	0	0	0	67	33	0	0
80	0	0	0	67	0	0	33	0	0
85	0	0	0	100	0	0	0	0	0
90	0	0	0	100	0	0	0	0	0
95	0	0	0	100	0	0	0	0	0
100	0	0	0	100	0	0	0	0	0
105	0	0	0	100	0	0	0	0	0
110	0	0	0	100	0	0	0	0	0
115	0	0	0	100	0	0	0	0	0

Graph theory classifier:

The average for organic overload at 20 g/L is:

time	milk	oo40	oo20	blc5	NaOH	blc1	Na10	HCl	Na20
0	0	0	0	0	0	0	0	0	0
5	0	0	0	0	0	0	0	0	0
10	0	0	0	0	0	0	0	0	0
15	0	0	0	0	0	0	0	0	0
20	0	0	0	0	0	0	0	0	0
25	0	0	0	0	0	0	0	0	0
30	0	0	0	0	0	0	0	0	0
35	0	0	0	0	0	0	0	0	0
40	0	0	0	0	0	0	0	0	0
45	0	0	0	0	0	0	0	0	0
50	0	0	0	0	0	0	0	0	0
55	0	0	0	0	0	0	0	0	0
60	0	0	0	0	0	0	0	0	0
65	0	0	0	0	0	0	0	0	0
70	0	0	0	0	0	0	0	0	0
75	0	0	33	0	0	0	0	0	0
80	0	0	100	0	0	0	0	0	0
85	0	0	100	0	0	0	0	0	0
90	0	0	100	0	0	0	0	0	0
95	0	0	100	0	0	0	0	0	0
100	0	0	100	0	0	0	0	0	0
105	0	0	100	0	0	0	0	0	0
110	0	0	100	0	0	0	0	0	0
115	0	0	100	0	0	0	0	0	0

FIS classifier:

The average for organic overload at 20 g/L is:

time	milk	oo40	oo20	blc5	NaOH	blc1	Na10	HCl	Na20
0	0	0	0	0	0	0	0	0	0
5	0	0	0	0	0	0	0	0	0
10	0	0	0	0	0	0	0	0	0
15	0	0	0	0	0	0	0	0	0
20	0	0	0	0	0	0	0	0	0
25	0	0	0	0	0	0	0	0	0
30	0	0	0	0	0	0	0	0	0
35	0	0	0	0	0	0	0	0	0
40	0	0	0	0	0	0	0	0	0
45	0	0	0	0	0	0	0	0	0
50	0	0	0	0	0	0	0	0	0
55	0	0	0	0	0	0	0	0	0
60	0	0	0	0	0	0	0	0	0
65	0	0	0	0	0	0	0	0	0
70	0	0	33	0	0	0	0	0	0
75	0	0	100	0	0	0	0	0	0
80	0	0	100	0	0	0	0	0	0
85	0	0	100	0	0	0	0	0	0
90	0	0	100	0	0	0	0	0	0
95	0	0	100	0	0	0	0	0	0
100	0	0	100	0	0	0	0	0	0
105	0	0	100	0	0	0	0	0	0
110	0	0	100	0	0	0	0	0	0
115	0	0	100	0	0	0	0	0	0

Graph theory classifier:

The average for organic overload at 40 g/L is:

time	milk	oo40	oo20	blc5	NaOH	blc1	Na10	HCl	Na20
0	0	0	0	0	0	0	0	0	0
5	0	0	0	0	0	0	0	0	0
10	0	0	0	0	0	0	0	0	0
15	0	0	0	0	0	0	0	0	0
20	0	0	0	0	0	0	0	0	0
25	0	0	0	0	0	0	0	0	0
30	0	0	0	0	0	0	0	0	0
35	0	0	0	0	0	0	0	0	0
40	0	0	0	0	0	0	0	0	0
45	0	0	0	0	0	0	0	0	0
50	0	0	0	0	0	0	0	0	0
55	0	0	0	0	0	0	0	0	0
60	0	0	0	0	0	0	0	0	0
65	0	0	0	0	0	0	0	0	0
70	0	0	67	0	0	0	0	0	0
75	0	100	0	0	0	0	0	0	0
80	0	100	0	0	0	0	0	0	0
85	0	100	0	0	0	0	0	0	0
90	0	100	0	0	0	0	0	0	0
95	0	100	0	0	0	0	0	0	0
100	0	100	0	0	0	0	0	0	0
105	0	100	0	0	0	0	0	0	0
110	0	100	0	0	0	0	0	0	0
115	0	100	0	0	0	0	0	0	0

FIS classifier:

The average for organic overload at 40 g/L is:

time	milk	oo40	oo20	blc5	NaOH	blc1	Na10	HCl	Na20
0	0	0	0	0	0	0	0	0	0
5	0	0	0	0	0	0	0	0	0
10	0	0	0	0	0	0	0	0	0
15	0	0	0	0	0	0	0	0	0
20	0	0	0	0	0	0	0	0	0
25	0	0	0	0	0	0	0	0	0
30	0	0	0	0	0	0	0	0	0
35	0	0	0	0	0	0	0	0	0
40	0	0	0	0	0	0	0	0	0
45	0	0	0	0	0	0	0	0	0
50	0	0	0	0	0	0	0	0	0
55	0	0	0	0	0	0	0	0	0
60	0	0	0	0	0	0	0	0	0
65	0	0	0	0	0	0	0	0	0
70	0	0	67	0	0	0	0	33	0
75	0	100	0	0	0	0	0	0	0
80	0	100	0	0	0	0	0	0	0
85	0	100	0	0	0	0	0	0	0
90	0	100	0	0	0	0	0	0	0
95	0	100	0	0	0	0	0	0	0
100	0	100	0	0	0	0	0	0	0
105	0	100	0	0	0	0	0	0	0
110	0	100	0	0	0	0	0	0	0
115	0	100	0	0	0	0	0	0	0

Graph theory classifier:

The average for NaOH is:

time	milk	oo40	oo20	blc5	NaOH	blc1	Na10	HCl	Na20
0	0	0	0	0	0	0	0	0	0
5	0	0	0	0	0	0	0	0	0
10	0	0	0	0	0	0	0	0	0
15	0	0	0	0	0	0	0	0	0
20	0	0	0	0	0	0	0	0	0
25	0	0	0	0	0	0	0	0	0
30	0	0	0	0	0	0	0	0	0
35	0	0	0	0	0	0	0	0	0
40	0	0	0	0	0	0	0	0	0
45	0	0	0	0	0	0	0	0	0
50	0	0	0	0	0	0	0	0	0
55	0	0	0	0	0	0	0	0	0
60	0	0	0	0	0	0	0	0	0
65	0	0	0	0	0	0	0	0	0
70	0	0	0	0	0	0	0	0	0
75	0	0	0	0	67	0	0	0	0
80	0	0	0	0	100	0	0	0	0
85	0	0	0	0	100	0	0	0	0
90	0	0	0	0	100	0	0	0	0
95	0	0	0	0	100	0	0	0	0
100	0	0	0	0	100	0	0	0	0
105	0	0	0	0	100	0	0	0	0
110	0	0	0	0	100	0	0	0	0
115	0	0	0	0	100	0	0	0	0

FIS classifier:

The average for NaOH is:

time	milk	oo40	oo20	blc5	NaOH	blc1	Na10	HCl	Na20
0	0	0	0	0	0	0	0	0	0
5	0	0	0	0	0	0	0	0	0
10	0	0	0	0	0	0	0	0	0
15	0	0	0	0	0	0	0	0	0
20	0	0	0	0	0	0	0	0	0
25	0	0	0	0	0	0	0	0	0
30	0	0	0	0	0	0	0	0	0
35	0	0	0	0	0	0	0	0	0
40	0	0	0	0	0	0	0	0	0
45	0	0	0	0	0	0	0	0	0
50	0	0	0	0	0	0	0	0	0
55	0	0	0	0	0	0	0	0	0
60	0	0	0	0	0	0	0	0	0
65	0	0	0	0	0	0	0	0	0
70	0	0	0	0	0	0	0	0	0
75	0	0	0	0	67	0	0	0	0
80	0	0	0	0	100	0	0	0	0
85	0	0	0	0	100	0	0	0	0
90	0	0	0	0	100	0	0	0	0
95	0	0	0	0	100	0	0	0	0
100	0	0	0	0	100	0	0	0	0
105	0	0	0	0	100	0	0	0	0
110	0	0	0	0	100	0	0	0	0
115	0	0	0	0	100	0	0	0	0

Graph theory classifier:

The average for HCl is:

time	milk	oo40	oo20	blc5	NaOH	blc1	Na10	HCl	Na20
0	0	0	0	0	0	0	0	0	0
5	0	0	0	0	0	0	0	0	0
10	0	0	0	0	0	0	0	0	0
15	0	0	0	0	0	0	0	0	0
20	0	0	0	0	0	0	0	0	0
25	0	0	0	0	0	0	0	0	0
30	0	0	0	0	0	0	0	0	0
35	0	0	0	0	0	0	0	0	0
40	0	0	0	0	0	0	0	0	0
45	0	0	0	0	0	0	0	0	0
50	0	0	0	0	0	0	0	0	0
55	0	0	0	0	0	0	0	0	0
60	0	0	0	0	0	0	0	0	0
65	0	0	0	0	0	0	0	0	0
70	0	0	0	0	0	0	0	0	0
75	0	0	0	0	0	0	0	33	0
80	0	0	0	0	0	0	0	100	0
85	0	0	0	0	0	0	0	100	0
90	0	0	0	0	0	0	0	100	0
95	0	0	0	0	0	0	0	100	0
100	0	0	0	0	0	0	0	100	0
105	0	0	0	0	0	0	0	100	0
110	0	0	0	0	0	0	0	100	0
115	0	0	0	0	0	0	0	100	0

FIS classifier:

The average for HCl is:

time	milk	oo40	oo20	blc5	NaOH	blc1	Na10	HCl	Na20
0	0	0	0	0	0	0	0	0	0
5	0	0	0	0	0	0	0	0	0
10	0	0	0	0	0	0	0	0	0
15	0	0	0	0	0	0	0	0	0
20	0	0	0	0	0	0	0	0	0
25	0	0	0	0	0	0	0	0	0
30	0	0	0	0	0	0	0	0	0
35	0	0	0	0	0	0	0	0	0
40	0	0	0	0	0	0	0	0	0
45	0	0	0	0	0	0	0	0	0
50	0	0	0	0	0	0	0	0	0
55	0	0	0	0	0	0	0	0	0
60	0	0	0	0	0	0	0	0	0
65	0	0	0	0	0	0	0	0	0
70	0	0	0	0	0	0	0	0	0
75	0	0	0	0	0	0	0	33	0
80	0	0	0	0	0	0	0	100	0
85	0	0	0	0	0	0	0	100	0
90	0	0	0	0	0	0	0	100	0
95	0	0	0	0	0	0	0	100	0
100	0	0	0	0	0	0	0	100	0
105	0	0	0	0	0	0	0	100	0
110	0	0	0	0	0	0	0	100	0
115	0	0	0	0	0	0	0	100	0

Graph theory classifier:

The average for milk is:

time	milk	oo40	oo20	blc5	NaOH	blc1	Na10	HCl	Na20
0	0	0	0	0	0	0	0	0	0
5	0	0	0	0	0	0	0	0	0
10	0	0	0	0	0	0	0	0	0
15	0	0	0	0	0	0	0	0	0
20	0	0	0	0	0	0	0	0	0
25	0	0	0	0	0	0	0	0	0
30	0	0	0	0	0	0	0	0	0
35	0	0	0	0	0	0	0	0	0
40	0	0	0	0	0	0	0	0	0
45	0	0	0	0	0	0	0	0	0
50	0	0	0	0	0	0	0	0	0
55	0	0	0	0	0	0	0	0	0
60	0	0	0	0	0	0	0	0	0
65	0	0	0	0	0	0	0	0	0
70	0	33	0	0	0	0	0	0	0
75	0	100	0	0	0	0	0	0	0
80	100	0	0	0	0	0	0	0	0
85	100	0	0	0	0	0	0	0	0
90	100	0	0	0	0	0	0	0	0
95	100	0	0	0	0	0	0	0	0
100	100	0	0	0	0	0	0	0	0
105	100	0	0	0	0	0	0	0	0
110	100	0	0	0	0	0	0	0	0
115	100	0	0	0	0	0	0	0	0

FIS classifier:

The average for milk is:

time	milk	oo40	oo20	blc5	NaOH	blc1	Na10	HCl	Na20
0	0	0	0	0	0	0	0	0	0
5	0	0	0	0	0	0	0	0	0
10	0	0	0	0	0	0	0	0	0
15	0	0	0	0	0	0	0	0	0
20	0	0	0	0	0	0	0	0	0
25	0	0	0	0	0	0	0	0	0
30	0	0	0	0	0	0	0	0	0
35	0	0	0	0	0	0	0	0	0
40	0	0	0	0	0	0	0	0	0
45	0	0	0	0	0	0	0	0	0
50	0	0	0	0	0	0	0	0	0
55	0	0	0	0	0	0	0	0	0
60	0	0	0	0	0	0	0	0	0
65	0	0	67	0	0	0	0	0	0
70	0	33	0	0	0	0	0	67	0
75	0	100	0	0	0	0	0	0	0
80	100	0	0	0	0	0	0	0	0
85	100	0	0	0	0	0	0	0	0
90	100	0	0	0	0	0	0	0	0
95	100	0	0	0	0	0	0	0	0
100	100	0	0	0	0	0	0	0	0
105	100	0	0	0	0	0	0	0	0
110	100	0	0	0	0	0	0	0	0
115	100	0	0	0	0	0	0	0	0

VITA

Alexandra Maria Almeida Carvalho Pinto, daughter of José Leite de Carvalho and Ilca Almeida Carvalho, was born on March 25, 1967, in Três Lagoas, Mato Grosso do Sul, Brazil, and has three sisters Andréa, Débora and Lygia. She entered the Universidade Estadual Paulista at Ilha Solteira, SP, Brazil, in March, 1988, where she received her Bachelor's degree in Civil Engineering in January, 1993. She married João Onofre Pereira Pinto in September 1992. Her son, João Vitor Carvalho Pereira Pinto, was born in January 1993. In March 1993, she entered the master program at the Universidade Federal de Uberlândia, MG, Brazil and received her Master of Science Degree in Electrical Engineering in August 1995. In August 1997 she entered graduate school at the University of Tennessee in Knoxville and received her Doctor of Philosophy degree in Biosystems Engineering in December 2001.